SEISMIC STRENGTHENING OF REINFORCED CEMENT CONCRETE (RCC) STRCTURES

Thesis of Bachelors in Engineering

By

Hesham Ahmed 2011-NUST-SCEE-BE-CE-34

Muneeb Ahsan Malik 2011-NUST-SCEE-BE-CE-90

M. Shaheryar Bakhtiar 2011-NUST-SCEE-BE-CE-74

Kulsoom Abbas 2011-NUST-SCEE-BE-CE-134

NUST Institute of Civil Engineering (NICE)

School of Civil and Environmental Engineering (SCEE)

National University of Sciences and Technology (NUST)

Islamabad, Pakistan

2015

SEISMIC STRENGTHENING OF REINFORCED CEMENT CONCRETE (RCC) STRCTURES

By

Hesham Ahmed	2011-NUST-SCEE-BE-CE-34
Muneeb Ahsan Malik	2011-NUST-SCEE-BE-CE-90
M. Shaheryar Bakhtiar	2011-NUST-SCEE-BE-CE-74
Kulsoom Abbas	2011-NUST-SCEE-BE-CE-134

A DISSERTATION

Submitted to

National University of Sciences and Technology

in partial fulfilment of

the requirements for the degree of

Bachelors of Engineering

In

CIVIL (STRUCTURAL) ENGINEERING

Department of Civil Engineering

National University of Sciences and Technology, Pakistan

This is to certify that

The thesis entitled

SEISMIC STRENGTHENING OF REINFORCED CEMENT CONCRETE (RCC) STRCTURES

Submitted by

Hesham Ahmed	2011-NUST-SCEE-BE-CE-34
Muneeb Ahsan Malik	2011-NUST-SCEE-BE-CE-90
M. Shaheryar Bakhtiar	2011-NUST-SCEE-BE-CE-74
Kulsoom Abbas	2011-NUST-SCEE-BE-CE-134

Has been accepted towards the partial fulfilment of the requirements

of

Bachelors in Civil Engineering

_____

Dr. Shaukat Ali Khan, PhD

NUST Institute of Civil Engineering

National University of Sciences and Technology, Islamabad, Pakistan

2015

ABSTRACT

The Reinforced Concrete building stock of Pakistan is highly vulnerable to seismic hazard due to poor construction practices and lack of proper design. The aim of this research work is to analyze and assess the seismic vulnerability of reinforced concrete bare frames and compare with fiber reinforced polymer (FRP) wrapped frames.

The experimental work done by Lam and Teng (2003) was used to model the stress strain behavior of FRP confined concrete. A program was developed to generate the model of reinforced concrete frames and their behavior under seismic excitation was analyzed using Drain 3DX software. It was tried to incorporate all the known structural responses such as slippage and bar pullout phenomenon which occur during a seismic event to precisely simulate the behavior of buildings. The frames were first analyzed as bare frames and then again by applying FRP to the joints. The purpose was to compare the extent to which the FRP improves the behavior of the frames under seismic loading.

The procedure adopted was Non Linear Static Procedure (modified capacity spectrum approach) for the simulation of the structures response. It is specified by FEMA 440 and ATC-4. Work done by (Kyriakides, 2007), (Fajfar, 1996) is used to develop vulnerability curves for low, medium and high rise RC structures of Pakistan both with and without FRP wrapping. Comparison of the bare and wrapped vulnerability curves of different structures allows to draw conclusion over how effective the FRP wrapping technique is to reduce the extent of damage to the buildings. Comparison by varying storeys, bays and number of wraps has also been done. A method of economic comparison of damage to building has also been developed. The work allows for the comparison of any sort of retrofitting technique by just varying the stress strain models.

DEDICATED TO

OUR LOVING PARENTS

ACKNOWLEDGEMENTS

All the praises be to Allah, the Gracious, the Most Merciful and the Best Guide, for His help and guidance that has always been with us at every step and every moment of life. Glory be to Him that He enabled us to accomplish this research work.

We also thank Dr. Shaukat Ali Khan, for supervising our work and guiding us throughout the project. He has been an inspiration and his work and knowledge in the field of seismic domain encouraged us to do our project in the same area.

We also appreciate all the help provided by our seniors especially by Uzair Maqbool Khan. Their support and guidance was invaluable for our project and we are thankful for their time.

Table of Contents

List of Tables

List of Figures

List of Abbreviations & Notations

Abbreviations

PMD	Pakistan Meteorological Department
VBA	Visual Basic Applications
ERA	Earthquake Risk Assessment
FRP	Fiber Reinforced-Polymers
DPM	Damage Probability Matrices
PSa	Pseudo Spectral Acceleration
ATC	Applied Technology Council
SDOF	Single Degree of Freedom System
RSM	Response Spectrum Method
FEMA	Federal Emergency Management Agency
HVAC	Heating, Ventilation, and Air Conditioning
CFRP	Carbon Fiber Reinforced Polymer
GFRP	Glass fiber reinforced polymer
FRP	Fiber Reinforced Plastic
PSHA	Probabilistic seismic hazard analysis
PGA	Peak Ground Acceleration
CSM	Capacity Spectrum Method
ERM	Earthquake Risk Mitigation
RCC	Reinforced Cement Concrete
BCP	Building code of Pakistan
ASCE	American Society of Civil Engineers
ACI	American Concrete Institute
UBC	Uniform Building Code
ADRS	Acceleration Deceleration Response Spectrum
MADRS	Modified Acceleration Displacement Response Spectrum
DI	Damage Index
HAZUS	Hazard of United States *Abbreviations*

BS	British Standards
CDF	Cumulative distribution function
CDP	Construction and design Practice
DG	Damage Grade
DR	Damage Ratio
EC	Euro code
ERA	Earthquake Risk Assessment
ISD	Inter-storey drift
LR	Low-rise buildings
MR	Mid-rise buildings
HR	High-rise buildings
LHS	Latin Hypercube Sampling
MDR	Mean Damage Ratio
MMI	Modified Mercali Intensity
NIBS	National Institute of Building Science
PDF	Probability Distribution Function
PGA	Peak Ground Acceleration

Notations

a/d	aspect ratio
b	breath of cross-section
d	depth of cross-section
d_{bl}	longitudinal bar diameter
f_c	concrete compressive strength
f_s	stress in a reinforcement bar
f_{ys}	steel bar yield strength
f_{yw}	shear link yield strength
h_i	height of floor i
l	anchorage length
m	total mass
s	shear link spacing

u_i	uniform random number
F_d	Design shear force capacity
F_y	Yield shear force capacity
F_{ult}	Ultimate shear force capacity
M_d	Design moment capacity
M_L	Local magnitude
M_s	Surface magnitude
M_y	Yield moment capacity
M_{ult}	Ultimate moment capacity
N	Number of floors
S	Soil parameter *Notation*

S_A	Spectral acceleration
S_D	Spectral displacement
$T_{initial}$	Initial period of vibration
T_{sec}	Secant period
V_c	Concrete shear contribution
W_i	Weight of floor i
A_s	Area of steel bar
E_s	Steel elastic modulus
α_0	mass damping coefficient
α_1	element damping coefficient
α_g	design ground acceleration
ε_s	steel strain
λ	correction factor
μ	mean value
σ	standard deviation
τ_e	bond strength for elastic steel
τ_y	bond strength for yielded strength
ω	angular frequency

CHAPTER 1

INTRODUCTION

1.1 Background

Pakistan is a highly seismically active region. Numerous earthquakes have jolted this region and caused high life and economical losses. In Pakistan the construction requirements of the buildings are mentioned and made mandatory in the Building Code of Pakistan (BCP). It governs the quality and strength requirement for buildings necessary for safe living. The provisions in the old Building Codes of Pakistan before 2007 focus solely on gravity loads. They do mention the recommended provisions needed for attainment of strength against lateral loading, but complying with those provisions was not compulsory.

After the devastating earthquake in 2005, the building Code of Pakistan was revised, provisions against lateral loading were improved and complying with these new provisions was made obligatory. This new Code was published in 2007.

Several earthquakes in the history have caused massive deaths and economic losses in Pakistan. These include the most recent 2005 Kashmir earthquake; 1945, Makran earthquake of magnitude 7.5; 1935, Quetta earthquake of magnitude 7.7, and many others. The economic loss caused due to 2005 earthquake was 5.2 billion dollars and more than a million lives were lost (Haseeb & Haseeb, 2011). Four hundred thousand plus buildings were reduced to rubble. The Quetta earthquake, 1935, caused more than sixty thousand deaths and was ranked the 23rd most deadly earthquake worldwide to date (Anon., 2014).

The unsuitable location of Pakistan considering seismic activity is the main cause of the huge damages caused in earthquakes and this has repeatedly highlighted the need for improved and better provisions against lateral

loading to ensure the safety of the building occupants. Pakistan is located on two tectonic plates: the Eurasian plate and the Indian plate. A fault in the North-south direction divides Pakistan into two and this makes the region highly prone to earthquakes.

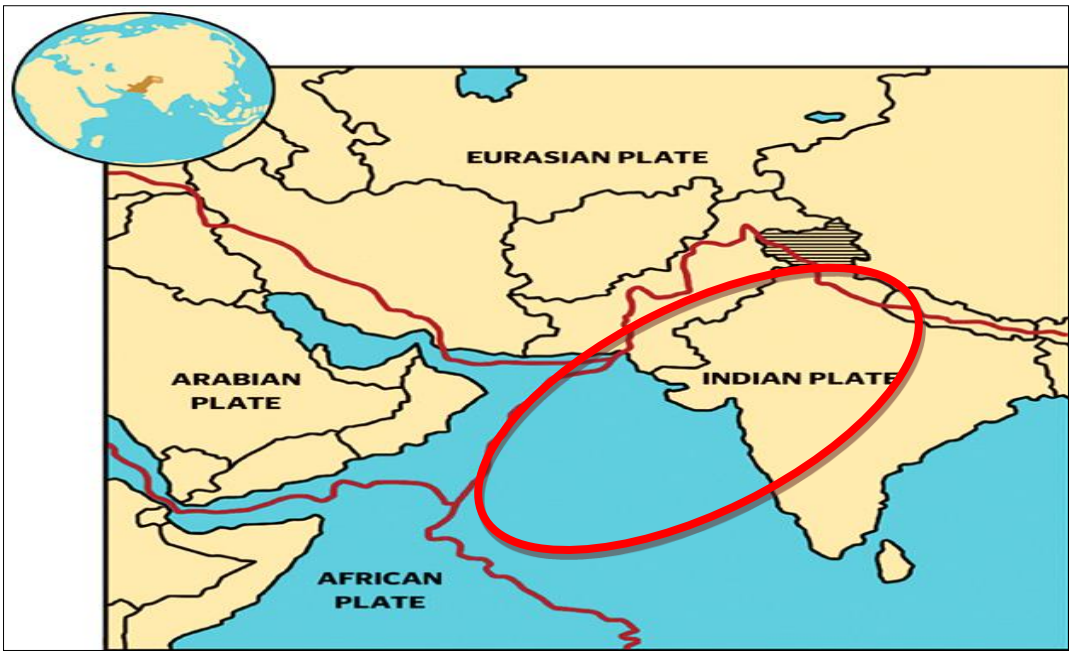

Figure 1. 1 Tectonic Location of Pakistan (TRIBUNE, 2013)

The losses suffered in an earthquake are due to the structures' inability to withstand the lateral loads induced during the earthquake. The structure, under lateral loads, deforms due to decrease in the stiffness of the structural members and can collapse if the deformation is excessive. In case of Pakistan, the old Building Code of Pakistan didn't provide vital provisions against earthquake loads (lateral loads) making the building stock highly vulnerable to seismic action. These provisions were later provided in the Building code of Pakistan 2007.

Pakistan has been divided into seismic zones and according to those zones vulnerability can be determined for various areas. Figure 1.2 shows division of areas with respect to seismic hazard level and fundamental details of earthquakes occurring in the zones.

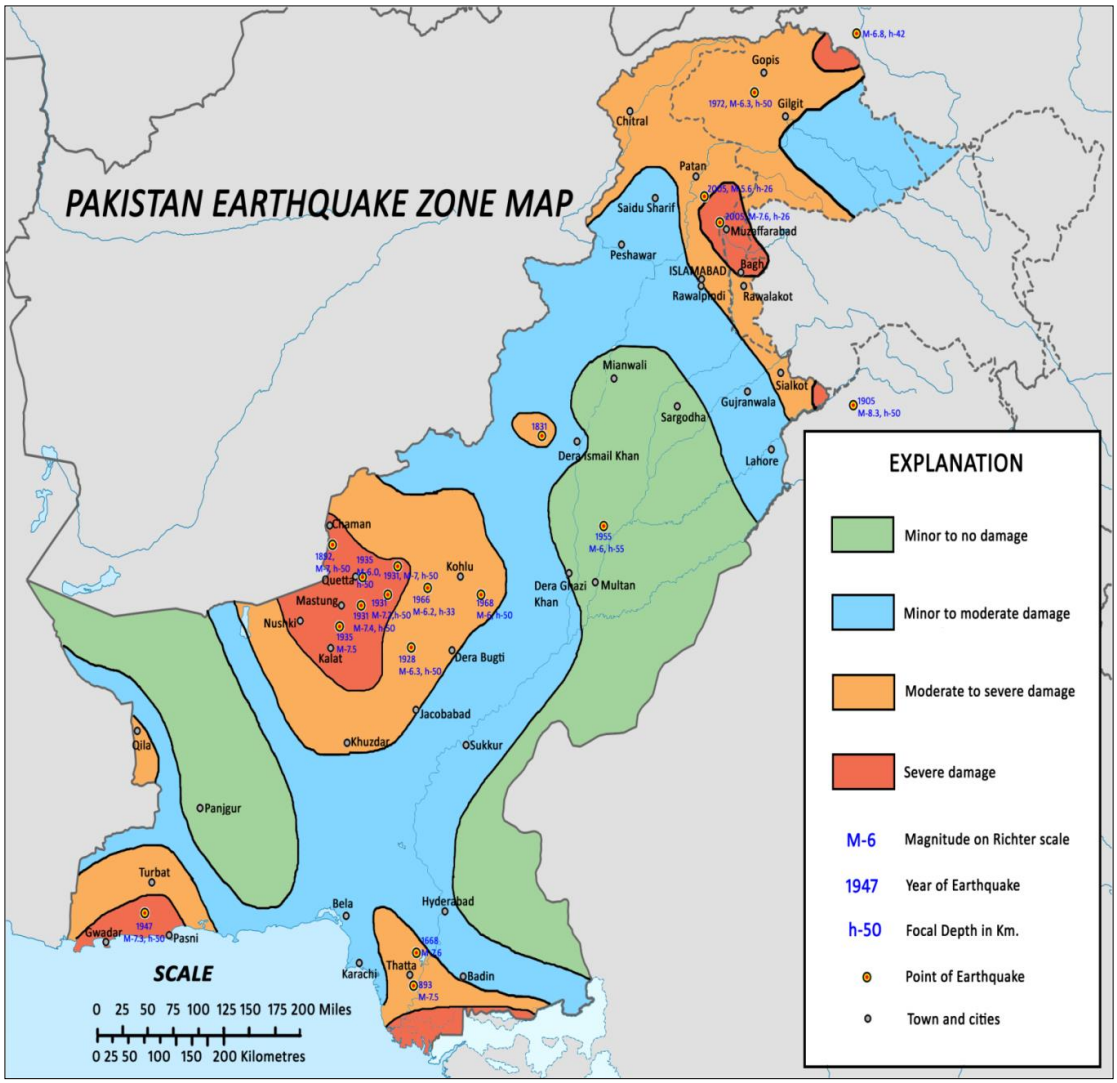

Figure 1. 2 Seismic Zone Map of Pakistan (Wikipedia, 2011)

However, the existing building stock is still unsafe against the earthquake loads. Several vulnerability studies have been carried out pointing out to the inability of the existing building stock constructed before 2007 in resisting the earthquake loads and based on these studies measures are needed to provide the necessary strength to the structures through retrofitting techniques. Actions need to be taken to assure the safety of the building stock constructed before 2007 in order to avoid further loss of human life and economic losses.

Figure 1. 3 Jinnah Road after Quetta Earthquake, 1935 (Telegraph)

Pakistan has always faced massive structural loss in the earthquakes with major destruction to the structures, buildings and the infrastructure including the bridges and roads. Despite the various studies conducted on the failures in RCC structures as RCC is the major construction material in Pakistan, very little has been done in the field of retrofitting.

Figure 1. 4 Structural Damage of Kashmir Earthquake, 2005 ((PWP), 2011)

The damage shown in Figure 1.4 demonstrates structural failure which demands a rapid action towards economical ways of retrofitting in existing

structures against lateral loads and seismic hazards. One of such methods includes wrapping of fibre reinforced polymers (FRPS) which provide confinement to the structural members and therefore makes them more resistance towards seismic loading. Brittle failure if prevented may result in longer durability and serviceability of the structures; therefore retrofitting by FRPs stands as the most viable solution since most of the constructed stock in Pakistan lacks seismic resistance measures.

1.2 Problem Statement

This study focuses to address the problem experienced by Pakistan in relation to the seismic hazards and loss. Developing an economical and feasible method of retrofitting stands as the need of time and strengthening the existing structures as well as the newly built ones stand equally significant for the construction industry of Pakistan. Table 1.1 summarizes the loss Pakistan has witnessed over its life and even before emerging as a separate geographical entity which shows drastic increase in subsequent loss and damage which needs to be fixed and addressed on urgent basis.

Date	Magnitude	Deaths	Areas affected
August 24, 1931	7	-	Sharigh valley, Baluchistan
August 27, 1931	7.4	-	Mach, Baluchistan province
May 31, 1935	7.7	60,000	Districts of Baluchistan
November 27, 1945	7.9 or 8 (tsunami)	4,000	Makran-Sindh coastal areas
December 28, 1974	6.2	5,300	Districts of the Khyber province
October 8, 2005	7.8	80,000	Parts of Khyber and Azad Kashmir
October 29, 2008	6.4	216	Quetta, Baluchistan
January 18, 2011	7.2	2	Baluchistan

Table 1. 1 Casualties Resulting from Deadliest Earthquakes in Pakistan (Anon., 2011)

Failures incurred in these earthquakes are primarily due to the bad material selection, poor construction practices, weak joints, brittle nature

of members, reinforcement failures, shear failure in columns, improper bonding of the columns. To address these problems, proposed methodology of retrofitting by FRPs is a valid option and this study aims at achieving the desired resistance and addressing the seismic vulnerability of the buildings of Pakistan.

1.3 Aims and Objectives

The aims following this research project involves developing seismic vulnerability assessment framework and the effect on these frameworks after the retrofitting of Fibre Reinforced Polymers (FRPs). The objectives can be further classified into the following steps:

- Review of the behaviour of FRP strengthened RC structures and the resistance provided against the seismic loading.
- Selecting significant number of RC frame structures with variation in the number of storey and bays to represent the building stock of Pakistan.
- Development of vulnerability curves.
- Comparison of retrofitted structure against un retrofitted structures in relation to their seismic vulnerability and resistance.
- Economic comparison of using FRP for retrofitting against repairing or replacing the damaged structures.

CHAPTER 2

LITERATURE REVIEW

2.1 Introduction

Pakistan's seismicity varies from moderate to high level. Numerous structures collapsed as a result of October 8, 2005 earthquake validated the assumption of high seismic vulnerability in the country (Virk, 2010). In the 2005 Kashmir Earthquake approximately 400,153 residential building were destroyed and damaged. It is also estimated that 50-70% important official buildings were destroyed and damaged including administration, police, military buildings etc. (Haseeb & Xinhailu, 2011). Out of 780,000 damaged buildings only 250,000 reinforced concrete constructions or combinations of reinforced concrete with masonry infill walls. (Nienhuys, 2010). The extent of damage due to earthquakes in this region especially in the existing building stock has led to the requirement of seismic retrofitting. For this purpose various techniques have been developed. This chapter covers previous studies on seismicity of Islamabad, seismic risk assessment and management, structural damage indictors, methods of retrofitting in general and fibre reinforced polymers in particular etc.

2.2 Seismicity of Islamabad

Pakistan is mostly experiencing compressional and transpressional forces. The compressional forces are believed to be a result of the ongoing collision of the Eurasian and Indo- Pak continental plates that result in the formation of the Himalayan ranges. The Indo-Pak plate, relative to the Eurasian plate is still moving northwards at a rate of about 3.7 cm/year near 73' longitude east (Molnar & Tapponier, 1975). The major portion of this convergence was taken up by deformation along the northern collision boundary involving folding and thrusting of the upper crustal layers in the shape of MKT (Main Karakoram Thrust), MMT (Main Mantle Thrust), MBT (Main Boundary Thrust) and SRT (Salt Range Thrust). In the NW

Himalayan Fold and Thrust Belt, the areas of Kohat and Potwar plateaus have been interpreted to be a result of transpression (Monalisa, Khwaja, & Javed, 2004). In the east, separating the fold belt from the central Himalayas fold belt of India is the N-S trending complex tectonic zone called the Hazara-Kashmir Syntaxis. Many thrust faults occur along the syntaxial loop, which on the western side terminate into the strike-slip Jhelum fault, whereas in the north they continue into the Nanga Parbat-Hararnosh region. Islamabad is located on the western side of the Hazara-Kashmir Syntaxis. On the east of the axis, the geological features show predominantly northwest trend while their trend changes to northeast towards the west of the axis.

The city of Islamabad is situated in the Potwar plateau, which is an area between Main Boundary Thrust (MBT) and Salt Range Thrust. In the north, Margalla and Hazara ranges while in the west, mountainous region of Kalachitta ranges covers the area. The southward portion encompasses the Salt range. The area contains a series of thrusts. General trend of these thrusts changes from E-W to northeast direction in the eastern part of the Potwar Plateau. Two seismically active faults i.e. MBT in the north and Riwat Fault in the' south of Islamabad are passing nearby, indicating that the study area is located within the seismically active environment. The Riwat thrust trending in the NE-SW direction lies about 20 km south of Islamabad. (Jadoon, Khwaja, & Jamshed, Thrust Geometries and Evolution of the Eastern North Potwar Deformed Zone, Pakistan., 1995) Believe that cessation of movement along the Riwat thrust stopped at about 2.7 Ma. Soan (Dhurnal) back-thrust is another distinctive feature of the Eastern Northern Potwar Deformed Zone. It occurs on the northern limb of the Soan Syncline immediately south of Islamabad. The MBT itself is represented by many high angle thrusts along which Eocene and older rocks have been thrusted over the molasses of the Potwar plateau. The Soan (Dhurnal) back-thrust is a passive back thrust and the area bounded by it and the Khair-i-

Murat Fault is a triangle zone of complex geology (Jadoon, Frisch, Jaswal, & Kemal, 1999).

On the basis of research five tectonic features i.e. MBT (Main Boundary Thrust), Nathiagali Thrust, Thandiani Thrust, Sangargali Thrust and Riwat Thrust having peak horizontal accelerations of 0.44g, 0.23g, 0.18g, 0.17g and 0.13g and maximum potential magnitudes of 7.8, 7, 6.8, 6.9 and 6.8 respectively have been designated as most hazardous to site of Islamabad. (Monalisa, Khwaja, & Javed, 2004).

2.4 Structural Damage Indicators

A large number of damage indicating parameters exist which have been broadly classified as follows by (Timchenko, 2002).

2.4.1 Dynamic parameters of the structure

The most widely used analytical damage indicators using the dynamic parameters of the structure are discussed below.

2.4.1.1 Maximum Softening

DiPasquale and Cakmak (1989) developed a damage index based on the evolution of the natural period of a time-varying linear system equivalent to the actual non-linear system. This global damage index depends on a combined effect of stiffness degradation and plastic deformation (Ghobarah, 1999). Although it is a global index, the complexity in the calculation of the maximum period as well as the fact that it does not account for the dissipated hysteretic energy and strength deterioration are its main disadvantages.

2.4.1.2 Final Softening

In the same paper, DiPasquale and Cakmak (1989) utilised the concept of the final softening as a damage indicator. They used the change in the fundamental period of the structure as a measure of the change in the stiffness caused by the earthquake. The advantage of final softening method is that it can be evaluated from the initial natural period and the final

period determined from vibration field-testing after the earthquake. On the other hand, it does not provide any information about local and storey damage. The period calculation at the final time step of the excitation may be affected by the randomness of the instantaneous tangent stiffness at the end of the dynamic load (Ghobarah, 1999). Nevertheless, it is a reliable method for rapid field assessment.

The proposition that damage is related to the increase in period (or decrease in frequency) was recently verified by using experimental data. Calvi *et al.* (2006) concluded from results of experimental tests on RC frames that *a significant period elongation occurs during strong ground motion and this can be attributed to the accumulation of damage in the structure.*

2.4.1.3 Stiffness Index

A more recent approach, using the dynamic parameters of the building for seismic damage evaluation, was conducted by Ghobarah *et al.* (1999) and resulted in a global stiffness index. Ghobarah *et al.* (1999) proposed a methodology in which two nonlinear static analyses are conducted before and after subjecting the structure to an earthquake. The earthquake is applied with the use of time-history analysis. The stiffness damage index $(DI)_K$ of the whole structure is calculated as shown in equation 2.1.

$$(DI)k = 1 - (^{Kfinal}/_{Kinitial}) \quad (2.1)$$

Where:

K initial is the initial slope of the base shear-top deflection relationship resulting from the pushover analysis before the time-history analysis and K final is the initial slope of the same relationship after the time-history analysis.

2.4.2 Displacement parameters

Displacement parameters are the most commonly used for vulnerability assessment purposes since they can easily be obtained analytically. In addition, it is generally accepted (Priestley, Displacement-based seismic

assessment for reinforced concrete buildigns, 1997), that displacement parameters such as drift and ductility simulate better the structural response in the inelastic range. (Priestley, Myths and Fallacies in Earthquake Engineering - Conflicts between Design and Reality, 1993) argued that seismic damage is related to material strains, which are related to maximum response displacements rather than accelerations.

Ductility Ratio (DR): Ductility ratio is defined as the ratio of maximum deformation to yield deformation. As a DI it can be shown to be unsatisfactory, especially when shear distortion in joints and bar pull-out are anticipated. Additionally the ductility ratio fails to take into account the damage induced by repeated loading cycles of inelastic action leading to the underestimation of cumulative damage. It is commonly assumed that failure occurs when the ductility demand exceeds the structural ductility capacity.

Inter-Storey Drift (ISD): It is defined as the maximum relative displacement between two storeys, normalized to the storey height. It was chosen as a damage indicator for structural and non-structural damage by (Rossetto & Elnashai, 2003). An initial attempt was conducted by (Culver, 1975) to estimate the threshold ISD values at different levels of damage using results from damaged buildings. It was suggested that a value of inter-storey drift equal to h/100 corresponds to damage to non-structural components, while h/25 corresponds to severe structural damage or collapse. (Napetvaridze, 1985) concluded that the threshold values of inter-storey drift for a variety of building types i.e. moderate damage on RC buildings at IDS= h/250. (Elenas & Meskouris, 2001) suggested the values of ISD=h/200 for low damage, h/83 for medium and h/58 for great damage.

2.4.3 Displacement and cumulative damage

Damage models were also developed to take both energy dissipation and peak displacement into account. The most popular DI of this category was derived by Park and Ang (1985). The ductility level at each displacement

increment is superimposed on the hysteretic energy dissipated in the structure up to the specific displacement. The calibration of this DI is rather demanding since laboratory or field data are required to calibrate its constant and, as with most of the cumulative damage indices, depends strongly on the hysteretic model of the elements.

However the model is based on the following two controversial assumptions,

- The contribution to damage of the extreme deformation and the dissipated energy can be superimposed linearly
- The related evolution in time of these components can be disregarded.

In addition, it has been suggested by Kappos and Xenos (1996) that, in general, cumulative indices are dominated by the ductility term and are only marginally affected by the energy term.

2.5 Joints

Joints are the most vulnerable part of reinforced concrete moment-resisting frames and can be subjected to large forces and deformations under earthquake loadings. In addition, their behaviour has a significant influence on the response of the structure as serious joint damage can severely threaten the integrity of the whole structure.

Joints have limited carrying capacity due to the strength limitations of beams and columns constituent materials. Deterioration in the joints due to a loss in strength or stiffness can lead to a substantial increase in lateral displacements of the frame, including possible instability due to P-delta effects. Repairing damaged joints is difficult, and so damage must be avoided by proper design which requires an adequate understanding of joints behaviour and failure mechanisms (Murty, 2003) and (Naeim, 2001).

2.5.1 Type of Joints

In RC buildings, portions of columns that are common to beams at their intersections are called beam-to-column joints (Murty, 2003).Three types of

joints in a moment resisting frame can be identified; interior joint, exterior joint and corner joint. When two beams are framed into a column on adjacent vertical sides, it forms a corner joint; when three beams frame into a column on three of its vertical sides, an exterior joint is formed (Uma & Parsad, 2004).

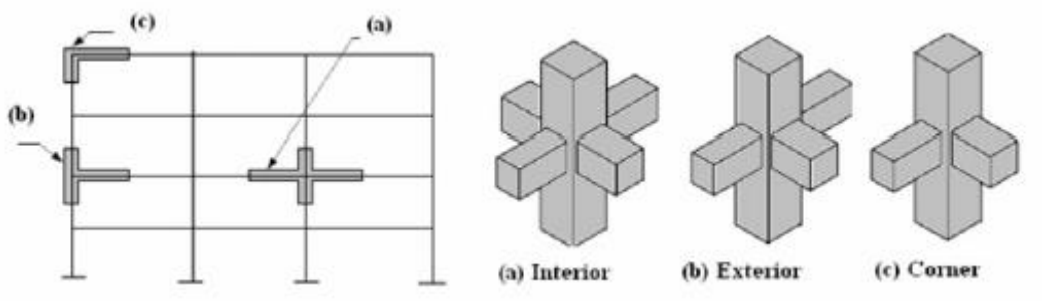

Figure 2. 1 Types of Joints

2.5.2 Modes of Failure

Energy dissipation is a very important concept especially when it comes to seismic design. As previously mentioned, the seismic design aims to provide a favourable failure mechanism. One of the most favourable failure mechanisms, in the case of reinforced concrete frames, is the formation of plastic hinges at beams in beam-column joints. The common name for this mode of failure is strong column-weak beam which can be achieved by the fulfilment of the capacity design method. According to (Eurocode 8, 2004), the strong column-weak beam design concept ensures that the formation of plastic hinges and energy dissipation mechanism take place in the beams at their ends. In the same matter, beams are expected to develop flexural over-strength beyond the design strength. When columns are the case, adequate strength should be provided so that the selected mechanism can be maintained. Proper detailing of the plastic hinge regions is very important in order to provide high ductility to the member, consequently to the structure which will limit the possibility of a total failure (collapse) during large seismic actions.

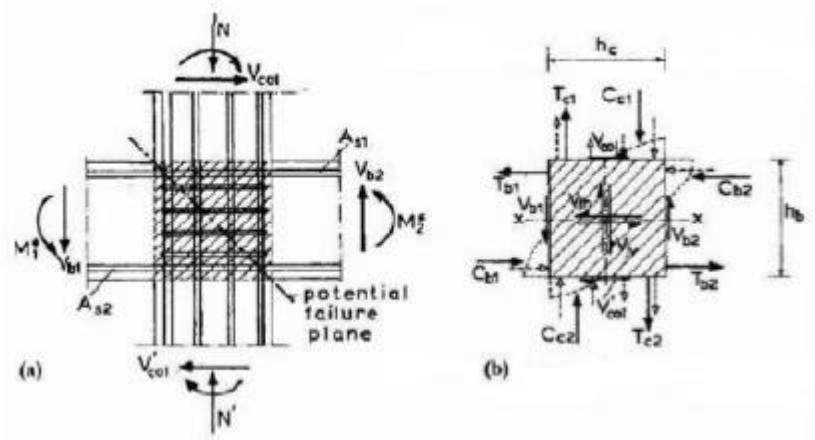

Figure 2. 2 Beam Column Joints subjected to earthquake

One of the most undesirable modes of joints failure is when plastic hinges develop in columns instead of beams. This is another fundamental rule of the capacity design method as plastic hinge formation in columns of RC buildings should be avoided. On the other hand, if for some reason plastic hinges are allowed to form in columns, the inelastic rotational demands imposed are very high that it is very difficult to be catered with any possible detailing. The mechanism with such a feature is called according to (Eurocode 8, 2004) strong beam-weak column mechanism or storey mechanism (Penelis and Kappos, 1997) and (Uma and Prasad, 2004).

Spalling of concrete cover at the faces of the joint is another possible mode of joints failure. The importance about spalling is that it leads to a major reduction sometimes of both the strength and the bearing capacity of the column. The severity of the reduction level depends upon the extent of the affected area (Penelis and Kappos, 1997).

Another type of joints failure is when the anchorage of beams longitudinal bars passing through the joint take place. The main effect of this failure is strength deterioration and significant permanent deformations. As a result, additional effects come out, as local rotations at the beam-column interface which cause severe reduction of the stiffness (Penelis and Kappos, 1997).

The development of tension forces at one boundary and compression forces at the other boundary of the joint has the potential to transfer a significant amount of force to the joint through bond along its perimeter. Therefore, it is important to realize that either of these two modes of forces application can develop what would be recognized as joint shear. Any corresponding failure to resist these applications of forces may be recognized as joint shear failure. This is the case when the joint fails to sustain diagonal tension or diagonal compression strut in joint core due to shear (CEB 231, 1996), and leads to strength and stiffness degradation.

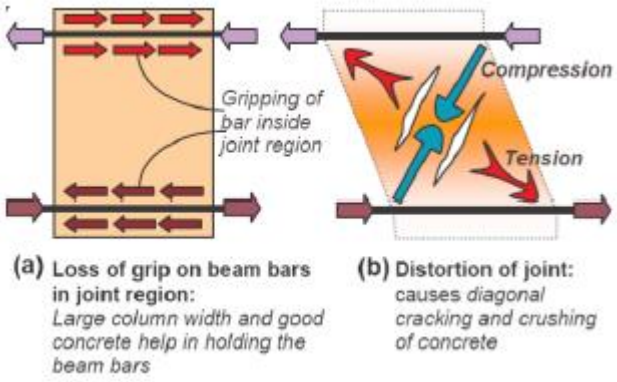

Figure 2. 3 Forces in Joints

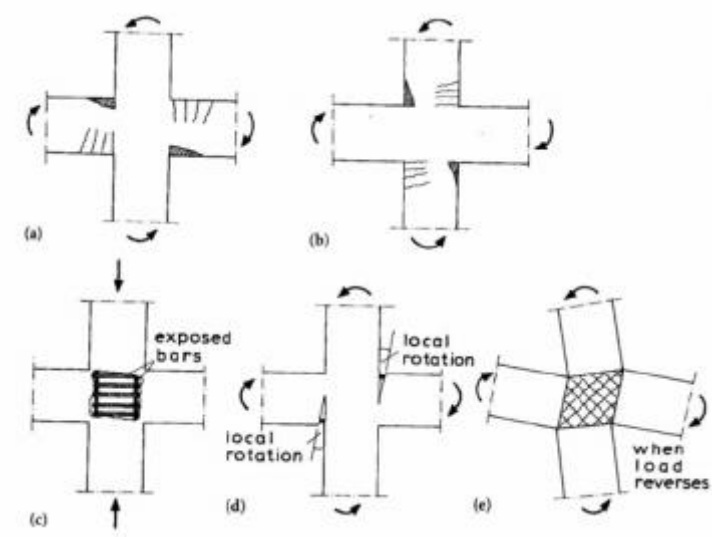

Figure 2. 4 Modes of failure

2.9 Fibre Reinforced Polymers (FRP)

Fibre reinforced polymers (FRP) is a composite material that consists of fibres imbedded in resin matrix. Fibres are usually carbon, glass, basalt or aramid fibres and resins are generally epoxy, polyester and vinyl ester. They can be 10 times as strong as mild steel but quarter as heavy and are noncorrosive. FRP have been in use in numerous other industries such as aerospace and automobiles but it was about only two decades ago that engineers found their use in construction industry due to its potential for application not only in retrofitting building but also in constructing new structures. With the constant price fall over the past few years and also the need to maintain and upgrade structures FRP composites have found their increasing wide application in the construction industry over the past few years. (Teng, 2002)

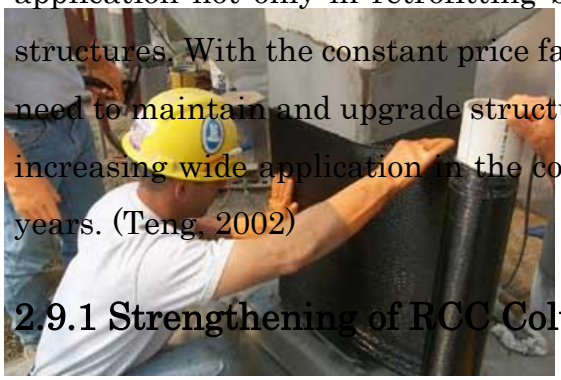

2.9.1 Strengthening of RCC Columns with FRP

As compared to other uses in construction industry the use of FRP in strengthening of RC- structures has been the most common due to their high strength to weight ratio, ease of installation and excellent corrosion resistance.

Within this domain, a very popular use of FRP is to provide confinement to RC columns to enhance their load carrying capability and ductility. This method of strengthening is based on the concept that axial compressive strength and ultimate strain can be improved by providing lateral confinement. RC columns are strengthened by using FRP for generally two purposes: i) to increase axial load capacity for better performance of column under static load such as increase in dead load or live load; ii) To increase the ductility if column for better performance under seismic loads.

In-situ FRP wrapping is the most common method used to confine RC structures in which fibres are impregnated with resins and wrapped continuously or discretely around column in wet layup process with main

fibres oriented in the hoop direction. This technique is most effective in circular columns; in case of rectangular columns sharp edges need to be rounded or their shape is modified. For example a rectangular section may be modified into elliptical section before jacketing (Teng, 2002). Figure 2.14 shows the installation of FRP wraps on columns and Figure 2.15 shows shape modification of rectangular column.

Figure 2. 5 Installation of FRP wraps on square and circular columns (Bank, 2006)

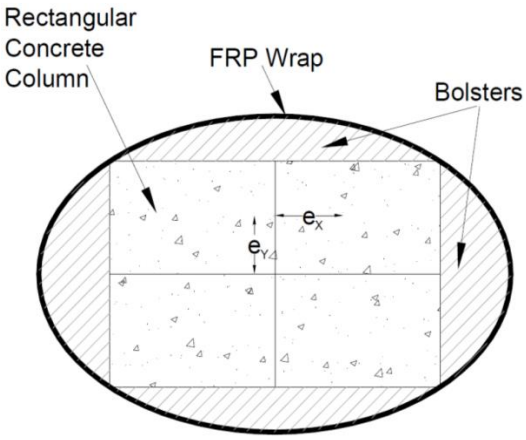

Figure 2. 6 Shape modification of rectangular column with bolsters to increase FRP confinement effectiveness (Brighton & Parvin, 2014)

2.9.2 Confining Action of FRP Jacket

Lateral confinement provided by FRP to concrete is passive in nature. When concrete is subjected to axial compression it expands laterally. This expansion is confined by FRP jacket which is loaded in tension is hoop

direction. Different from steel confined concrete in which lateral confinement pressure is following yielding of steel, Confining pressure by FRP increases as lateral strain increases because FRP does not yield. The confining action of FRP wrapped concrete is shown in Figure 2.16.

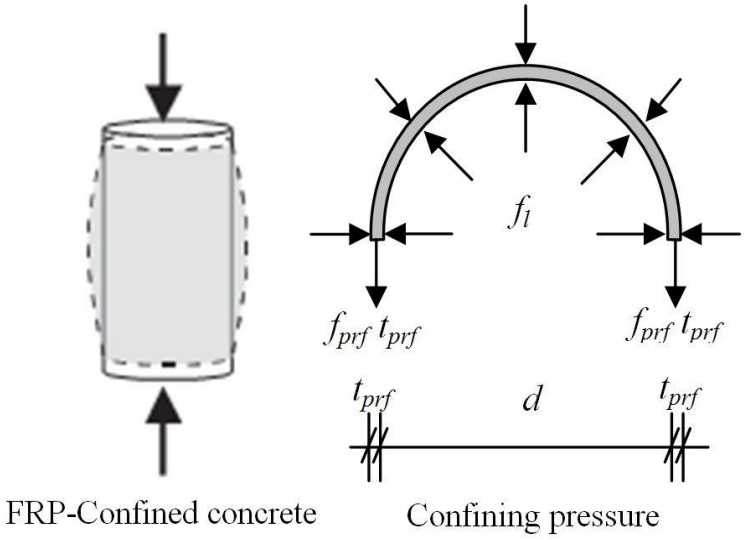

Figure 2. 7 Confining action in FRP-Confined concrete (Benzaid & Mesbah, 2013)

The lateral confining action pressure acting in the concrete core σ_l is given by

$$\sigma_l = \frac{2\sigma_h t}{D} \tag{2.3}$$

Where, σ_h is stress in FRP hoop direction, t is the thickness of the FRP jacket and D is the diameter of the confined core. If the FRP is loaded in hoop tension only, then the hoop stress in the FRP jacket σ_h is proportional to the hoop strain ε_h due to linearity of FRP and is given by

$$\sigma_h = E_{frp}\varepsilon_h \tag{2.4}$$

Where, E_{frp} is the elastic modulus of FRP in the hoop direction.

The lateral confining pressure at rupture reaches its maximum value f_l with

$$f_l = \frac{2\sigma_{h,rup}t}{D} = \frac{2E_{frp}\varepsilon_{h,rup}t}{D} \quad (2.5)$$

Where; $\sigma_{h,rup}$ and $\varepsilon_{h,rup}$ are the hoop stress and strain of FRP at rupture respectively.

2.9.3 Dilation Properties

Under axial compression unconfined concrete experiences volumetric compaction up to 90% of the peak stress (Jiang & Teng, 2007). Therefore concrete shows unstable volumetric dilation due to rapidly increasing lateral to axial strain ratio. This dilation could be effectively contained by confining concrete using FRP. Due to radial displacement compatibility, the lateral dilation results in continuously increasing lateral confining pressure provided by FRP which gradually reduces the rate of lateral dilation itself. The dilation properties of FRP-confined concrete depend both on force equilibrium and geometric compatibility.

The secant dilation ratio μ_s is commonly used to characterize the dilation properties. μ_s Is defined as the absolute value of the secant slope of the lateral to axial strain curve of FRP-confined concrete and is given as

$$\mu_s = \left|\frac{\varepsilon_l}{\varepsilon_c}\right| \quad (2.6)$$

Where, $\varepsilon_l$and ε_c are lateral strain and axial strain of concrete respectively. It should be noted that their magnitude is equal in case of circular section.

Typical experimental secant dilation ratio-axial strain curve is shown in Figure 2.17. It is noted that at the initial stage, the secant dilation ratio is equal to the Poisson's ratio and then it increase as the concrete core dilates. The confining action is activated after the compressive strength of unconfined concrete is reached. As a result, the secant dilation ratio decreases due to the increasing confining pressure.

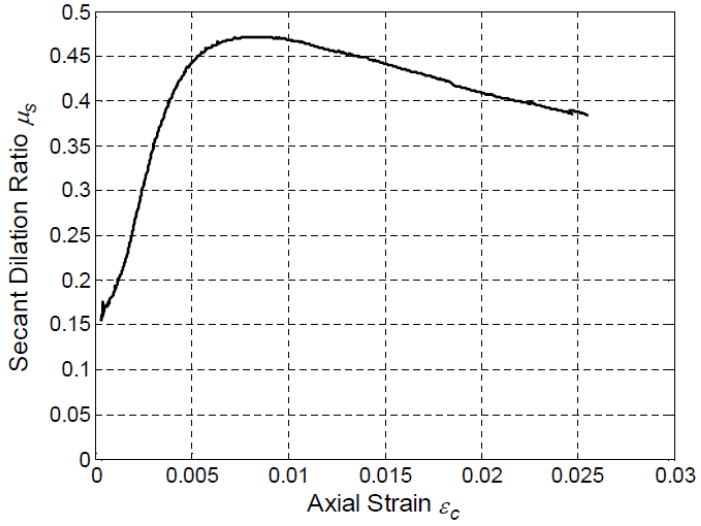

Figure 2. 8 Typical secant dilation-ratio curve (Jiang T., 2008)

2.9.4 Ultimate Condition

The ultimate conditions of FRP wrapped concrete refers to its compressive strength and ultimate axial strain. The ultimate conditions are dependent on the confining pressure provided by the FRP jacket when it ruptures. Initially it was assumed that the confining pressure is equal to the tensile strength of the same FRP material (Samaan, Mirmiran, & Shahawy, 1998). However lateral experimental results suggested that the material tensile strength of FRP cannot be reached in FRP-confined concrete as the hoop rupture strains of FRP measured in compression tests have been found to be considerably smaller than those obtained from material tests (Xiao & Wu, 2000). The ratio of the FRP rupture strain to the ultimate tensile strain is an important for the stress-strain model. Serval possible causes that may result in this phenomenon have been proposed, including the non-uniform deformation of concrete, local misalignment and waviness of fibres, residual strain and multi axial stress state effect of curvature of FRP jacket, and existence of overlapping zone. (Lorenzis & Tepfers, 2003). Lam and Teng were the first one to carry out carefully designed test to investigate these possible issues (Lam & Teng, 2004).

2.9.5 Stress-Strain Curve

It has become well-known after extensive experimental work that the stress-strain curve of FRP-confined concrete features a monotonically ascending bi linear curve with sharp softening in transition zone around the stress level of unconfined concrete strength if the amount of FRP exceeds a certain threshold value as shown in Figure 2.18(a). This type of curve was obtained in the vast majority of test results. With this type of curve both the compressive strength and ultimate axial strain are reached simultaneously and significantly enhanced as compared to unconfined concrete. However recently it has been found that in some cases bilinear curve cannot be expected (Xiao & Wu, 2000) instead it features a post peak descending branch and the compressive strength is reached before the tensile rupture of FRP jacket (descending type). This type of stress strain curve may end up at the stress value either smaller or larger than the compressive strength of unconfined concrete as shown in Figure 2.18(b) and (c).

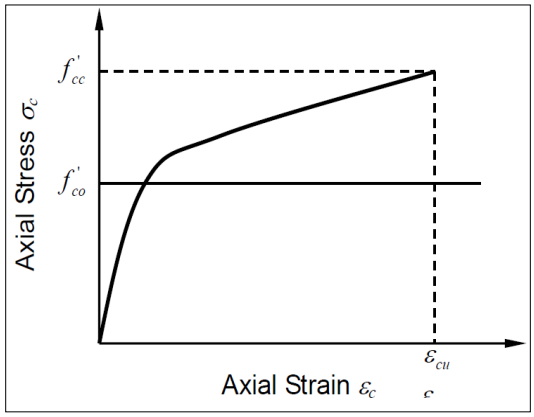

(a) Ascending Type

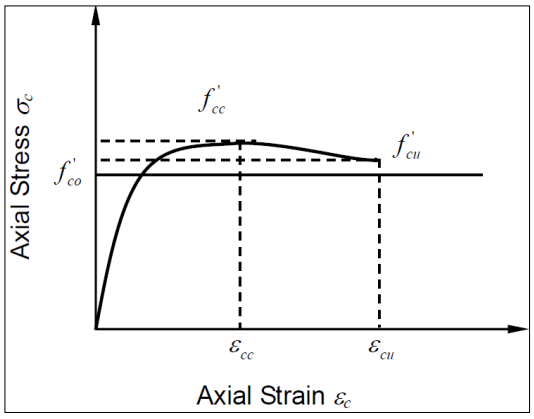

(b) Descending Type with $f'_{cu} \geq f'_{co}$

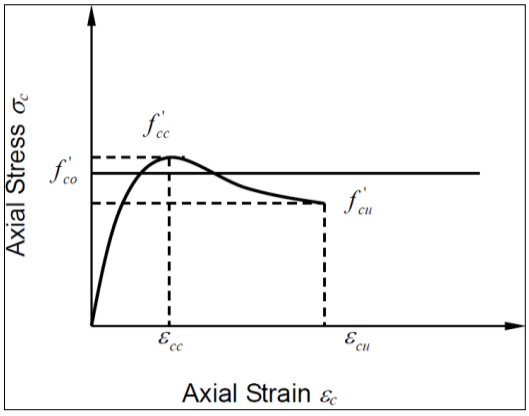

(c) Descending Type with $f'_{cu} < f'_{co}$

Figure 2. 9 Classification of stress-strain curves of FRP-confined concrete. (Jiang & Teng, 2007)

2.9.6 FRP Confined Concrete in Rectangular Columns

The effect of FRP confinement in rectangular column has been a topic of interest over the past few years. It is a well-known fact now that FRP confinement is less effective in rectangular column due to non-uniformity of confinement as shown in Figure 2.19. To enhance the confinement effect the sharp corners of rectangular columns should be rounded before wrapping as shown in Figure 2.20. However, due to existence of internal reinforcement the radius of the corner is limited in practical application.

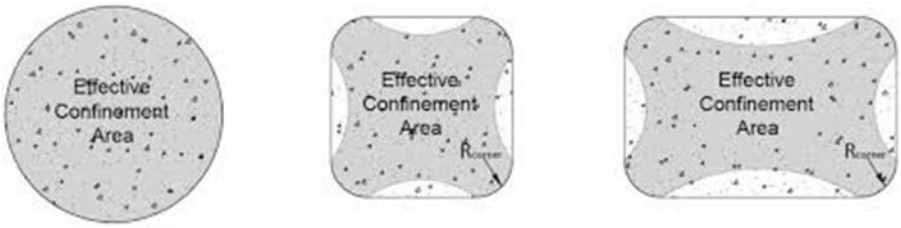

Figure 2. 10 Comparison of FRP-confinement in circular, square and rectangular columns. (Brighton & Parvin, 2014)

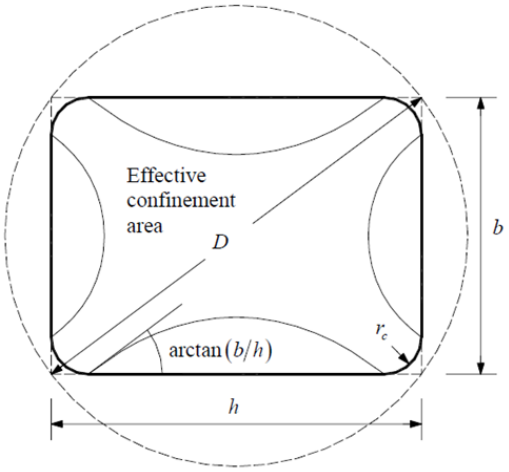

Figure 2. 11 Model for FRP-confined concrete in rectangular columns. (Jiang & Teng, 2007)

2.9.7 Failure in FRP-wrapped Rectangular Columns

A significant number of experimental studies have been carried out on FRP-confined rectangular columns. Failure was generally observed to occur at the corners by FRP tensile rupture. The key parameters that effect failure are the amount of confinement, the radius of rounded corners, and the aspect ratio of the cross section (ratio of the longer side to the shorter side of the cross section) (Lam & Teng, 2004). The test results showed that the effectiveness of confinement increases as the amount of FRP or the corner radius increases and the aspect ratio decreases (Jiang T. , 2008).

2.9.8 Size Effect

Vast majority of experimental tests were conducted on small scale specimens; the actual effect of confinement on actual size columns is still unclear. Recently some studies have been done on large-scale columns; these studies indicated that the behaviour of realistically sized circular columns could be reasonably well extrapolated from small scale specimens. (Youssef, Feng, & Mosallam, 2007). In case of rectangular columns it is difficult to identify size effect because of the large scatter of test results

(Rocca, Galati, & Nanni., 2006). Therefore, the size effect in rectangular columns is still unclarified.

2.9.9 Stress Strain Models

A significant number of stress-strain models for FRP-confined concrete have been proposed. These models can be classified into two basic categories (a) design-oriented models (b) analysis oriented models. (Lam & Teng, 2004). Design oriented models generally comprise of a closed-form stress-strain equation and ultimate condition equation directly derived from the interpolation of experimental results. The accuracy of these models depends on the definition of the ultimate condition of FRP-confined concrete (Jiang T. , 2008). In case of analysis oriented models the stress strain curves of FRP-confined concrete are generated using an incremental numerical procedure which accounts for the interaction between the FRP jacket and the concrete core. The accuracy of these models depends on the modelling of the lateral-to-axial strain relationship of FRP-confined concrete (Jiang T. , 2008).

2.9.10 Examples of Stress Strain Models

2.9.10.1 Analysis Oriented Models

(Mirmiran & Shahawy, 1997), (Harajli, Hantouche, & Soudki, 2006), (Harmon, Ramakrishnan, & Wang, 1998), (Spoelstra & Monti, 1999), (Fam & Rizkalla, 2001), (Chun & Park, 2002), (Becque, Patnaik, & Rizkalla, 2003), (Harries & Kharel, 2002), (Marques, Marques, Lins da Silva, & Cavalcante, 2004), (Binici, 2005), (Jiang & Teng, 2007)

2.9.10.2 Design Oriented Models

(Fardis & Khalili, 1982), (Karbhari & Gao., 1997), (Samaan, Mirmiran, & Shahawy, 1998), (MIYAUCHI, INOUE, KURODA, & KOBAYASHI, 1999), (Saafi, Toutanji, & Li., 1999), (Lillistone & Jolly, 2000), (Xiao & Wu, 2000), (Lam & Teng, 2003 (a)), (Berthet, Ferrier, & Hamelin., 2006), (Harajli, Hantouche, & Soudki, 2006), (Saenz & Pantelides, 2007), (Wu, 2007), (Youssef, Feng, & Mosallam, 2007)

(Fardis & Khalili, 1982)

Fardis and Khalili were the first one to consider the effect of confinement in FRP-wrapped cylinders. They conducted compressive strength test on a sum of 46 specimens. Two different types of concrete cylinders were used (75×150 mm for compressive strength of 34.5 MPa and 100×200 mm of compressive strength 31 MPa). Concrete cylinders were confined with four kinds of GFRP with the number of FRP layers varying from 1 to 5. It was proposed that the tri-axial failure criterion suggested by Richart *et al.* (1929) (Equation 2.7) and by Newman (1971) (Equation 2.8) both can give satisfactory approximation for the ultimate strength of concrete confined by FRP.

$$f'_{cc} = f'_{co}\left(1 + k_1 \frac{f_l}{f'_{co}}\right) \tag{2.7}$$

Where, f'_{cc} is compressive strength of FRP-confined concrete, f'_{co} is strength of unconfined concrete and $k_1$is the confinement effectiveness factor. Richart *et al.* (1929) recommended using $k_1 = 4.1$

From test results it was proposed that coefficient of confinementk_1, have the following value for FRP-wrapped specimen:

$$k_1 = 3.7\left(\frac{f_l}{f'_{co}}\right)^{-0.14} \tag{2.8}$$

This confinement coefficient yielded the following value for FRP-confined specimen:

$$f'_{cc} = f'_{co}\left(1 + 3.7\left(\frac{f_l}{f'_{co}}\right)^{0.86}\right) \tag{2.9}$$

For the corresponding, axial strain at failure was proposed to be:

$$\varepsilon'_{cc} = \left(0.002 + 0.001\frac{E_{FRP}.n_{FRP}}{D.f'_{co}}\right) \tag{2.10}$$

Where, ε'_{cc} is the longitudinal strain of confined concrete at failure, E_{FRP} is modulus of elasticity of FRP jacket.

They predicted the complete stress-strain response of the FRP-confined concrete in the form of hyperbola. The initial tangent modulus of unconfined concrete was suggested for the initial slope of the confined concrete response.

$$f_c = \frac{E_{co}.\varepsilon_c}{\left(1+\varepsilon_c\left(\frac{f'_{cc}}{E_{co}}-\frac{1}{\varepsilon_{c\,max}}\right)\right)} \quad (2.11)$$

Where, E_{co} is the initial tangent modulus of unconfined concrete.

Shortcomings Model has no validity for large scale columns, due to the following reasons:

- It was calibrated using limited test data, also size effect is unknown.
- It was calibrated using Normal Strength Concrete so its validity on high strength concrete is required.

(Lam & Teng, 2003 (a))

A constitutive model was proposed for FRP-confined concrete based on a bilinear stress-strain curve. Parabolic first portion and a straight-line second portion were used to describe the complete response as shown in Figure 2.21.The following equations governed the plot:

$$f_o = E_c\varepsilon_c - \frac{(\varepsilon_c - E_c)^2}{4\,f_{oc}}\varepsilon_c{}^2 \text{ , for } 0 < \varepsilon_c < \varepsilon_o \text{ (parabolic first portion)} \quad (2.12)$$

$$f_o = f_{oc} + E_2\varepsilon_c \text{ , for } \varepsilon_o \leq \varepsilon_c \leq \varepsilon_{cmax} \text{ (linear second portion)} \quad (2.13)$$

Where f_{oc} was said to be independent of confinement ratio and was set to bef'_{co}, elastic modulus of unconfined concrete was calculated to be $E_c = 4730\sqrt{f'_c}$, ε_o is the axial strain at which parabolic portion meets the linear.

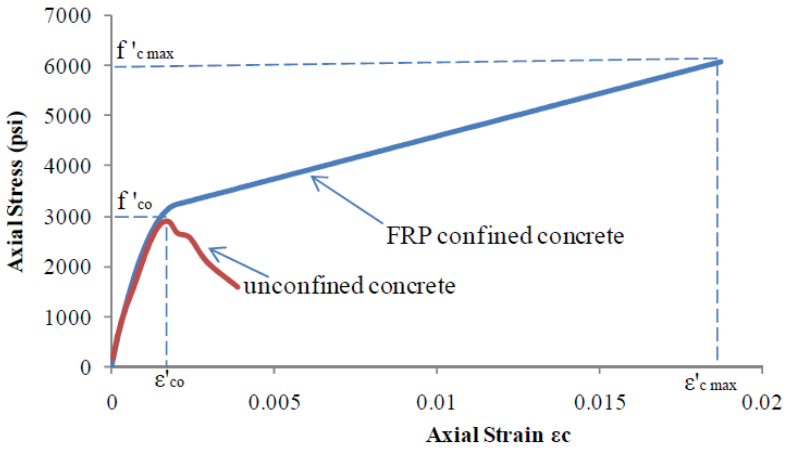

Figure 2. 12 Axial stress-strain curve of FRP-confined concrete (Lam & Teng, 2003 (a))

$$\varepsilon_o = \frac{2f_{oc}}{E_2 - E_c} \tag{2.14}$$

The slope of linear portion was computed as

$$E_2 = \frac{f_{cc}' - f_o}{\varepsilon_{cu}} \tag{2.15}$$

For the peak confined concrete stress $f_{c\,max}'$ and $\varepsilon_{c\,max}'$ the following expression was proposed:

$$\frac{f_{cc}'}{f_{co}'} = 1 + 3.3\frac{f_{l,a}}{f_{co}'} \tag{2.16}$$

Where $f_{l,a}$the actual confining pressure is given by:

$$f_{l,a} = \frac{2E_{frp}t\varepsilon_{H.rup}}{d} \tag{2.17}$$

Where, E_{frp} is the modulus of elasticity of FRP, t is the thickness of wrap, d is the diameter of concrete specimen and $\varepsilon_{H.rup}$ is the hoop rupture strain of FRP. (Lam & Teng, 2003 (a)) Proposed the ratio of actual hoop rupture strain $\varepsilon_{H.rup}$ and hoop rupture strain ε_{frp}, to be 0.586 for convinience in applying the equation of actual confining pressure and also the ultimate strain, which is given by:

$$\frac{\varepsilon_{cu}}{\varepsilon_{co}} = 1.75 + 5.53\left(\frac{f_{l,a}}{f_{co}'}\right)\left(\frac{\varepsilon_{frp}}{\varepsilon_{co}}\right)^{0.45} \quad (2.18)$$

This model is workable for normal strength concrete. As both peak strain and stress were related with measured rupture strain of the FRP jacket, the workable rupture strain of FRP jacket needs to be carefully calculated.

2.9.10.3 Models for Rectangular Columns

Stress strain models of circular columns are not directly applicable to rectangular columns because of non-uniform confinement in rectangular section as discussed before. Various models have been presented, most of which are design oriented aiming to predict the average stress strain curve. Many researchers have extended their circular stress-strain models to rectangular considering the effect of non-uniformity. Some examples are (Lam & Teng, 2003 (b)), (Harajli, Hantouche, & Soudki, 2006), (Wu, 2007), & (Youssef, Feng, & Mosallam, 2007). Lam & Teng, 2003 (b) model is discussed over here in detail to illustrate the commonly accepted approach.

(Lam & Teng, 2003 (b))

This model is an extension of (Lam & Teng, 2003 (a)) for FRP-confined concrete in circular column. Two new parameters were introduced, shape factor and equivalent diameter. The stress-strain equations become

$$\frac{f_{cc}'}{f_{co}'} = 1 + k_{s1}3.3\frac{f_{l,a}}{f_{co}'} \quad (2.19)$$

$$\frac{\varepsilon_{cu}}{\varepsilon_{co}} = 1.75 + k_{s2}12\left(\frac{f_{l,a}}{f_{co}'}\right)\left(\frac{\varepsilon_{frp}}{\varepsilon_{co}}\right)^{0.45} \quad (2.20)$$

Where k_{s1} and k_{s2} are shape factors for stress and strain respectively and are calculated as:

$$k_{s1} = \left(\frac{b}{h}\right)^{\alpha}\left(\frac{A_e}{A_c}\right) \quad (2.21)$$

$$k_{s2} = \left(\frac{h}{b}\right)^{\beta}\left(\frac{A_e}{A_c}\right) \quad (2.22)$$

Where, b and h are cross-sectional dimensions of column and α and ß were found to be 2 and 0.5.

This model has been confirmed to give accurate results when used for normal strength concrete.

CHAPTER 3

ANALYTICAL TOOL: Drain 3DX

To find out structural response and to develop the analytical vulnerability curves, an analytical tool is required. This tool needs to be verified first with experimental results to be used in risk assessment procedures. Therefore, it depends on the use and selection of suitable analytical tool and suitable element models in order to assess and verify their capability against experimental data obtained from full-scale seismic tests.

3.1 Background

After the development of capacity-spectrum method in the mid-1970s (Freeman, 1978) static nonlinear analysis has become the main alternative for performance evaluation purposes since it provides a simple and effective alternative to complicated non-linear time-history analysis. (Kyriakides, 2007). It compares the nonlinear capacity of the structure with the reduced force-based demand from a seismic event to evaluate the performance of the structure for the particular event.

The most significant parameter for the accurate simulation of the nonlinear seismic behaviour of RC frames is the modelling of the structural elements. It is necessary to select element models that can simulate any possible damage potential. Possible damage on RC frames includes:

- Cracking of concrete in tension.
- Local buckling of the reinforcement.
- Plastic hinge formation through yielding of reinforcement.
- Slip of the reinforcement due to excessive bond deterioration.
- Shear failure due to inadequate shear reinforcement, inadequate spacing of the shear links, diagonal compressive failure, or cumulative deterioration.
- Concrete deterioration and crushing

Realistic RC modelling should cover flexural, shear and bond failures in members and joints.

In most frame analysis tools non-linearity is added to the element through finite hinges at the element ends with lumped plasticity moment-rotation models that accounts for the:

- formation of plastic hinges at member ends
- dissipation of energy in the hinges
- ductility of the members

A possible approach for determining element behaviour is to utilize resistance models for each potential failure type.

3.2 Resistance models

3.2.1 Flexure

To increase the accuracy of flexural behaviour modelling a multi-section (fibre) analysis element which enables distributed plasticity needs to be introduced. The element should be able to produce the moment-curvature envelopes and interaction diagrams using only the cross-section details and material properties.

3.2.2 Shear

Most studies treat shear deformations in an elastic manner and assume abrupt shear failure when the shear capacity is reached in members (Dymiotis, 2000). Although this is a conservative assumption, since shear failure may exhibit different post-peak characteristics. In particular, shear failure in joints is a very common failure mode for sub-standard construction. This is due to the fact that in most cases no shear links are placed in the joint region (due to practical reasons), and also due to the fact that in most cases the joint capacity is less than that of the corresponding of the beam.

3.2.3 Bond

The flexural forces from beams and columns cause tension and compression forces in the longitudinal reinforcement passing through the joint. Bond stresses increase as the force in the bar increases up to the yield level. When the longitudinal bars passing through the joint are stressed beyond yielding, de-bonding along the bar can cause the deterioration of bond between steel and concrete. This deterioration may cause slip which can contribute to additional apparent flexural deformations. (Kwak & Filippou, 1990) analysed the deformations on an interior joint and concluded that bond-slip of the reinforcing bars in the joint contributed approximately 33% of the total deformation near the ultimate load. (Sezen, 2002)Also monitored slip deformations on columns and concluded that these contribute between 25-40% of the total lateral displacement. Slip of the reinforcement is only prevented by providing adequate development length and confinement detailing in the lapping regions placed outside the yield penetration zone, which is defined as the length of the reinforcement

3.3 Choice of Analytical Tool

After a wide literature search it was decided to use DRAIN-3DX as it includes local elements with degradation characteristics fulfilling the requirements discussed above. The 3D version is preferred to the 2D since it includes a cyclic shear element (Prakash, Powell, & Campbell, 1994). In addition to having an extensive element library (Powell & Campbell, 1994) and accessible source code it has been widely used for both static and dynamic analyses (Dymiotis, 2000) (Deng C., 2000) (Kyriakides, 2007) etc. and proven to have a reliable solver (good convergence). Its main drawback is that it lacks Graphical User Interface, which makes it difficult to use.

The following paragraphs describe the elements used both for member and joint modelling based on the requirements mentioned above.

3.3.1 Drain-3DX (Flexure)

The element library of DRAIN-3DX includes a section analysis element (element 15), which is used to model the flexural behaviour of beams and columns. This element can have rigid zones (to simulate joints) and deformable regions (Kyriakides, 2007). Within the length of the deformable region the element has distributed plasticity accounting for the spread of the inelastic behaviour both over the cross section and along the member length (Powell & Campbell, 1994). It also accounts for the interaction between axial force and bending in columns (P-M interaction).

A schematic representation of the element is shown in Figure 3.1. Each cross-section comprises of a number of concrete and steel fibres. The location of each fibre depends on a local axis system defined at the beginning of the analysis. The cross-section characteristics are defined by assembling these fibres based on their coordinates and sectional area. The response of each fibre is concentrated at its centre of gravity. The stiffness and strength of the section depends on the number and location of the fibres. The deformable part of the element can be divided into a number of segments. The cross-section properties are assumed to be constant within each segment, but can vary from segment to segment if required. The behaviour is monitored at the midpoint of each segment and accounts for the spread of the inelastic behaviour both over the cross section and along the member length (Powell & Campbell, 1994)

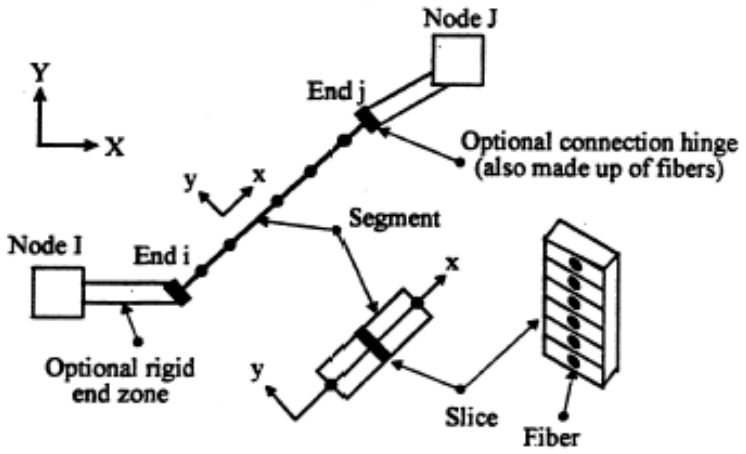

Figure 3. 1 Section analysis element (Prakash, Powell, & Campbell, 1994)

3.3.2 Drain-3DX (Anchorage)

Element 15 is also capable of modelling slip deformations at connection hinges at element ends. (Prakash, Powell, & Campbell, 1994). These connection hinges are defined as fibres having both pull-out and gap characteristics. Pull-out fibres can model slip movement of the reinforcement bars whereas gap fibres are used to account for gap opening of concrete. Therefore, pull-out and gap fibres replace steel and concrete fibres at member ends.

3.3.3 Drain-3D (Shear)

The nonlinear shear behaviour of members and joints can be modelled using element 8 in DRAIN-3DX with the use of shear hinges distributed along the element length. (Kyriakides, 2007). These hinges account for additional elastic and inelastic shear deformations. The inelastic shear model in DRAIN-3DX is used in parallel to a linear elastic model accounting for the elastic flexural deformations prior to the attainment of the shear capacity. The calibration of the model requires the definition of the shear capacity values and the corresponding elastic and post elastic stiffness.

3.4 Capabilities and limitations of DRAIN 3DX

- Linear/ nonlinear static analysis.

- Calculate mode shape or period in initial state or any later state
- Response spectrum analysis.
- Pushover analysis
- Nonlinear dynamic analysis under-ground displacement history
- Nonlinear dynamic analysis under dynamic force
- Nonlinear dynamic analysis for nodal velocities
- The elements are capable of modelling various degradation effects of reinforced concrete element by defining a hinge at its ends.

CHAPTER 4

DATA COLLECTION

4.1 Introduction

In this section the selected buildings for the study has been discussed and the methodology undertaken in selecting these buildings. According to a survey, the reinforced concrete structured buildings are on a continuous rise in Pakistan and currently they count up for almost 15 % of the entire buildings being constructed. Frame construction is also on the rise in Pakistan and in all the major cities across the country, many domestic and commercial building are being constructed using reinforced cement concrete technology. The modern construction practices being used currently in Pakistan including all the major cities are based on frame construction for the purposes of either domestic apartments or commercial utility. The buildings used in this study include frame structure selected from 5 major cities Pakistan and their respective structure and classification has been discussed in this chapter.

4.2 Background

Reinforced concrete buildings are most commonly constructed in the urban areas of Pakistan. However, it is not unusual to see reinforced-concrete structures in the sub-urban cities too, though in the majority of the cases, their use is restricted to commercial purposes (offices, hotels, shopping malls etc.). Major cities of Pakistan have seen rise in the construction of reinforced concrete frame structures in the past two decades. This rise in construction of reinforced-concrete structures can be attributed to the improvement in the economic conditions of the people as well as awareness of the fact that these are a better alternative as compared to traditional unreinforced brick masonry load bearing structures in many aspects, particularly in performance during earthquakes, other reason being the increase in vertical development of cities due to increase in population and

in such cases UMB(Unreinforced Masonry Buildings) can't be used. Also due to population burst in Pakistan in the past couple of decades, the land prices have risen appreciably. This has forced builders to adapt to reinforced concrete structures as residential units in addition to their previous role of accommodating commercial facilities only.

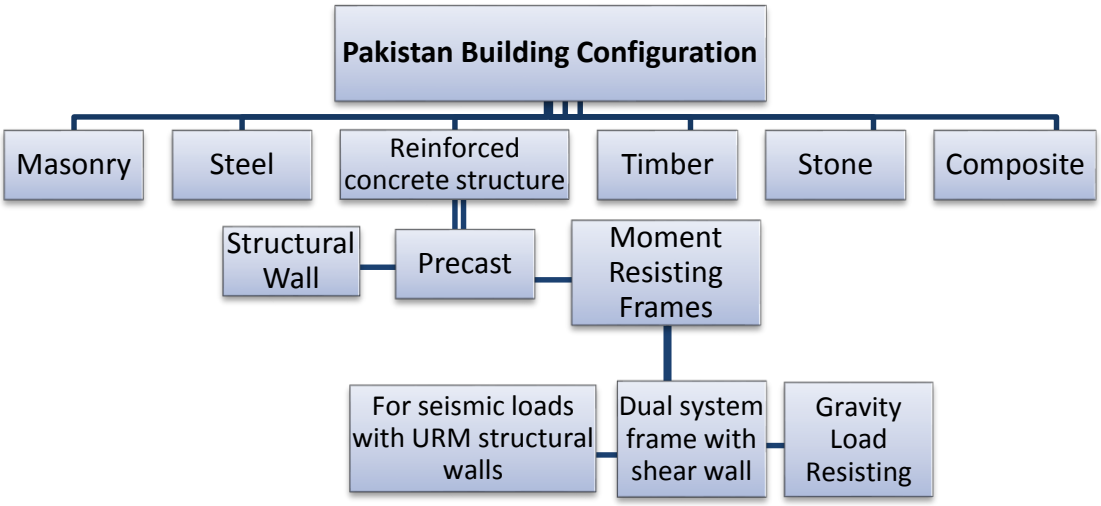

Figure 4. 1 Building Configuration of Pakistan

4.3 Building Configuration & Frame Selection

4.3.1 Building Configuration

In this section, the structural forms of buildings have been highlighted. The frame structures usually are composed of rectangular plan commonly practiced apart from a few aesthetically modified structures including curvatures and irregular geometry. The elevation is also regular usually to aid in symmetrical construction and ease of designing and maintenance. The buildings selected for this study are regular and rectangular with equal bay widths and storey heights to keep uniformity in design and analysis and bringing it close to the real practices in Pakistan.

The most commonly observed plan dimensions of buildings in Pakistan have the following dimensions:

- Length: Ranging between 10 -40 meters

- Width: Ranging between 10-20 meters
- Storey height - Ranging between 3-5 meters
- Number of storeys: Ranging between 3-8

Keeping these dimensions in view, the frames selected for the analysis on the software include the storey height of 3.3 m and bay width as a constant 4.5 m for all frames. These spans are variable as depending upon the area of the building and the utilization. Depending on the location and the type of material available, frames built based on reinforced concrete vary significantly with respect to the number of storeys as in the lesser developed cities the range is from 3 to 8 storeys which fall under the small to medium rise configuration. Moving towards to more developed and technologically active cities the trend prevails of medium rise buildings ranging from 8 and even touching the horizon of high rise buildings of 15 storeys. If the structure is built on naturally stable and firm ground then the storeys may be increased but due to fluctuation of geography within Pakistan, the buildings vary significantly with respect to configuration.

4.3.2 Frame Selection

The selected frames for this study will represent the actual frame network of Pakistan and therefore the collected data has been divided in to sub categories. For ease of analysis, three distinctive categories have been chosen:

1. Low rise
2. Medium rise
3. High rise

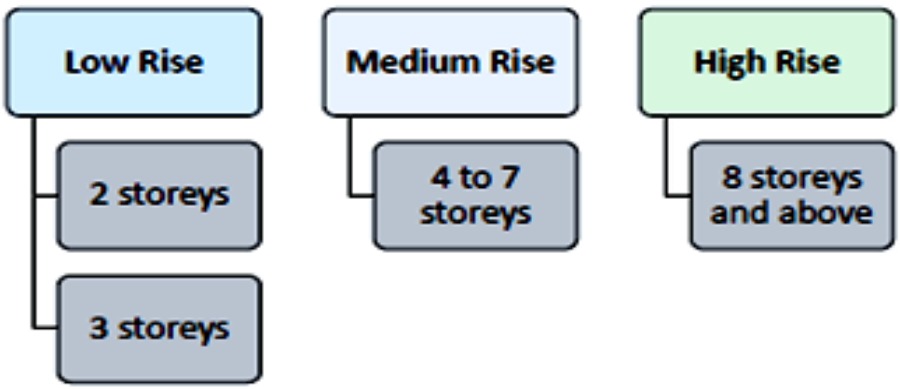

Figure 4. 2 Distribution of Frames

The RCC building stock of Pakistan has been grouped into these categories on basis of their frequency of occurrence and risk of seismic activities. Moreover for each category the frames have been further divided acknowledging for the variations of bays with respect to storeys. This will also assist us in understanding the relationship of bays and storeys to the vulnerability during the analysis phase. The frames chosen for vulnerability assessment will cover all aspects of RCC building utility in Pakistan which prominently includes residential, recreational, commercial and industrial utilities.

4.3.2.1 Low Rise Buildings

This category is the most frequently observed one in Pakistan and currently the most vulnerable one. Mostly in the rural and urban settlements of various cities in Pakistan, low rise buildings are constructed with storey height varying between 2 storeys to 3 storeys and bays may range in between 2 to 5. These buildings are primarily designed on basis of gravity loading without any concentration given to the dynamic loading conditions. The frames included for this category are:

2 storeys & 2 bays (2x2)	**3 storeys & 2 bays (3x2)**
2 storeys & 3 bays (2x3)	**3 storeys & 3 bays (3x3)**
2 storeys & 4 bays (2x4)	**3 storeys & 4 bays (3x4)**
2 storeys & 5 bays (2x5)	**3 storeys & 5 bays (3x5)**

These buildings are utilized for commercial usages mostly ranging from shops to malls and plazas for official utility. Residential apartment buildings in suburbs of Islamabad are usually falling in this category. The design parameters are weak and therefore they often fail to support the fundamental gravity loading and fail in the earlier stages of its lifecycle. Retrofitting these buildings is a fundamental need of time as they cater almost 60-70% of the population which makes them at risk in case of any seismic event.

4.3.2.2 Medium Rise Buildings

The most common range of storeys falls under this category when considering commercial utility in Pakistan. Due to various regulations imposed by the local government within the residential zones, heights are regulated to usually 3 storeys but in commercial zones this limit exceeds from 4 storeys to 7 storeys. Many commercial buildings, offices, public buildings fall under this category and 50% of residential apartments are also beyond 4 storeys high. The frames include in this category are:

4 storeys & 2 bays (4x2)
4 storeys & 3 bays (4x3)
4 storeys & 4 bays (4x4)
4 storeys & 5 bays (4x5)

These buildings are also been designed only for the gravity loads ignoring the effect of any dynamic or lateral loading events. These buildings are also prone to earthquake risks and therefore retrofitting them may reduce their hazard level and make them safer for the inhabitants.

4.3.2.3 High Rise Buildings

The last category covers the high rise building stock of Pakistan, yet in the exploration phase but gaining acknowledgement with a faster pace. These buildings are usually for large corporations, multinational firms, and offices of government or luxury apartments. Some hotels also fall in this category. During the design phase wind loading is usually neglected but in 25% of the designs seismic forces are accounted for. Even though their increasing numbers with the development in construction industry, they are at risk to certain seismic hazards and therefore stand vulnerable.

The frames for this category include:

8 storeys & 3 bays (8x3)
8 storeys & 4 bays (8x4)
8 storeys & 5 bays (8x5)

These buildings are usually considered more significant due to the nature of occupancy being highly crucial therefore retrofitting techniques to cease the risk occurrences and improve their strength is a fundamental focus.

4.4 Material Parameters

To analyse the selected frames certain strength and material parameters are to be incorporated in the analytical tools i.e. DRAIN 3D.To show Pakistan's true RCC building stock the data pertaining to concrete and reinforcement was first to be collected. For this purpose various qualitative and quantitative methods were implemented. Firstly the available data was collected through the work of already carried out projects which include (Uzair Maqbool Khan, 2010) and (Usman, 2010), their works have been utilized for the analysis phase throughout. Moreover survey was conducted in Pakistan cities including Islamabad, Lahore, Peshawar and parts of Kashmir (seismically active zones) and the existing buildings were evaluated. To configure the frames and design their reinforcement and structural plan, this data was sufficient for our analysis. Another researcher (Shahzada, 2011) worked specifically for the vulnerability assessment and the frame network he utilized was also incorporated in deciding the final frame configuration.

To achieve the data relating to the strength of materials used and other material properties, aid was taken from the work of (Usman, 2010) and (Uzair Maqbool Khan, 2010), in which the data was collected using various testing laboratories all over Pakistan. The testing was either carried out commercially through various firms including NESPAK, or through the institutional testing being carried out in National University of Sciences and technology (NUST), Islamabad, University of Engineering and Technology (UET), Peshawar and Lahore. The data was reassessed through and matched with the various results from both the sources and the parameters for modelling the frames were finalized.

The selected parameters which govern the nature of reinforced buildings are:

- Strength of concrete (f'_c)
- Yield strength of Steel (F_y)

4.4.1 Strength of Concrete (f'c')

Concrete plays an important role and forms the bulk constituent in RCC buildings. The compressive strength of concrete holds importance in framing the failure mode of concrete buildings and governing their behaviour under loading. To obtain the compressive strength for the frames of our analysis the data obtained from UET (Peshawar) was rearranged and outliers were removed from the results. Then for the strength, statistical evaluation was carried out and a mean value was evaluated.

The mean value for strength of concrete (f'_c) was 16.5 MPa and this strength was used for all the modelled frames which acted as a true representation of Pakistan's building's incorporated concrete strength.

Figure 4. 3 Concrete Specimen Failures (UET, Peshawar)

4.4.2 Yield Strength of Reinforcement (Fy)

The reinforcement in concrete structures provides tensile strength which concrete is weak in, therefore it should be designed accordingly. The data was again collected from the testing laboratories across Pakistan and these testing were carried out on Universal Testing Machine (UTM). The data

was arranged for various tests and to increase the accuracy the average value after omission of outliers was considered for the analysis.

Yield Strength (F_y) from the collected data was 316.7 MPa and this value has been consistently used throughout the study. This value again depicted the true nature of steel reinforcement being used in Pakistan.

Figure 4. 4 Universal Testing Machine (UTM), Central Process Laboratory (Pakistan)

4.5 Modelling Parameters of Frames

In this section, the frame configuration and parameters chosen for seismic vulnerability design and retrofitting by FRP have been discussed. The essential part of any RCC frame is the beam and column dimensions and the reinforcement detailing which has been mentioned in the following section. The loading considered for modelling these frames have been also summarized in the following sections.

4.5.1 Detailing of the Modelled Frames

The structures which were considered for the vulnerability assessment were representative of the building stock currently in Pakistan. Therefore

a total of fifteen frames were chosen which adequately depicted the building configuration of Pakistan. The considered RCC frames were designed for gravity loading as in Pakistan, the existing structures are not designed for seismic loads and very occasionally wind loading is considered.

Therefore these 15 frames represent the vulnerable buildings in Pakistan. According to the collected data the beam and column sizes have been summarized below with respect to the chosen number of storeys. The following table illustrates the chosen frame structures with their corresponding beam and column dimensions and steel reinforcement.

Storeys	Beam Dimension	Column Dimension	Reinforcement Detailing	
			Beam	Column
2	9”x15”	9”x9”	6 # 6 bars	6 #5 bars
3	9”x15”	12”x12”	6 # 6 bars	6 #6 bars
4	9”x15”	12”x12”	6 # 6 bars	1st storey - 8#6 bars 2nd-4th storey- 6#6 bars
8	9”x15”	15”x15”	6 # 6 bars	1st-4th storey- 8#7 bars 5th-8th storey-6#7 bars

Table 4. 1 Parameters of the Modelled frames

4.5.2 Loading Details

As the existing frames of Pakistan are usually designed for gravity loadings and therefore are vulnerable to seismic hazards, we considered only the gravity loading and no lateral load was incorporated in the design procedure. For effective impact of the wrapped FRPs it was necessary to design those frames which already exist in Pakistan and are at risk of seismic activities. Table 4.2 below summarizes the loads that were considered during the design procedure.

No.	Load Type	Magnitude
1	Concrete (Density)	24 KN/m3
2	Super Imposed Dead Load	2.15 KN/m2
3	Typical Live Load	2.9 KN/m2
4	Typical Roof Live Load	0.575 KN/m2

Table 4. 2 Load Distribution

4.6 Conventional Construction Methods

In Pakistan, construction industry has not yet reached the international standards and practices and therefore the buildings face tremendous damage during any natural calamity. In this section the common practices of Pakistan's construction industry has been discussed in detail and their respective drawbacks have been also mentioned. These practices make structures more prone to seismic hazards as they are usually not in accordance to the seismic loading. The fact needs to be acknowledged that although they frequency of earthquake events may be less but their magnitudes on occurrence are considerably high so buildings designed should be considered for lateral forces and those buildings already constructed should be adequately retrofitted to minimize the damage caused.

4.6.1 Strength of Reinforcement Steel

Steel needs to be checked and verified for strength during the phases of manufacturing and placement. Steel is usually added as a reinforcing material providing the required tensile strength to the concrete which concrete itself is weak.

The yield strength (F_y) is the parameter to monitor the strength of steel bars and according to the importance of the structure selection is carried out. In Pakistan, the testing of rebar is inadequately performed and therefore no standards are met. Grade 60 steel is most commonly being utilized and recent development has started in the field of high strength steel but it is not yet practiced.

(Shahida Manzoor, 2013), worked on testing of the steel rebar being used in construction industry in Pakistan. Their results showed that the acquired yield strength of all the tested bars were greater than the prescribed minimum value of 60 Ksi. The comparison was drawn by (Shahida Manzoor, 2013) between the idealized analytical and the experimental behaviour of the rebar and they concluded that the ultimate tensile strength of the idealized curve was higher than experimented result values and the deformation capacity of the rebar were adequate within a strain on 0.218% whereas the analytical idealized had capacity within a strain of 0.15%. The results of their experimentation are shown in the Figure 4.5 given below.

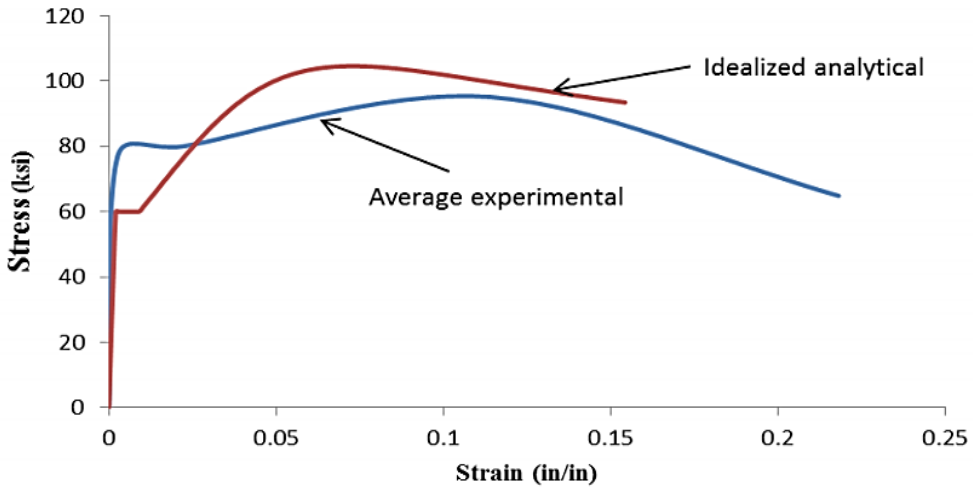

Figure 4. 5 Comparison of Idealized and Experimental Results of Steel Rebar, Grade 60 (Shahida Manzoor, 2013)

4.6.2 Placement of Reinforcement Steel

Another parameter to consider after the strength of steel is the placement of steel during construction process. Rebar are specified in the drawings and plans and their respective spacing, positioning, cover are also specified in the specifications which need to be followed for durability and better service life of the structures. In Pakistan, as most of the construction is carried out under the inspection of contractors and engineers are not actively involved, it results in poor placement, inadequate cover, corrosion of steel

reinforcement, inappropriate protection against weather and fire hazards, weaker joints, too less or too more spacing. All these result in deteriorating the structure's life and significantly damaging the structure's strength to bear excessive loads.

Placing is crucial for the structure's strength and load carrying capacity, for instance placing top rebar lower or bottom rebar above by 0.5 inch results in 20% strength reduction of a 6" thick slab. Furthermore during the concrete laying process, rebar should neither be readjusted or positioned nor removed as it results in disturbing the distribution of concrete around the reinforcement.

Figure 4. 6 Rebar Corrosion due to Inappropriate Cover

4.6.3 Column Construction

Columns are a critical structural part of any RCC structure and their failure is considered crucial as their mode of failure is brittle. Therefore more care should be taken while constructing columns and the recommended dimensions and design should be followed. In Pakistan due to traditional construction practices, no special considerations are made in column construction and usually failures of structures reveal defect such as poor lap splice, bad joints, weak column, inadequate reinforcement, insufficient

lateral reinforcement, tie or spiral spacing being inappropriate. These all result in reduction of the strength of the structures sufficiently.

Detailing of columns should also be done carefully as it acts as primary support of many structural loads. When deficient column structures are loaded by seismic forces, they result in poor resistance thus failure as shown in figure 4.7 below.

Figure 4. 7 Failure of a Column due to Shear Forces Generated in the Kashmir Earthquake

4.6.4 Concreting and Curing

After discussing the tensile reinforcement, it is imperative to highlight the common practices being utilized regarding the pouring of concrete and its curing. Concrete is considered to be actively participating in taking the compressive loading for the structures. As concreting is usually done by the contractors and therefore they are unaware of the many defects bad concreting may result into. Some of the prominent ones are bleeding, segregation, cracking, poor aggregate distribution, early setting, hardening

before placement, shrinkage, temperature related variations in volume, creep.

All these problems arise solely due to bad concreting routines and improper curing periods. Curing and concreting both needs to be done in accordance with the ACI code requirements which unfortunately are not followed actively in Pakistan. Curing temperatures, curing timings, rate of pouring concrete, mixing, handling, placement, finishing, mix ratios, water cement ratios all are extremely critical for the desired strength of the structures.

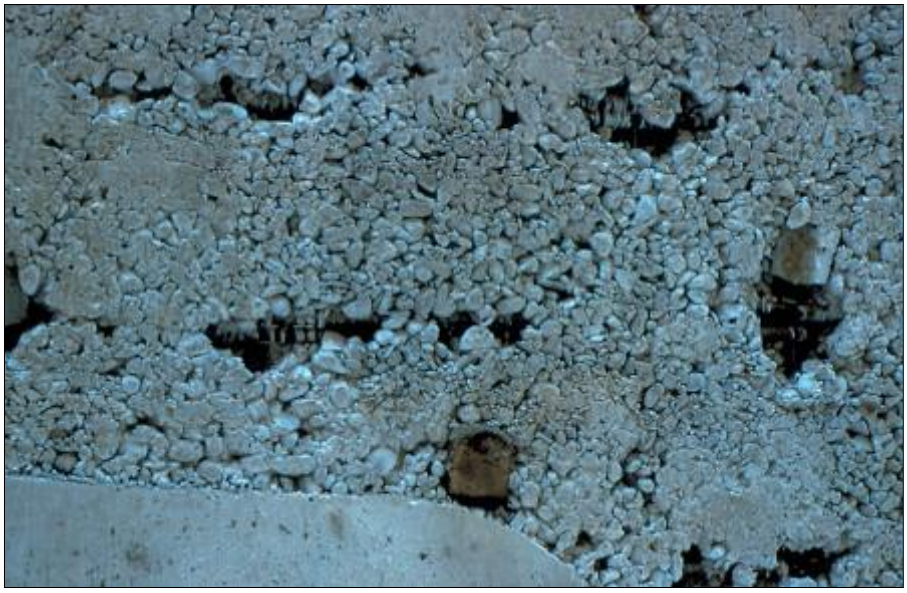

Figure 4. 8 Honeycombing in Concrete

4.6.5 Strength of Concrete

In the past use of hand-mixed concrete in residential and low-rise commercial building was very common. Concrete mixed by using this technique is commonly low strength due to improper mixing of constituents, adding unspecified amount of water and poor handling which results in segregation of the mix. Nowadays due to easy and cheap availability of concrete mixtures their use on job sites is becoming very common but due to the lack of properly trained labourer concrete of low quality is produced owing to the fact that no proper mix design is carried out, the proportioning of materials is done on a hit and trail basis, to increase the workability of

concrete and make their job easier water is added in unspecified quantity resulting in high water-cement ratio. Moreover, it is not mixed properly for the required amount of time which results in inconsistent mix. This ultimately weakens the concrete and high water cement ratio produces cracks in hardened concrete. This low strength concrete fails very easily when subjected to seismic load.

Figure 4. 9 Hand Mixing Concrete (left); Drum Mixing Concrete (right)

In case of medium and high rise building ready mixed concrete is used. Even in this case placement is an issue. If it is not placed and compacted properly it results in loss of strength.

Figure 4. 10 Ready Mixed Concrete Placement

ACI 304 R-89 sets different criteria for storage, batching, mixing, transporting, placing, compaction, and finishing of Concrete. These must be followed in the job site to achieve the desired strength of concrete.

Figure 4. 11 Poor quality concrete subjected to seismic load (Kashmir, 2005)

4.6.6 Development Length

The development length may be defined as the length of the rebar required on either side of the section to develop the required stress in steel at that section. Continuous bars of steel cannot be provided throughout the structure. There are always connections, joints and splices, if adequate development length is not provided then at the location of these critical areas the structure will fail easily. But if sufficient amount of length is provided to give a continuity to the strength of the structure then the strength will be same everywhere. Sufficient length of embedment of steel must be provided so that bond strength between steel and concrete develops to an infinity level, which is a basic assumption of Concrete technology. The development length is a function of the bar size, yield strength of steel,

concrete strength and other factors such as coating of the bar. It is dependent on whether the bar is in tension or compression. Tension development lengths are larger than compression development lengths. ACI 318-11 provides methods to calculate the required development length.

In Pakistan it is a common practice that the required development length is not provided. Local contractors disregard its importance and therefore tend to neglect the standard practice. Sufficient embedment is not provided; therefore bar slippage occurs during a seismic activity. This causes cracks in joints and stiffness is lost as a result. The basic assumption of rigid joints therefore becomes null and void. As a result structure becomes vulnerable to severe damage

Figure 4. 12 Inadequate Development Length (Kashmir, 2005)

4.6.7 Formwork Malpractices

Formwork is a temporary structure used to contain poured concrete, mould it to the required dimensions and support until it is able to support itself. It comprises primarily of the face contact material and the bearers that directly support the face contact material. The time between pouring and formwork stripping depends on the job specifications, the cure required, and

whether the form is supporting any weight, but is usually at least 24 hours after the pour is completed.

In Pakistan, the traditional timber formwork is commonly used, it requires skilled craftsmen and labour; along with fine quality of formwork, which is rare thus compromising the strength and safety of concrete structure. If formwork is not properly aligned it results in eccentric loading in columns. Also if cover is not considered it affects the gross area of concrete column. In most cases formwork is removed before concrete has attained sufficient strength which causes permanent damage to concrete. ACI-347-04 provides guideline to formwork for concrete.

4.6.8 Strong Beams and Weak Column Arrangement

Current practices stress on making strong column weak beam arrangement, in order to reduce the damage. The idea is to design column much stronger than beams so that the beams and horizontal elements of the structure should break, (without total collapse if possible) always before the columns, and, even better, the beams in the upper levels should break always before the beams of the lower levels, creating a cascade effect that helps the structure to dissipate seismic energy without total collapse. The plastic hinges developed in the beams lead to reduced deflection of the building. By the creation of these plastic joints, the initial ductility of the untouched structure, now partially broken, increases enormously, and can absorb bigger amount of lateral displacements. Moreover, columns are primary supporting member of a structure and a building fails with the failure of any column as shown in figure 4.13. However, beams are localized members and their failure leads to localized failure.

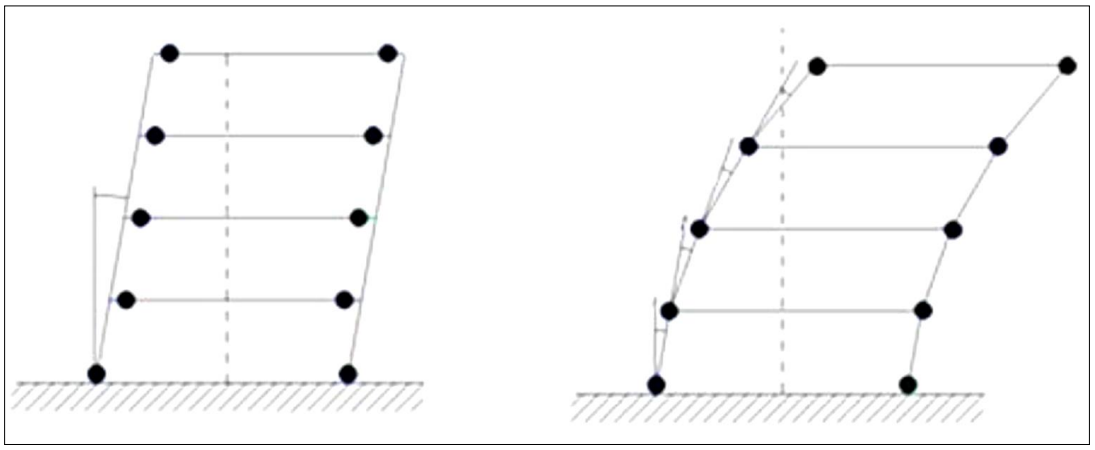

Figure 4. 13 Deflection of frame structures due to strong beam weak column arrangement

Analysing the present buildings in our country, one can reach upon the conclusion that most of the existing structures have not been designed according to Strong Column-Weak Beam analogy. This makes them vulnerable to severe damage in case of a seismic event.

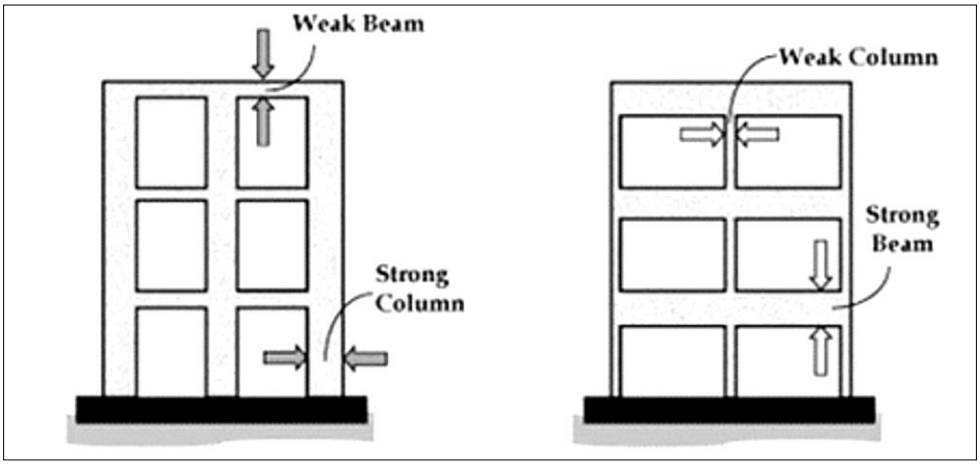

Figure 4. 14 Comparison of Strong Column Weak-Beam design (left) and Weak-Column Strong-Beam Design (right)

Figure 4. 15 Failure due to strong beam weak column arrangement (Kashmir, 2005)

CHAPTER 5

PROCDURE: VULNERABILITY ANALYSIS

5.1 Introduction

The ultimate goal of this chapter is to understand the development of Vulnerability Curve. Non-linear static analysis will be carried out on different RC frame structure as discussed in previous chapter using the prescribed methods and codes. Damage to the frame structures will be evaluated against certain displacements due to seismic hazards called Damage Index. Later for each damage index calculated, a corresponding Peak Ground Acceleration (PGA) will be calculated representing Hazard Level. This plot will be called Vulnerability Curve. Following tasks are required to develop this procedure:

a. For different RC frame structures, predict structural response at various PGA levels
b. For the predicted structural response calculate the damage potential

The following sections contain detailed procedure to achieve the above mentioned results.

5.2 Non-Linear Static Analysis

Nonlinear static procedures requires capacity of a structure to be represented by a capacity curve, which is a plot of the base shear at ordinate and roof displacement at abscissa, obtained from non-linear static cyclic analysis. As static cyclic analysis simulates the nature of seismic loading in a better way (Kyriakides, 2007), so for this study non-linear static cyclic analysis shall be used to develop the capacity curve of the structure.

Static cyclic analysis may be performed using a chained sequence of Static analyses, while each Static analysis pushes the structure in opposite direction and would use stiffness from preceding analysis. Each cycle has a

specified displacement; lateral loads are applied until that displacement is reached.

This specified displacement is increased in each cycle by a displacement step. The displacement steps determine the accuracy of the structure. The smaller the steps, the more accurate results will be, but at the cost of analysis time and increased chance of convergence error. Therefore a suitable value of displacement step is to be selected. Direction of load pattern is reversed after each cycle and the cycles are repeated until desired displacement has been achieved. Multiple deflections are given to the structure in order to displace it until it reaches the maximum limit. DRAIN 3D gives the result in the form of Hysteresis Loop.

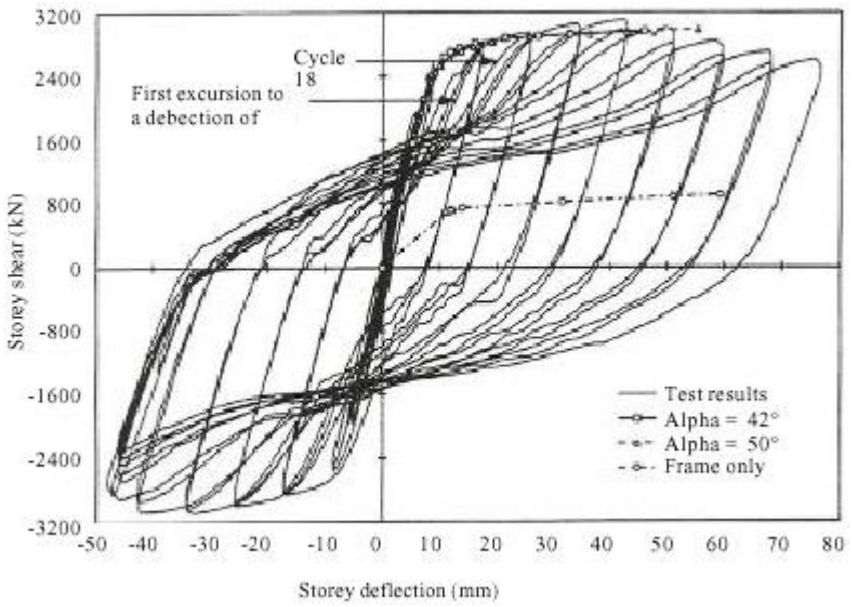

Figure 5. 1 Hysteresis Loop from Cyclic Pushover Analysis

This pushover curve is a better representation of the overall structure rather than its individual components. Under the scope of work of this study, the pushover curve is considered a good estimate of structural response. The Backbone/ Pushover curve obtained from this analysis is used for vulnerability assessment. The name of Backbone is given to the curve because of the reason that it gives the response of the structure and its shape resemble to the human backbone. It is obtained by connecting maximum positive points on the Hysteresis Loop.

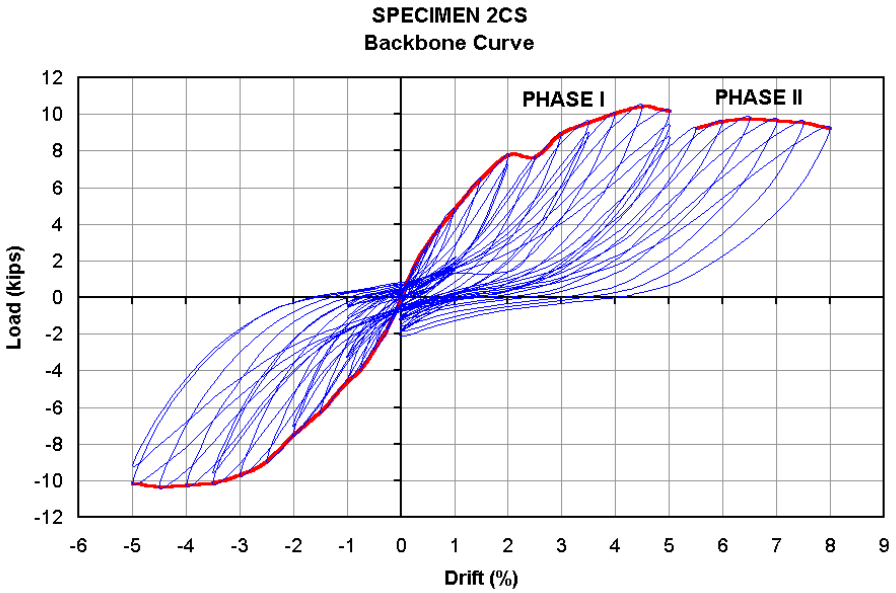

Figure 5. 2 Backbone/ Pushover Curve of the Hysteresis Loop

5.3 Selection of Parameters and Guidelines

As the capacity of building has been evaluated in the form of backbone curve, now the next step is to evaluate the seismic hazards corresponding to various levels of damage in the building. In this research work, methodology developed by (Kyriakides, 2007)for seismic vulnerability is employed, which is a reverse procedure of Capacity Spectrum method (CSM) defined by FEMA 440. The Capacity Spectrum Method (CSM) is a non-linear static analysis method which provides the graphical representation of expected seismic performance of structure. The philosophy behind this method is based on the assumption that the performance of a Multi-degree of freedom (MDOF) system under a specific earthquake event can be anticipated by comparing the demand from earthquake event with the capacity of an equivalent Single degree of freedom (SDOF) system.

5.4 Earthquake Response Spectrum

In capacity spectrum method, the earthquake response spectrum represents the demands imposed by an earthquake event on a structure. Response Spectrum is essentially a plot of peak response (acceleration,

displacement or velocity) with specified damping and varying natural time period, produced by the earthquake's ground motion. For this study, the Design Spectrum given in UBC-97 shall be used which is also adopted by BCP-2007. This Design Spectrum is basically used for performance based design and given area specific earthquake hazard response spectrum. This Design Spectrum depends upon various parameters such as:

- Soil type
- Distance of site from nearest active Fault line
- Earthquake zone

The Design Spectrum is prepared according to UBC-97. Islamabad is placed in Zone-2B and has soil type S_D (Table 16-J, UBC-97) with near source factors equal to one.

$$T_0 = 0.2T_s \tag{5.1}$$

$$T_s = \frac{C_v}{2.5C_a} \tag{5.2}$$

Where,

C_a = Seismic acceleration coefficient representing Design Spectrum's PGA, obtained from *Table 16-Q (UBC-97)*

C_v = Seismic velocity coefficient obtained from *Table 16-R (UBC-97)*

Z= seismic zone factor obtained from *Table 16-I (UBC-97)*

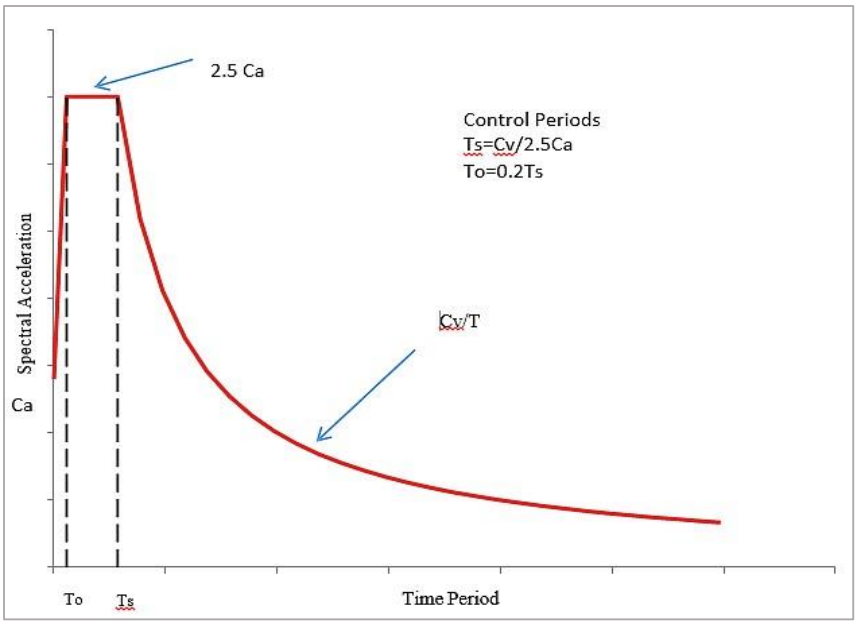

Figure 5. 3 UBC-97 Design Spectrum

For the application of Capacity Spectrum Method, the Design Spectrum is required to be converted into $S_a - S_d$ space which is termed as Acceleration-Displacement Response Spectrum ADRS (β_0), using the equation of an elastic SDOF system:

$$S_d = \left(\frac{T}{2\pi}\right)^2 S_a \tag{5.3}$$

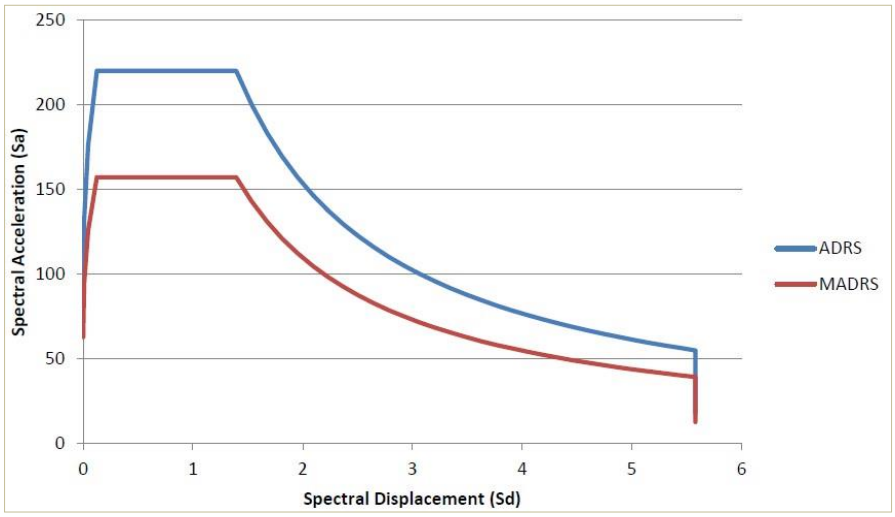

Figure 5. 4 Conversion of UBC-97 Design Spectrum into ADRS

5.5 Capacity Curve Generation

Capacity Curve is a graphical representation of Spectral Acceleration (S_a) versus Spectral Displacement (S_d), which is obtained using Capacity Spectrum Method. The method is comprehensively explained in ATC-40 manual, clause 8.2.2.1.1 and is also suggested by FEMA-440. The backbone curve obtained from the static cyclic analysis is representation of capacity of a Multi Degree of Freedom system. To use the Capacity Spectrum Method it is necessary to convert the capacity curve, which is in terms of the base shear and roof displacement to what is capped a capacity spectrum, which is a representation of capacity curve in Acceleration-Displacement Response Spectra (ADRS) format.

For this conversion, modal participation factor and modal mass coefficient for first mode shape are to be defined. In CSM it is assumed that fundamental mode is sufficient for prediction of response. The required equations to make the transformation are:

$$P.F = \left[\frac{\sum_{i=1}^{N}(w_i\phi_{i1})/g}{\sum_{i=1}^{N}(w_i{\phi_{i1}}^2)/g}\right] \tag{5.4}$$

$$\alpha_1 = \left[\frac{\left(\sum_{i=1}^{N}(w_i\phi_{i1})/g\right)^2}{\left(\sum_{i=1}^{N}(w_i)/g\right)\left(\sum_{i=1}^{N}(\frac{w_i{\phi_{i1}}^2}{g})\right)}\right] \tag{5.5}$$

Where,

$P.F$ = Modal Participation factor for the first natural mode

α_1 = Modal mass coefficient of the first natural mode

w_i/g = mass assigned to level i

ϕ_{i1} = Amplitude of mode 1 at level i

N = level N, the level which is the apparent portion of the structure

W = Building Dead weight plus likely live loads

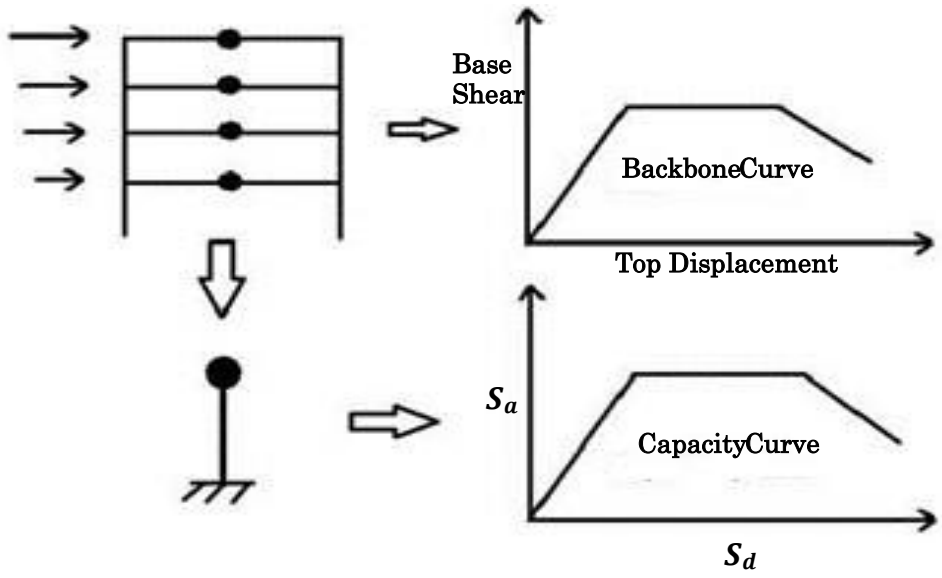

Figure 5. 5 Conversion of a MDOF system into an equivalent SDOF system

The base shear axis of backbone curve is replaced by the spectral axis and acceleration ordinate of Acceleration-displacement response spectrum (ADRS) curve is obtained by the following equation of ATC-40.

$$S_a = \frac{V/W}{\alpha_1} \tag{5.6}$$

Where,

S_a = Spectral Acceleration

V = Base Shear

w_i/g = mass assigned to level i

The displacement axis of backbone curve is replaced by spectral displacement and is calculated by the following relation:

$$S_d = \frac{\Delta_{roof}}{P.F\ \phi_{roof}} \tag{5.7}$$

Where,

S_d = Spectral Displacement

Δ_{roof} = Roof displacement

ϕ_{roof} = Amplitude of fundamental at the roof, taken as 1 for normalized amplitudes

5.6 Bilinear Idealization of Capacity Curve

A Bilinear representation of the Capacity Spectrum is needed to estimate the effective damping and appropriate reduction of spectral demand. The Capacity Curve is idealized as mentioned in the Chapter 8 of ATC 40. Idealization is also required to establish ductility levels for each of the selected or assumed performance point (Kyriakides 2007). According to Kyriakides (2007) the idealization of capacity envelope with the elastic plastic approximation does not yield sufficiently good results for substandard construction like in Pakistan and other developing countries as the ductility cannot be accurately approximated at every point on the capacity curve. Instead the equivalent elastic plastic system approximated using equal energy rules are more accurate which leads to the need of the bi-linear idealization of every point on the curve.

Every point on the curve (S_A – S_D) is selected and a bilinear idealized capacity curve is generated using equal energy principle stated above i.e. the area above the bi-linear curve and the area below the curve must be equal, neglecting the post yield area above the curve.

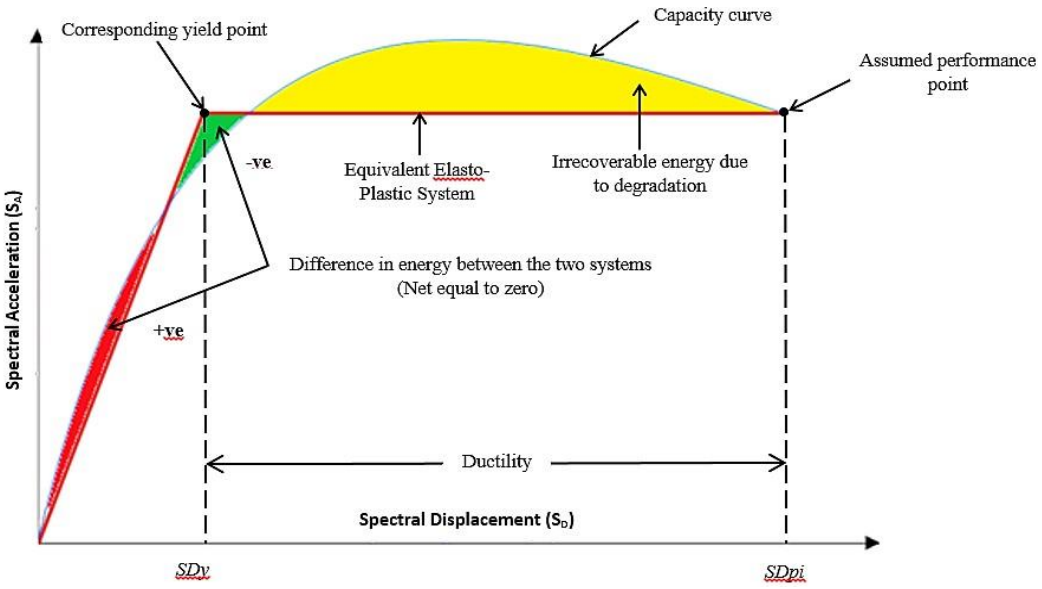

Figure 5. 6 Procedure for Bi-Linear Idealization

The above figure represents a case of ES approximation for assumed point. Blue curve is capacity curve, red one is the bi-linear elastic-perfectly plastic curve. Red area is the positive area, green is the negative area and the yellow area is the neglected area representing energy dissipated due to degradation.

As a result of idealization of curve, for every assumed performance point a corresponding yield point is obtained on the curve and hence ductility is calculated by dividing the spectral displacement of performance point to the spectral displacement of the yield point as given by the formula:

$$Ductility = \mu = \frac{SD_{pi}}{SD_y} = \frac{\Delta u}{\Delta y} \tag{5.8}$$

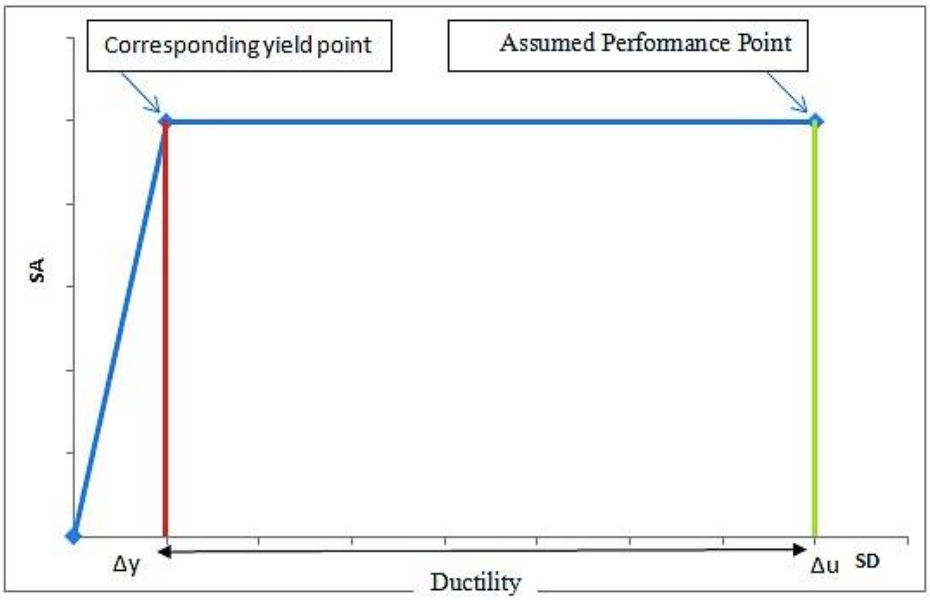

Figure 5. 7 Bi-Linear Idealized Curve along with Ductility of assumed Performance Point

5.7 Capacity Spectrum Method

In capacity spectrum method demands imposed on a structure by an earthquake event are estimated by comparing the capacity spectrum of the structure with the Response spectrum. Design Response spectrums given in building codes are elastic response spectrums for 5% damping level. These should be reduced to in-elastic spectrums and modified to account for damping level of the structure.

According to FEMA 440, the Performance Point in CSM is determined by iteration. The displacement response of non-linear SDOF is calculated using an equivalent linear system with effective damping $ß_{eff}$ and time period T_{eff}. Effective damping values, expressed as a percentage of critical damping, for all hysteretic model types and α values have the following forms:

For $1.0 < \mu < 4.0$:

$$\beta_{eff} = (\mu - 1)^2 + (\mu - 1)^3 + \beta_o \quad (5.9)$$

For $4.0 \leq \mu \leq 6.5$:

$$\beta_{eff} = C + (\mu - 1) + \beta_o \quad (5.10)$$

For $\mu > 6.5$:

$$\beta_{eff} = E\left[\frac{F(\mu-1)-1}{[F(\mu-1)]^2}\right]\left(\frac{T_{eff}}{T_o}\right)^2 + \beta_o \quad (5.11)$$

Values of the coefficients in the above equations for effective damping of the model oscillators are obtained from FEMA-440 Table 6-1 of Coefficients for use in Equations for effective damping. The coefficients in this table have been optimized to fit the empirical results for idealized model oscillators having well defined hysteretic behaviour designated earlier in this document as Elastic Perfectly Plastic (EPP), Stiffness Degrading (SD) and Strength and Stiffness Degrading (SSD). Real buildings, comprised of a combination of many elements, each of which may have somewhat different strength and stiffness characteristics, will seldom display hysteretic behaviours that match those of the oscillators, exactly.

Effective period values for all hysteretic model types and α values have the following form:

For $1.0 < \mu < 4.0$:

$$T_{eff} = [(\mu - 1)^2 + (\mu - 1)^3 + 1] \quad (5.12)$$

For $4.0 \leq \mu \leq 6.5$:

$$T_{eff} = [I + (\mu - 1) + 1] \quad (5.13)$$

For $\mu > 6.5$:

$$T_{eff} = \left\{K\left[\sqrt{\frac{(\mu-1)}{1+L(\mu-1)}} - 1\right] + 1\right\} T_o \quad (5.14)$$

Values of the coefficients in the above equations for effective period of the model oscillators are obtained from FEMA-440 Table 6-2 Coefficients for use in Equations for Effective Period. Note that these are a function of the characteristics of the capacity spectrum for the oscillator in terms of basic hysteretic type and post elastic stiffness α.

In order to evaluate the performance level of the building in a given earthquake, FEMA 440 gives an iterative process which involves the following steps:

- Assume a performance point on the capacity curve and calculate its ductility μ and secant period $T_{sec.}$

$$T_{sec} = 2\pi\sqrt{\frac{SD_i}{SA_i}} \quad (5.15)$$

- Calculate Effective damping $ß_{eff}$ and Time period T_{eff} for the specific ductility levels using the equations of FEMA 440.
- Reduce elastic spectrum ADRS ($ß_0$) by incorporating effective damping to obtain ADRS ($ß_{eff}$), by dividing acceleration ordinate with reduction factor *B*.

$$B = \frac{4}{5.6 - ln\beta_{eff}(in\%)} \quad (5.16)$$

- Generate Modified Acceleration Displacement Response Spectrum MADRS (ßeff, M) to incorporate the non-linearity of the structure by multiplying the acceleration ordinate with reduction factor *M*.

$$M = \left(\frac{T_{eff}}{T_{sec}}\right) \quad (5.17)$$

- The performance point (PP) is obtained by the intersection of MADRS (ßeff, M) with the Capacity Curve. If the estimated PP is within the acceptable limits to assumed one, then it is adopted. Otherwise, this process is repeated using another refined Performance Point.

5.8 Application of Capacity Spectrum Method

At every displacement step on the Capacity Curve, the corresponding hazard level (PGA) is the required output for the derivation of vulnerability curve. So, instead of varying performance point to suit the hazard level as mentioned above, the hazard level is varied in accordance with performance points as shown in Figure 4.9. Therefore, the above described method has to be reversed so as to determine hazard level for selected points on the capacity curve (Kyriakides, 2007).

To predict the PGA level, it is required that all the characterizing parameters of the structural response (Capacity Curve) should be known at all displacements steps. Every point on the capacity curve is treated as a Performance Point, with known initial period and ductility. Thus, the MADRS method of CSM (as stated above) is reversed for every performance point to calculate the SA ordinates of ADRS ($ß_0$) from respective MADRS ($ß_{eff}$, M) instead of calculating MADRS ($ß_{eff}$, M) from ADRS ($ß_0$). By using the equation:

$$SA(ADRS) = \frac{MADRS\ B}{M} \tag{5.18}$$

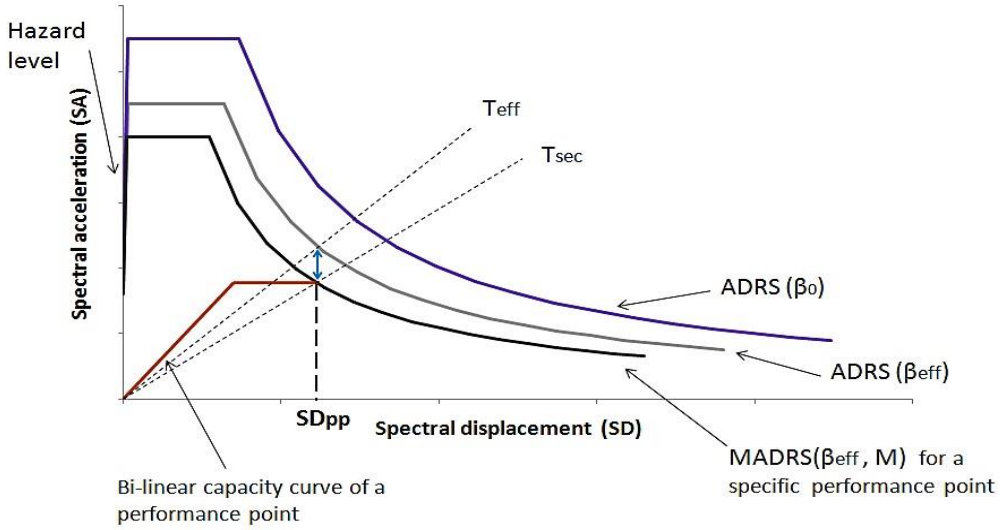

Figure 5. 8 Application of Capacity Spectrum Method for determination of PGA level

5.9 Quantification of Damage Potential

For derivation of analytical vulnerability curve, quantification of damage is necessary which can be plotted as Damage Index (DI) on ordinate of these curves. Damage index as discussed in the literature review section can be used in calculating the damage corresponding to PGA levels. Listed below are the parameters of above mentioned discussion:

- Dynamic parameters of the structure
- Displacement parameters
- Displacement and cumulative damage

The criteria for selection from one of these DI was based on expert reasoning .The selection is done the basis of the following factors:

- DI should account and represent damage of the whole structure
- It should be correlated to the capacity envelope
- Should take input of the data of damaged buildings for calibration

Keeping in view the above mentioned criteria, it was decided to use Dynamic parameters of the structure as a means to calculate DI. This would account for the increase in natural period of vibration of the structure as a basis for calculating DI. This was selected as an increase in natural period is a global effect of a structure rather than a local one. Period (T) can be easily calculated before and after an earthquake. Furthermore, as increase in period occurs due to strength loss and softening, it can be easily calibrated.

Calvi et al. (2006) confirmed in his research that increase in Natural period is due to damage to structure. Other researchers like Zembaty et al. (2006) also produced a damage scale which relate degree of damage and increase in frequency of structure. The equation to be used for DI corresponding to change in natural frequency is given below:

$$DI = \frac{T_{sec} - T_{initial}}{T_{100} - T_{initial}} x100 \qquad (5.19)$$

Here $T_{initial}$ refers to the Time period when damage is zero and T_{100} refers to Time period at complete collapse of structure. T_{100} values used can be calculated by using following formula:

$$T_{100} = 2\pi\sqrt{\frac{SD_{limit}}{SA}} \tag{2.20}$$

Following is the building types that are used in this project. This model building type is based on classification system of FEMA 178

The graph below shows the point on capacity curve for a specific PGA level, after which spectral displacement keeps increasing while spectral acceleration remains constant.

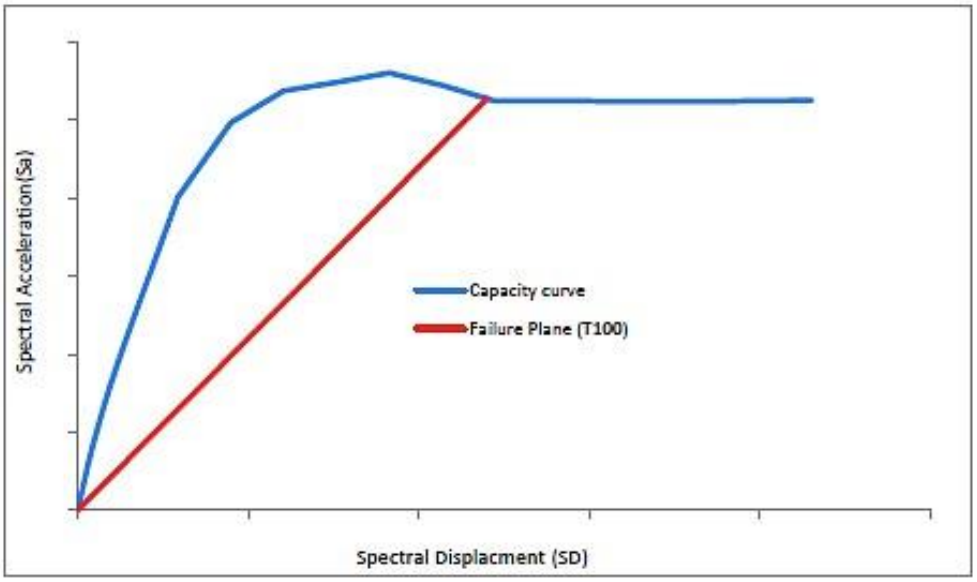

Figure 5. 9 Failure Plane on the Capacity Curve

5.10 Determination of Vulnerability Curves

In the case of generation of vulnerability curve, instead of varying performance point to suit the hazard level as mentioned above, the hazard level is varied in accordance with performance points. So the above described method has to be reversed so as to determine hazard level for selected points on the capacity curve. The details of the methodology used are as under:

1. A representative elastic spectrum is selected which is denoted as ADRS (ßo). This elastic spectrum is also known as a d9emand spectrum and is obtained by performing the detailed procedure of Eurocode 8.
2. Later, a performance is assumed on the capacity curve. These performance points are selected after the idealization of the capacity curve. Based on this performance point, the ductility is calculated as:

$$\mu = \frac{S_{D(P,F)}}{S_{D(Y,P)}} \tag{5.21}$$

3. After calculating the ductility (μ), the values of T_{eff} and $ß_{eff}$ are calculated corresponding to each ductility level using the equation defined in FEMA 440 chapter6.
4. After calculating the value of $ß_{eff}$, it is then substituted in elastic spectrum equation to adjust it for ADRS ($ß_{eff}$).
5. The elastic spectrum for ADRS is then converted into MADRS as discussed earlier by multiplying Sa with a factor 'M' where M is:

$$M = \left(\frac{T_{eff}}{T_{sec}}\right)^2 \tag{5.22}$$

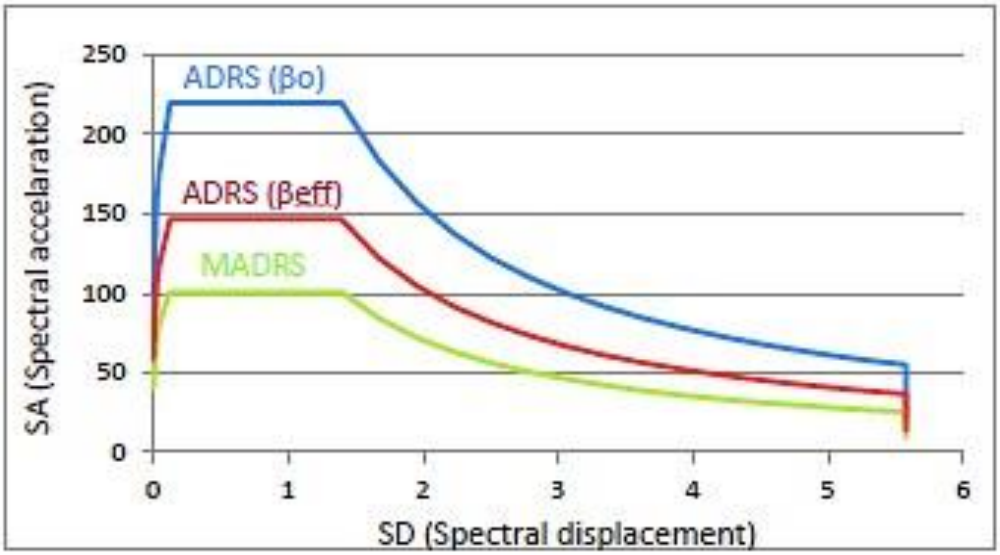

Figure 5. 10 MADRS in FEMA 440 used for Capacity Spectrum Method

6. Now by varying the PGA's that is by applying the reverse Kyriakides approach, performance point is calculated by intersecting the point of the idealized capacity spectrum to the MADRS.
7. At this point DI is calculated using the formula:

$$DI = \frac{T_{sec} - T_{initial}}{T_{100} - T_{initial}} x100 \quad (5.23)$$

8. This procedure is repeated by varying the performance point and PGA's and hence a vulnerability curve is plotted.
9. The damage index can be linked to the mean damage ratio which is the ratio of the total cost of the building to the repair cost. It is assumed that the DI is linearly correlated to the MDR with the correlation coefficient equal to 1 (Kyriakides, 2007). The function to relate MDR to DI is as follows:

$$MDR = f(DI) \quad (5.24)$$

5.11 Input Parameters

After selecting the representative frames as discussed in chapter 4 relative to their significance, the next step is to model these representative frames in the analytical tool for pushover analysis and later on the construction of vulnerability curves. Using DRAIN 3DX is a long iterative task as analysis carried on DRAIN 3DX acquires binary coding and adequate input generation files. With the use of many factors and variables, the input files are generated.

5.12 Element Generation

To define any structure in DRAIN 3DX, various nodes are generated to define the location of the joints commonly referred as nodes in DRAIN 3DX. These nodes are defined by four number sequences, in which the first two numbers represent the horizontal location and the last two numbers represent the location on vertical axis. For example 2020 means that the node is located at the second bay and at the second storey. Similarly for all storeys and variable bays the nodes are defined for each and every beam

and column joint of the frame. To define the frame in the software, we need to define certain groups by grouping similar members in to a single entity. The groups used for our analysis included the following:

- Group 1: Foundation Columns
- Group 2: Floor Columns
- Group 3: Beam Fibre

These are the fundamental groups which will adequately describe our frame network and will suffice for the analysis.

5.13 Restraint Assignment

The next step is to define the restraints for each and every node respectively and this step is crucial as restricting the translation and rotations have a deep impact on the results of analysis. The slab nodes were permitted translation in the X and Y plane whereas the restriction was in the Z plane. Moreover the foundation nodes are taken to be spring, as DRAIN 3DX does not permit the fix support on the floor nodes.

Moreover there are K nodes utilized in this analysis scheme, which are primarily used for orientation process. These nodes are used to orient each and every node with respect to the entire structure. To elaborate it basically represents the location of the node or the group relative to the global axis; i.e. definition of local axis.

5.14 Fibre Definition

To input the frames into the software i.e. DRAIN 3DX every cross section is divided into fibres as the software incorporates nodal values and reference on grid so the fibres are defined accordingly. This further demonstrates that in a particular fibre the strength and properties remain consistent and do not change within a respective fibre.

Concrete fibres are kept constant for the frames and each beam or column is sub divided into strips (fibres). Concrete has been divided into linear

segments of 4 fibres for both beams and columns whereas the reinforcement is defined by individual fibre i.e. a fibre for each reinforcing bar. As the reinforcement varies for each type of frame, therefore the total number of fibres will also differ from storey to storey. The concrete fibres are generated by equal division of the cross sectional area and therefore linear geometrical behaviour will exist. As shown in the figure below the fibres are defined and then their respective properties are then assigned on the software.

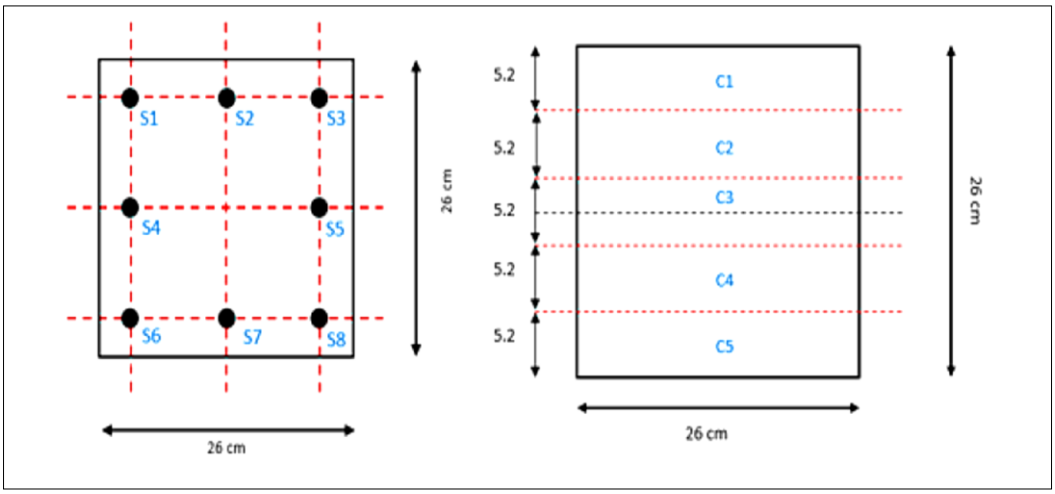

Figure 5. 11 Fibre Definition for a 26cm x 26cm beam cross section; Steel fibres (Left) & Concrete fibers (Right)

5.15 Incorporation of FRP

To incorporate the FRP as a retrofitting technique the nodes are defined according to the proposed location by (Garcia R., 2010) and FRP is incorporated in between these nodes. The locations are also taken as approximated to resist the shearing effect and slippage failures at the recommended locations. As the joints are a critical location for seismic vulnerable damages therefore they are considered while determining the location for the FRPs. In between these nodes the property of concrete will be that as proposed by (J.G Teng, 2004) which will show ample amount of confining action when subjected to any form of compressive loading.

The confinement action will be just incorporated in the region between the columns area forming joint with beams and all the other unwrapped

portions will have the concrete property of unconfined concrete as used for the bare frames. All other steps of analysis will remain constant.

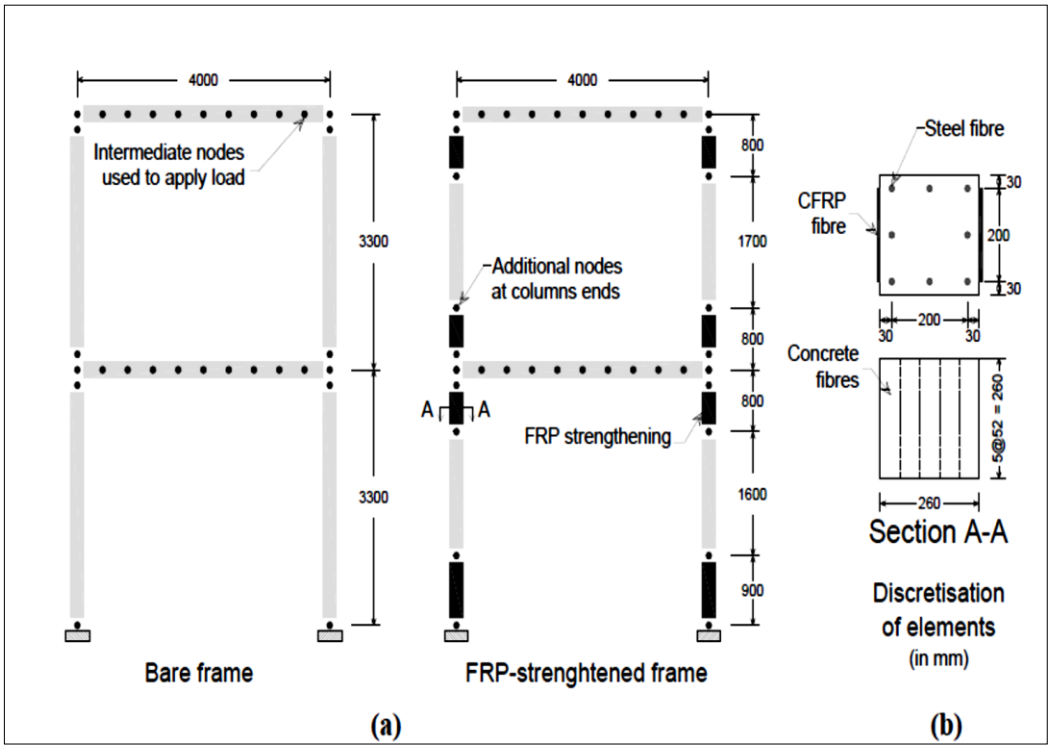

Figure 5. 12 Location of FRP wraps as proposed by (Garcia R., 2010); (a) the representation of bare and FRP wrapped frames, (b) the cross section of the section A-A

The figure above shows the idealistic wrapping locations which have been used in this study and the analysis performed for FRP retrofitted frames are based on these cross sectional details. The length of wrap near the foundation columns is greater than the length on the storeys above as the base shear is higher at the bottom columns and therefore they require higher resistance.

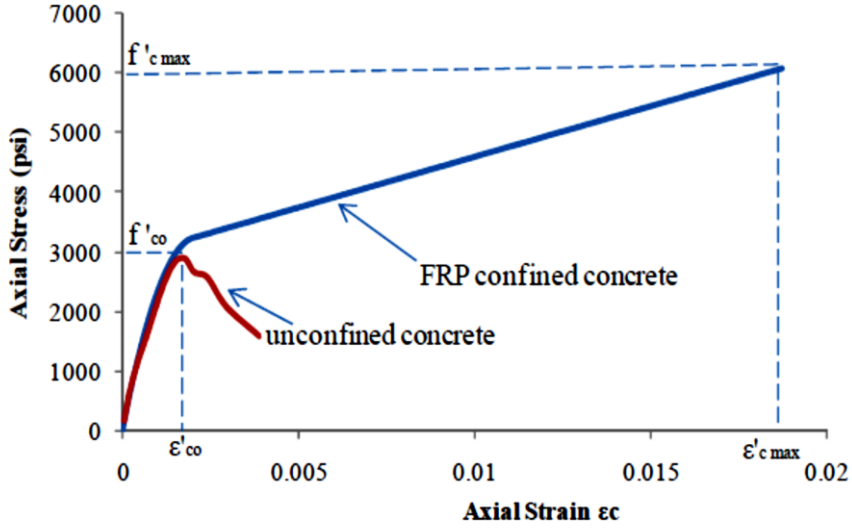

Figure 5. 13 Stress Strain Model for confined and unconfined concrete as proposed by (J.G Teng, 2004)

In the above figure the confinement properties can be visualized regarding the concrete sections and for this study these values have been incorporated. These values are close to the strength parameters of Pakistan's buildings. The increase of confinement action and increase in strength can be easily observed through this curve.

CHAPTER 6

RESULTS & DISCUSSION

6.1 Introduction

In this chapter the achieved results and their comprehensive analysis are drawn to assess the objectives of this study. After the successful construction of all the vulnerability curves, it is essential to evaluate their relationships and to compare them with each other. The comparisons drawn in this chapter will aid in the easy understanding of the subject of this study and moreover it will form the basis of risk assessment and viable economical aspects.

6.2 Results

To comprehend the achieved vulnerability curves, in this section the curves will be discussed. To demonstrate clearly the comparisons between the retrofitted and bare frames, the curves will be first discussed individually and later comparison will be drawn. A vulnerability curve is the demonstration of the seismic activity responding to a particular PGA value and the damage index it can impact on a structure. It is a depiction of the damage a structure is prone to under specific seismic event and therefore acts a strong framework for assessing the risk allocation and damage generated during any such activity.

A vulnerability curve has many distinctive points and features which signify either the material response or the structural capacity. To understand a vulnerability curve, an example of a representative building (2x2) bare frame is discussed in the following section.

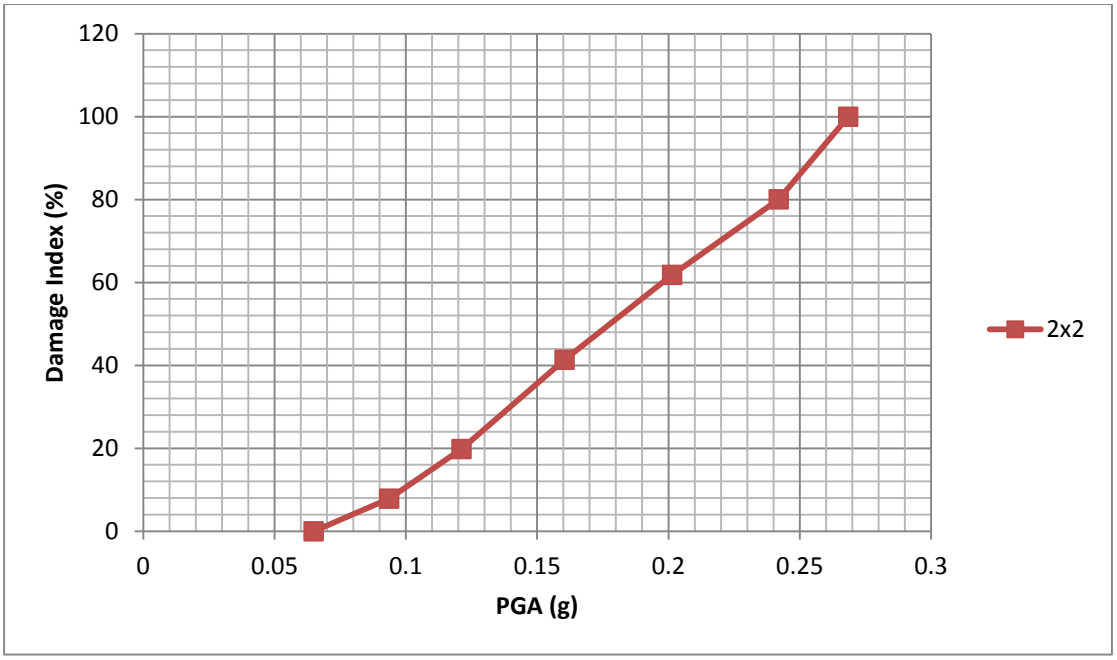

Figure 6. 1 Vulnerability Curve of a 2x2 Bare Frame

Figure 6.1 demonstrates a common shape of a seismic vulnerability curve and to understand the various stages in a progressing curve, an example of 2x2 frame without FRP wrap has been considered. The failure is initiated by the cracking of the structural elements and later on the steepness is representing the yielding of concrete in compression due to the seismic forces. Moreover as the curve progresses the slope becomes steeper which shows the simultaneous yielding of reinforcement and the concrete and primarily this failure mode is experienced in the columns of the frames at the perimeter.

Initiating from cracking and gradually reaching the pull out fibre state is the common characteristic of this vulnerability curve. The materials lose their strength with successive cycles and therefore the slope becomes steeper and steeper when we shift from higher buildings to lower buildings. Moreover the higher the building is lesser brittle damages are witnessed and more ductile nature is depicted.

6.2.1 Vulnerability Curves of Bare Frames

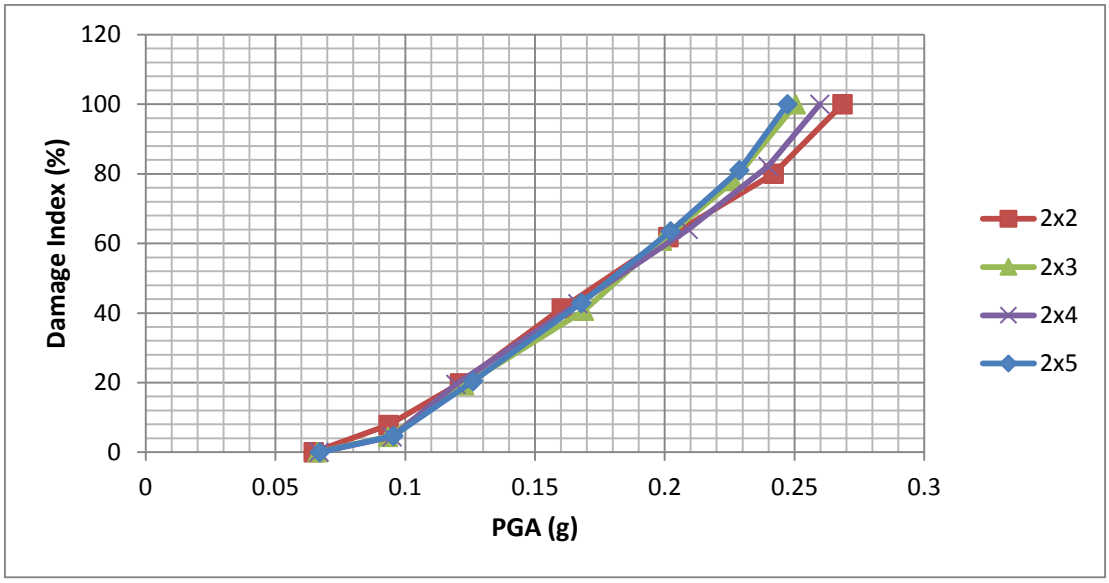

Figure 6. 2 Vulnerability Curve of all 2 Storeys Bare Frames

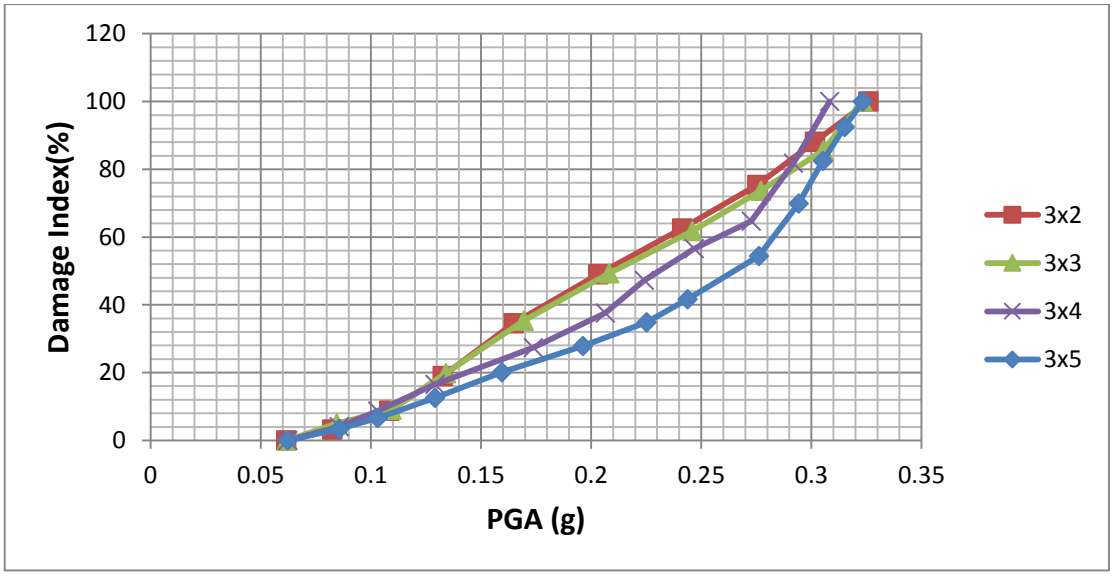

Figure 6. 3 Vulnerability Curve of all 3 Storeys Bare Frames

Figure 6.2 and 6.3 show the vulnerability curves achieved for two and three storey buildings and the damage range for two storey frames lie in between PGA of 0.25g to 0.27g whereas with successive increase of another storey the collapse range also increases to 0.31g to 0.33g. The PGA value decreases for successive increment of bays keeping the storey configuration constant. The curves show little fluctuation of collapse potential when considering nominal changes in the plan configuration.

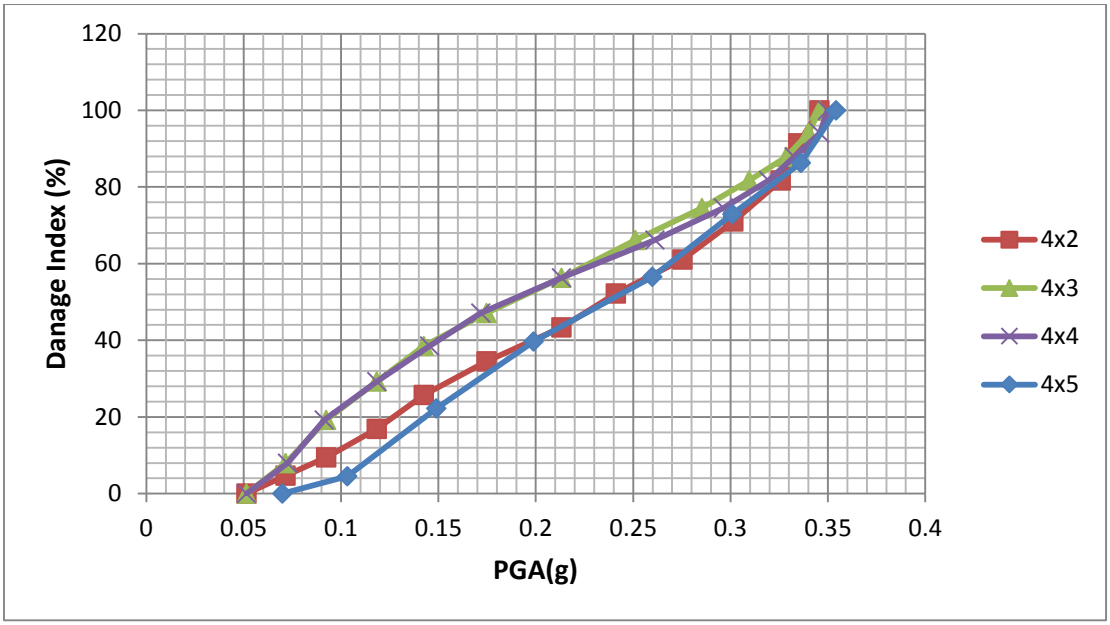

Figure 6. 4 Vulnerability Curve of all 4 Storeys Bare Frame

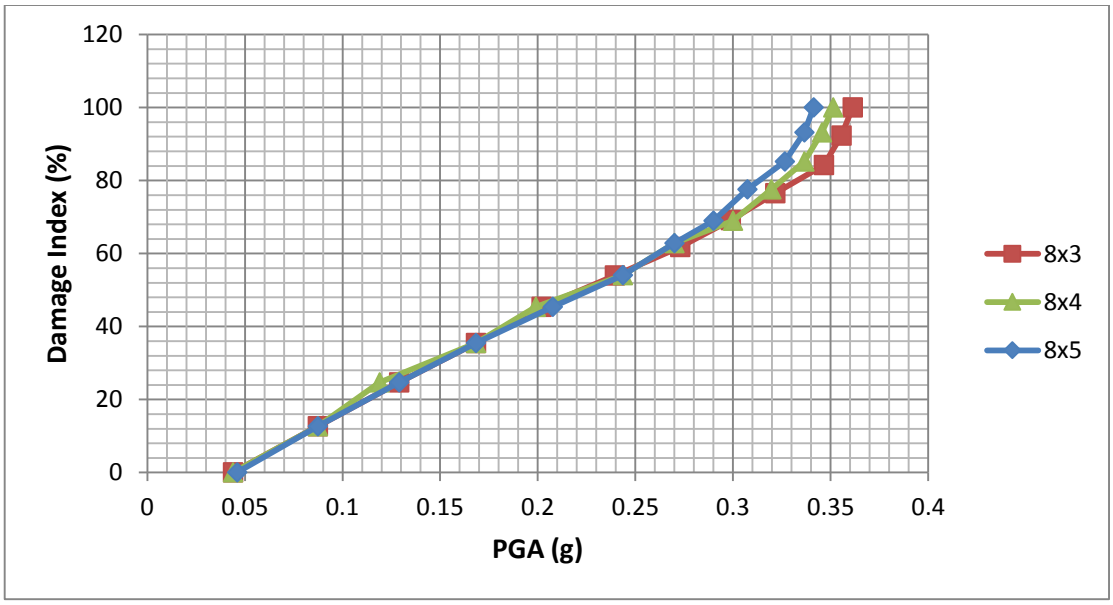

Figure 6. 5 Vulnerability Curve of all 8 Storeys Bare Frame

Figure 6.4 shows typical curve of a 4 storey frame structure and damage is observed at 0.35g almost for all storeys. The range of PGA for maximum collapse state of damage is hence increasing with increase in storeys. The curves show a convergence behaviour when near to collapse. Figure 6.5 shows a typical curve of 8 storeys frame, and a massive shift of behaviour is observed as for all storeys the curves are almost overlapping showing the

decreased effect of seismic forces on high rise buildings and failure occurs at a PGA value of 0.36g.

6.2.2 Vulnerability Curves of FRP Retrofitted Frames

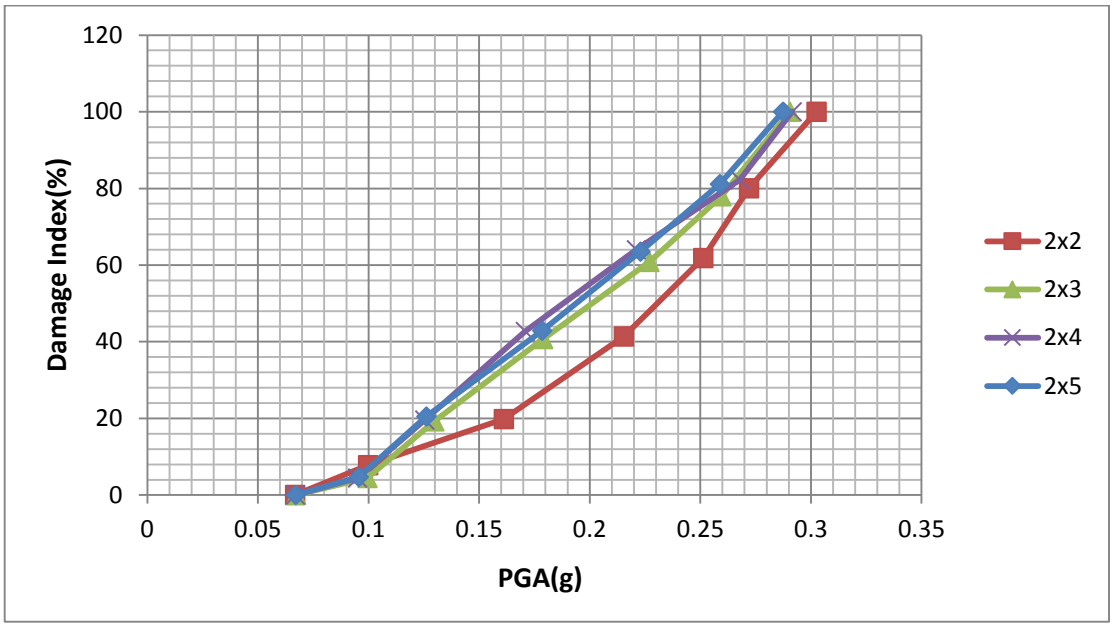

Figure 6. 6 Vulnerability Curve of all 2 Storeys FRP Wrapped Frames

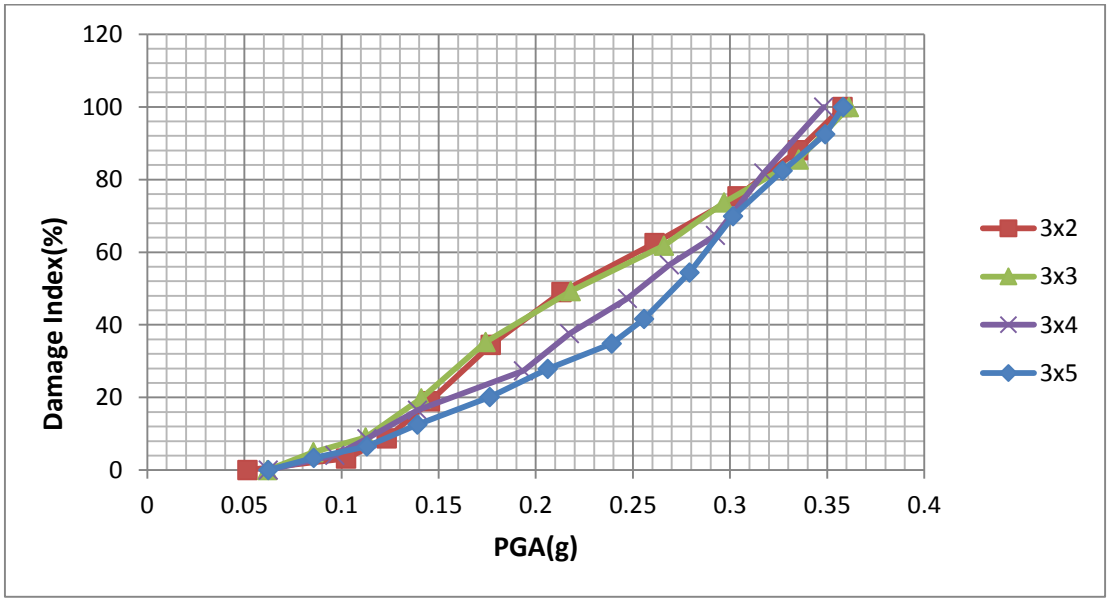

Figure 6. 7 Vulnerability Curve of all 3 Storeys FRP Wrapped Frames

Figure 6.6 shows the curve generated by the incorporation of a single FRP wrap around 2 storey frame network and the progressive damage is observed at a PGA value of 0.28 to 0.30 which is greater as compared to the

bare frames. Similarly a larger difference is observed for 2 storey frames in figure 6.7 where maximum damage state is attained at a PGA value of 0.35 with mild fluctuating trend line through the curve. The relationship for variable storeys and bays persists similarly to bare frame structures with mild variations.

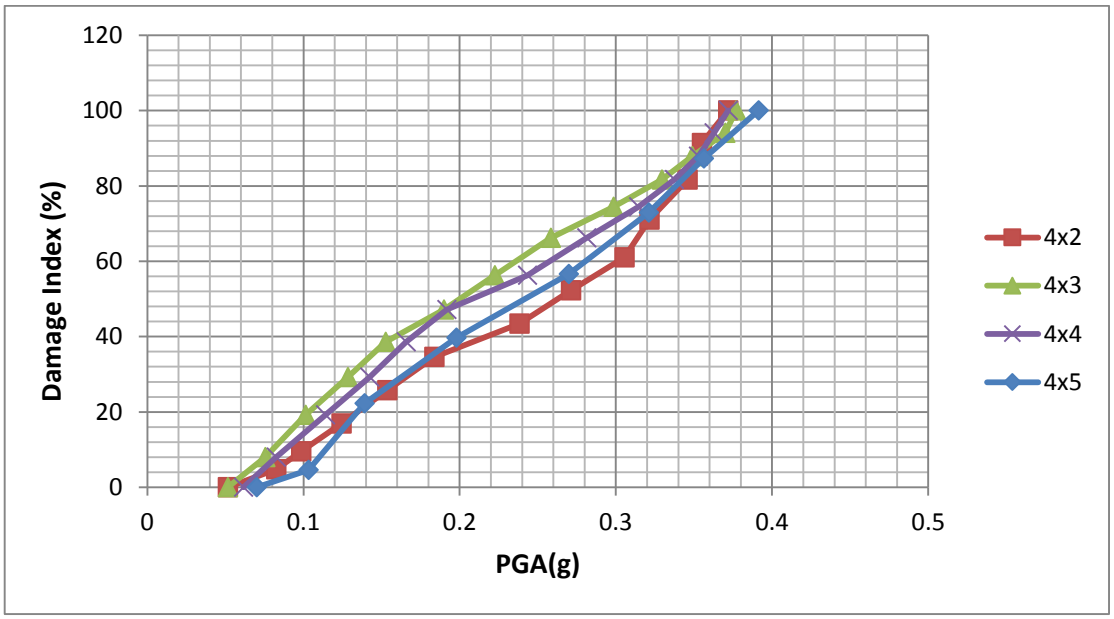

Figure 6. 8 Vulnerability Curve of all 4 Storeys FRP wrapped Frames

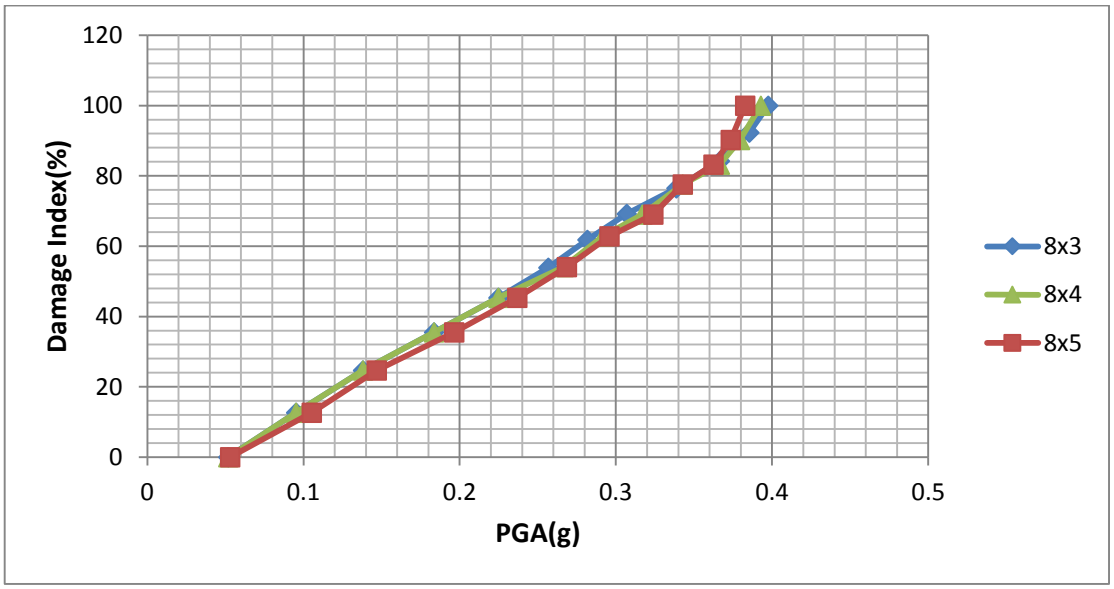

Figure 6. 9 Vulnerability Curve of all 8 Storeys FRP wrapped Frames

Figure 6.8 shows a typical behaviour of a 4 storey frame network and the collapse is observed at a PGA value of 0.38 which is an increase from the

bare frames of similar plan. Figure 6.9 shows the curve for FRP retrofitted 8 storey frames and they tend to again depict a very close curve trend irrespective of storeys with the complete failure at 0.4g value. The capacity hence is seen to be increased as comparable to the bare frames. Hence FRP tends to provide some confinement action.

6.3 Effect of Variable Storeys

Variation in the number of storeys in individual frames has a strong effect on the curve generation and the degradation of strength. The shape of the curve is also reformed when moving from shorter storeys to higher storeys or vice versa. This is primarily due to the change in the stiffness and the ductility parameters. Figure 6.10 below shows a comparison between variable storey heights and the impact it has on the PGA and the damage index. The curve constructed shows 2 frames of equal number of bays i.e. five but a difference in the number of storeys from two to four.

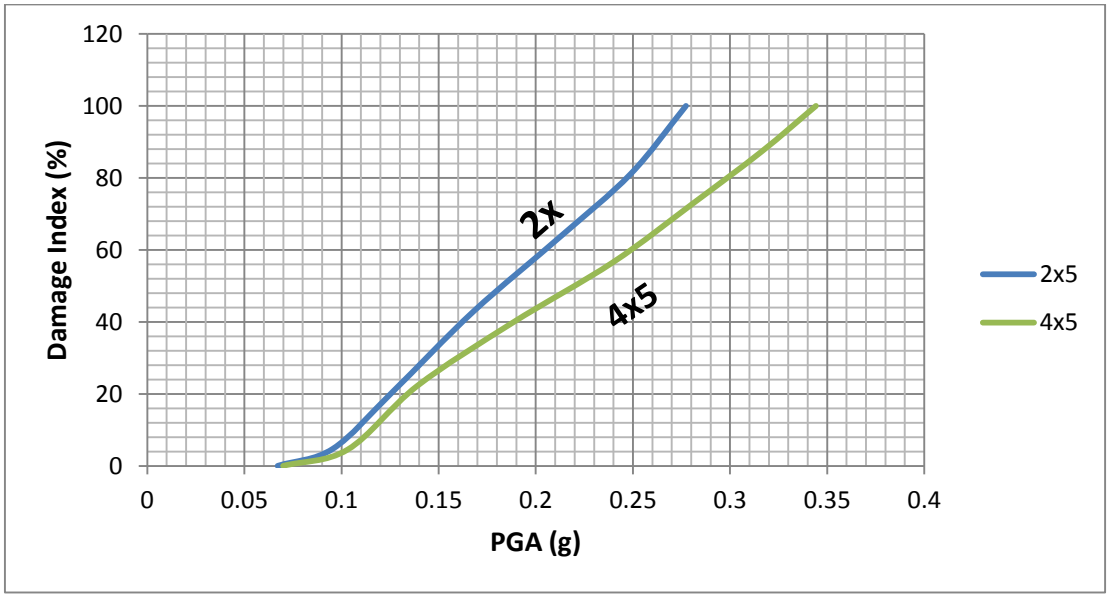

Figure 6. 10 Effect of Variable Storeys on Vulnerability Curve

Figure 6.10 shows the vulnerability curve showing the strong influence number of storeys has on the vulnerability of a frame structure. With significant increase of two storeys the building has become lesser stiff and more ductile, therefore the frame of 4x5 will exhibit more time periods under any earthquake event. This will result in excessive swaying of the

structure and therefore until a specific limit the swaying effect dominates the cracking of the concrete. The frame with two storeys shows a damage index of 100% at a PGA value of 0.28g whereas the four storeys frame has increased strength and resists the seismic forces up to a PGA value of 0.34g. The increase of ductility ensures higher strength under a seismic event which influences the failure modes of for any RCC structure. The percentage of increase of strength increases as the subsequent difference between the numbers of storeys increase. The curves tend to separate more when considering a greater storey difference.

6.4 Effect of Variable Bays

Similarly the vulnerability curves are highly impacted by the variation in the number of bays across a frame structure. Bays are the plan division of a frame structure and they are considered according to the utility purpose of the building. Usually bays are kept rectangular in plane and with uniform dimensions to aid in a uniform organization. At times the land costs, piping networks, beams and columns distribution effect the bay division. These bays demarcate a building into respective zones and panels which can be either separated by suitable mechanism or left undisturbed. The increase of lateral dimensions has a strong influence on the behaviour of buildings under seismic loading and therefore needs to be carefully dimensioned. Figure 6.11 below shows the effect of variable number of bays while all other variables are kept constant for example the storey heights, number of storeys, loadings, and material properties.

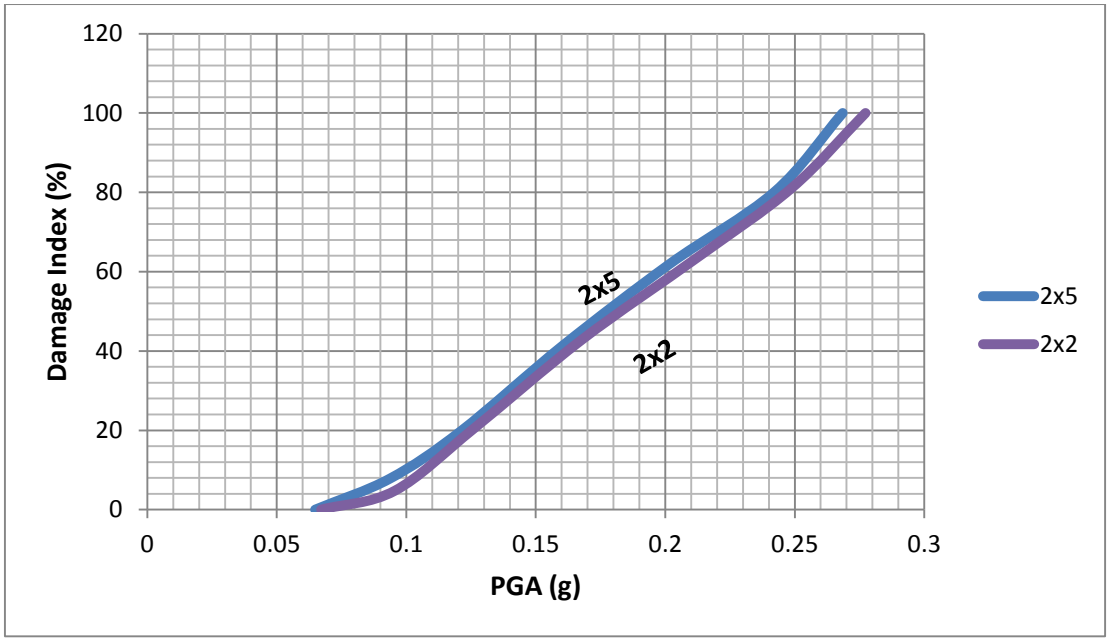

Figure 6. 11 Effect of Variable Bays on the Vulnerability Curve

The curve shows the difference in the vulnerability curves both belonging to same number of storeys i.e. two storeys but variable bays. The bays selected for this evaluation are both extremes, one is a curve for two bays and the other is of 5 bays. The shape and the trend of both curves tend to follow the standard pattern of vulnerability curves. The difference of both curves is not massively observed as compared to the difference of variable storeys. The increase of bays makes a structure stiffer in the longitudinal axis due to increase of mass and no corresponding change in height.

The stiffness decreases the capacity of the structure and results in a brittle range failure due to cracking of concrete at earlier stages. The failure mode is dependent on the cracking event of concrete for the vulnerability assessment. Therefore it can be observed that the frame with five bays reaches the ultimate damage index of 100% at a PGA value of 0.27g whereas the two bays frame yields at a higher PGA value around 0.28g. Although the difference is not as significant as seen for the variability of storeys but the difference becomes more obvious when the difference in number of bays becomes greater.

6.5 Effect of FRP Wraps on the Vulnerability Curves

The comparison has been made between the bare and the FRP wrapped frames in this section of similar configurations of frame network and the following figure will explain the damage reduction achieved.

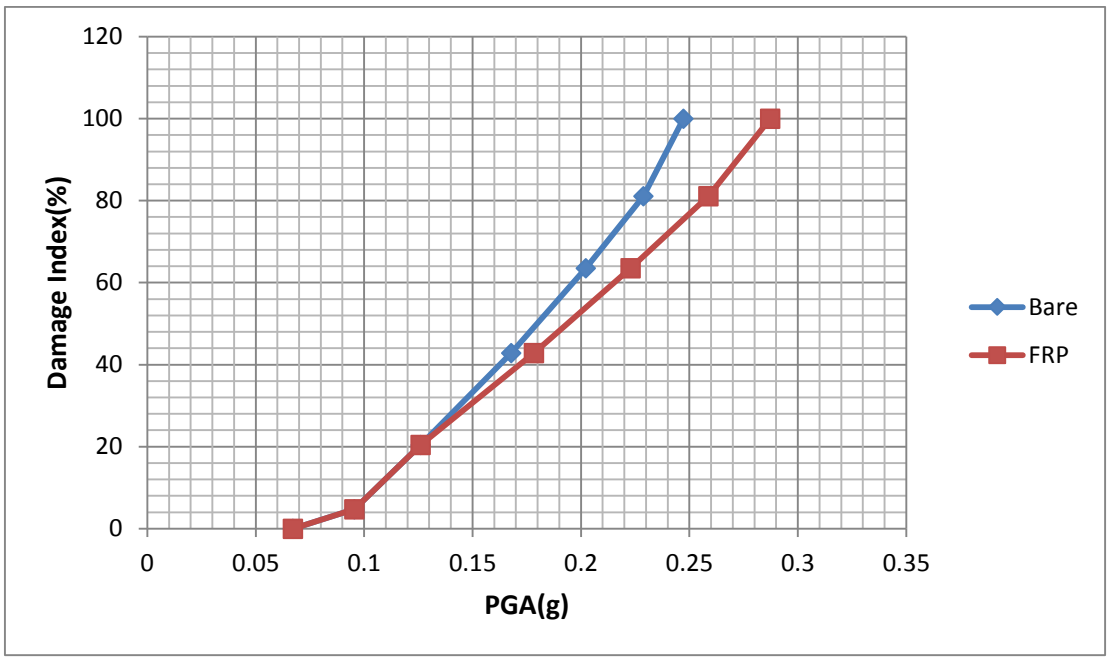

Figure 6. 12 Comparison of Bare and FRP Frame of Configuration 2x5

In figure 6.12, the impact of FRP wrap (single) is significantly observed and the increase in the strength due to FRP is also observed. For lower PGA values ranging between 0g to 0.15g, the difference in damage is not very significant and curves follow a similar pattern but for higher PGA values which are more common in scenario of Pakistan's seismic activity, the damage is more prominent. To further see the real impact of FRP the 100% damage state is observed which is in fact the collapse level and the PGA value has significantly increase by a difference of 0.05g for FRP wrapped frame. It shows the impact of FRP on the cracking of concrete which shows that the concrete has been confined and therefore exerts lesser damage for the same seismic activity. Moreover the capacity of the frame is seen to be increased massively by wrapping the FRP over the concrete members.

This difference is observed more in low to medium rise buildings and in 2 and 3 storeys frame structures. The difference reduces with increase of storeys while moving towards high rise buildings.

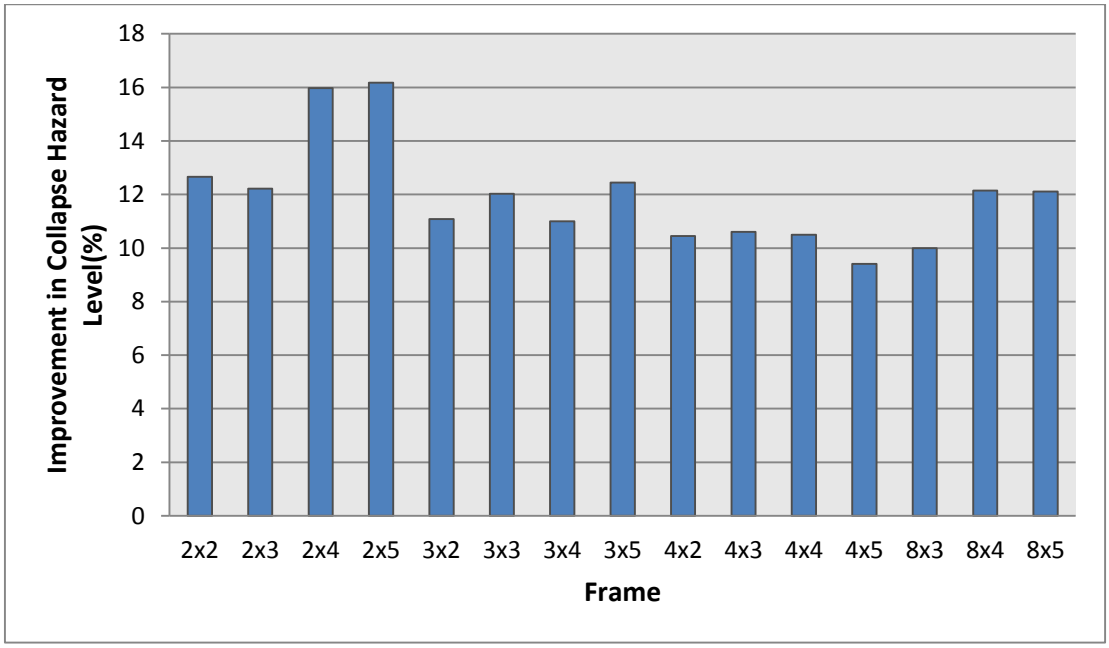

Figure 6. 13 Improvement in Collapse Hazard Level with Incorporation of FRP Wraps

Figure 6.13 shows the increase in PGA value for the retrofitted frame models and therefore identifies the improvement in the collapse hazard level. Percentages yield that the low to medium rise buildings seemingly have higher impact of FRP wraps as for 2 storeys the difference is maximum at a percentage of 16 but it decreases to 12 for 8 storeys. The increase in PGA value for 100% damage state is an indicator of the strengthening achieved by the frames during a seismic event. Confinement provided to columns ensures the ductile nature of frame elements which further increases resistance achieved by FRP wraps.

Within Pakistan PGA range of 0.2g to 0.4g, the performance increase is significantly enhanced by the FRP methodology of retrofitting. Moreover the wrapped frames show lesser damage for the same PGA value as compared to bare frames. Even on the lower side, the performance level many be enhanced by 8% due to incorporation of FRP wraps which can definitely assure reduced hazardous earthquake consequences.

6.6. Comparison of MDR bare vs FRP wrapped Frame

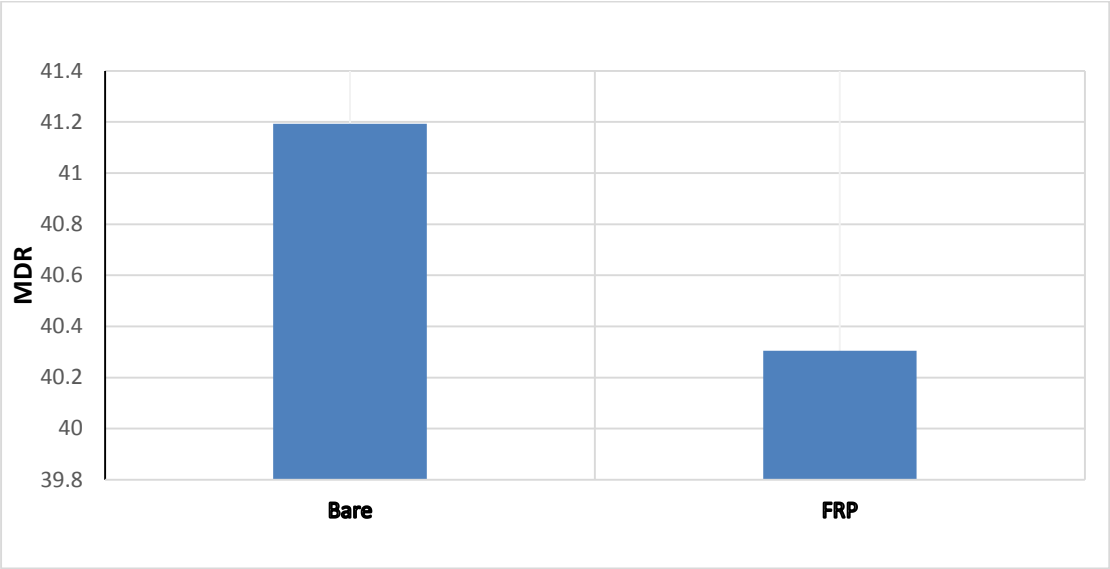

Figure 6. 14 Improvement of MDR for 4x5 frame bare vs FRP

The figure 6.14 shows the difference in the MDR of bare and FRP wrapped 4x5 frame subjected to an earthquake that produces 0.24g of PGA. The results indicate that in case of the bare frame the repair cost would be approximately 41.2 % of the initial construction cost whereas in case the same building was to be wrapped by FRP the cost of repair would be around 40.3 % of the total construction cost. Saving about 0.9 % of the initial construction cost and reducing the repair cost by 2.18 %.

6.7. Effect of Multiple Wraps of FRP

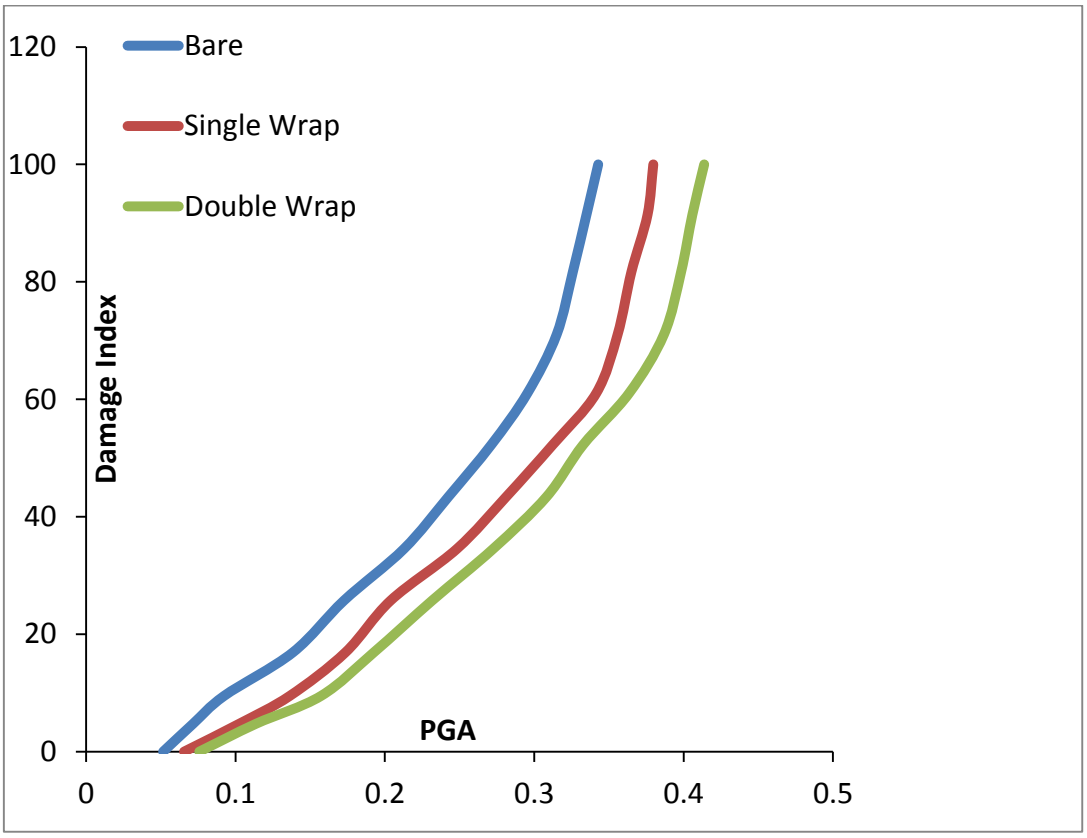

Figure 6. 15 Vulnerability Curves with Multiple Wraps of FRP

In figure 6.15, the impact of using multiple FRP wraps as a retrofitting technique is evident. The plot shows that with the increase of number of wraps the capacity of the structure also enhances. The frame with single FRP wrap fails at PGA value of .38g whereas that with double wraps of FRPs fails at .41g.

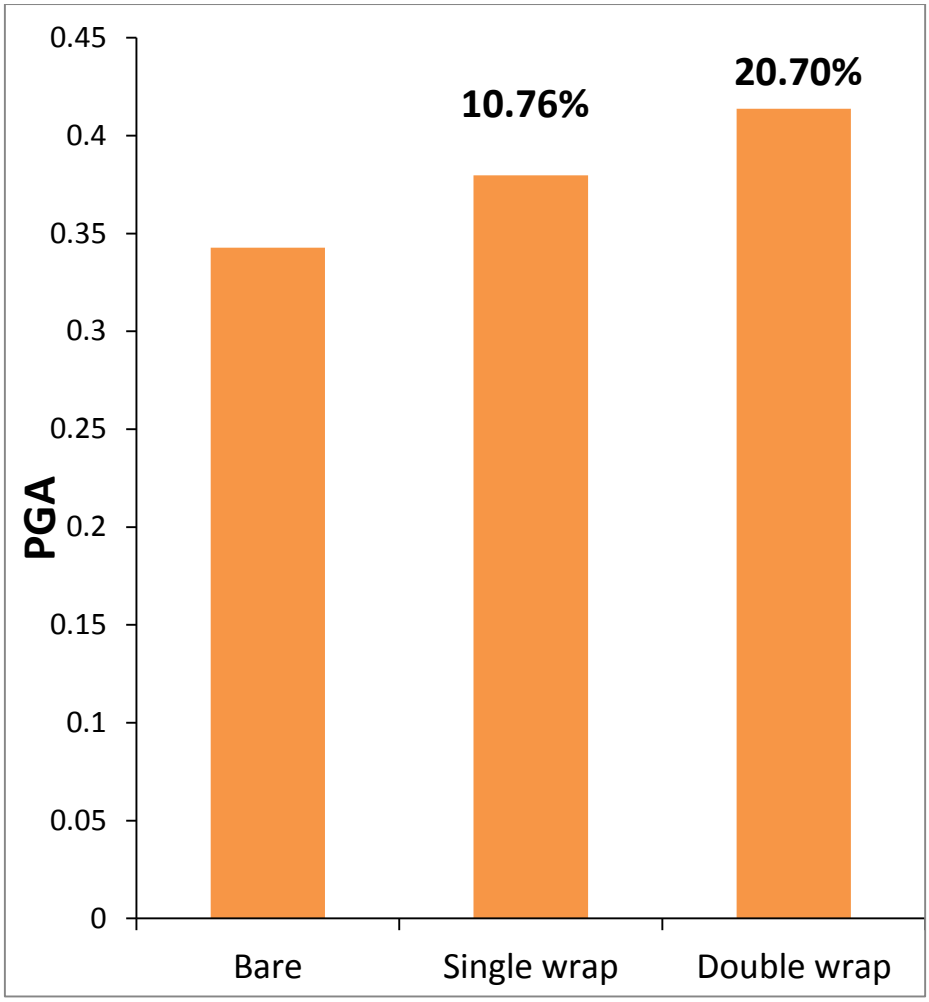

Figure 6. 16 Increase in Performance

In figure 6.16 the increase in the capacity of the structure is shown. The percentage increase for a single wraps yields a value of around 10% whereas a double wrap yields around 20%. This effect shows the increase in confinement to the column members by FRP jacketing hence increasing the capacity of the structure.

CHAPTER 7

CONCLUSION & RECOMMENDATIONS

7.1 Conclusion

The main aim of this study was based on analytical procedure in portraying the impact of using the retrofitting techniques of Fibre reinforced Polymers (FRPs) wraps on the behaviour of RCC buildings under seismic event.

1. Maximum improvement of 18% was observed in the damage index of FRP wrapped frames in comparison of bare frames.
2. Improvement in collapse hazard level may increase up to an average value of 15% for low to medium rise buildings with installation of FRP wraps.
3. Improvement around 23% increase in PGA for complete collapse state in case of double FRP wraps to frame.
4. Approximate increase of 25% increase in max PGA resisting capacity in case of increasing the number of storeys from 2 to 4.
5. Increasing the planar bays by 3 reduces the PGA for 100% collapse by approximately 5 %.
6. Up to 40 % reduction in repair cost of an FRP retrofitted structure was observed in comparison to a bare frame.

7.2 Recommendations

After detailed analysis of representative RC frames structures of Pakistan, including low, medium and high rise buildings, with variable number of bays and other parameter which effects the strength and seismic capacity of building, following recommendations are being made which will not only be open gates for future research but also will help to improve the design practices.

1. It revealed that before the earthquake of 2005 there was no seismic reinforcement used in buildings so they damaged much more than anticipated. Seismic hooks should be provided in buildings
2. It is observed that the most vulnerable part of the building are beams column joints and they are most important part of building and also most prone. So proper joints designed should me made against earthquake.
3. Full scale models of the building or its component should be tested and experimented to get more realistic results.
4. In the future a study to compare the effectiveness of different retrofitting techniques should be conducted to determine the most economical and suitable technique of retrofitting for the building stock of Pakistan.

APPENDICES

APPENDIX-A

DRAIN-3DX INPUT FILE

```
*STARTXX
! Nodal Restraints: Sequential Generation
  A1              0 1 0 0             3D Frame Analysis
!
!
*NODECOORDS
! Controle Nodes (C-lines)
C1010    0        0        0        0
C1020    4.5      0        0        0
C1030    9        0        0        0
C1040    13.5     0        0        0
C1050    18       0        0        0
C2010    0        3.3      0        0
C2020    4.5      3.3      0        0
C2030    9        3.3      0        0
C2040    13.5     3.3      0        0
C2050    18       3.3      0        0
C3010    0        6.6      0        0
C3020    4.5      6.6      0        0
C3030    9        6.6      0        0
C3040    13.5     6.6      0        0
C3050    18       6.6      0        0
C4010    0        9.9      0        0
C4020    4.5      9.9      0        0
C4030    9        9.9      0        0
C4040    13.5     9.9      0        0
C4050    18       9.9      0        0
C5010    0        13.2     0        0
C5020    4.5      13.2     0        0
C5030    9        13.2     0        0
C5040    13.5     13.2     0        0
C5050    18       13.2     0        0
C1111    0        0        1        0
C2222    0        1        0        0
C3333    8        0        0        0
C1910    0        3.1      0        0
C1920    4.5      3.1      0        0
C1930    9        3.1      0        0
C1940    13.5     3.1      0        0
C1950    18       3.1      0        0
C2110    0        3.5      0        0
C2120    4.5      3.5      0        0
C2130    9        3.5      0        0
C2140    13.5     3.5      0        0
```

```
C2150    18      3.5     0       0
C2910    0       6.4     0       0
C2920    4.5     6.4     0       0
C2930    9       6.4     0       0
C2940    13.5    6.4     0       0
C2950    18      6.4     0       0
C3110    0       6.8     0       0
C3120    4.5     6.8     0       0
C3130    9       6.8     0       0
C3140    13.5    6.8     0       0
C3150    18      6.8     0       0
C3910    0       9.7     0       0
C3920    4.5     9.7     0       0
C3930    9       9.7     0       0
C3940    13.5    9.7     0       0
C3950    18      9.7     0       0
C4110    0       10.1    0       0
C4120    4.5     10.1    0       0
C4130    9       10.1    0       0
C4140    13.5    10.1    0       0
C4150    18      10.1    0       0
C4910    0       13      0       0
C4920    4.5     13      0       0
C4930    9       13      0       0
C4940    13.5    13      0       0
C4950    8       1       0       0
!
!
*RESTRAINTS
! Nodal Restraints: Sequential Generation
S  1111111010    1010    0
S  1111111020    1020    0
S  1111111030    1030    0
S  1111111040    1040    0
S  1111111050    1050    0
S  0011102010    2010    0
S  0011102020    2020    0
S  0011102030    2030    0
S  0011102040    2040    0
S  0011102050    2050    0
S  0011103010    3010    0
S  0011103020    3020    0
S  0011103030    3030    0
S  0011103040    3040    0
S  0011103050    3050    0
S  0011104010    4010    0
S  0011104020    4020    0
S  0011104030    4030    0
```

```
S  0011104040     4040     0
S  0011104050     4050     0
S  0011105010     5010     0
S  0011105020     5020     0
S  0011105030     5030     0
S  0011105040     5040     0
S  0011105050     5050     0
S  1111111111     1111     0
S  1111112222     2222     0
S  1111113333     3333     0
S  0011101910     1910     0
S  0011101920     1920     0
S  0011101930     1930     0
S  0011101940     1940     0
S  0011101950     1950     0
S  0011102110     2110     0
S  0011102120     2120     0
S  0011102130     2130     0
S  0011102140     2140     0
S  0011102150     2150     0
S  0011102910     2910     0
S  0011102920     2920     0
S  0011102930     2930     0
S  0011102940     2940     0
S  0011102950     2950     0
S  0011103110     3110     0
S  0011103120     3120     0
S  0011103130     3130     0
S  0011103140     3140     0
S  0011103150     3150     0
S  0011103910     3910     0
S  0011103920     3920     0
S  0011103930     3930     0
S  0011103940     3940     0
S  0011103950     3950     0
S  0011104110     4110     0
S  0011104120     4120     0
S  0011104130     4130     0
S  0011104140     4140     0
S  0011104150     4150     0
S  0011104910     4910     0
S  0011104920     4920     0
S  0011104930     4930     0
S  0011104940     4940     0
S  1111114950     4950     0
!
!
*MASSES
```

```
! Nodal Masses: Sequential Generation
S 10041.02     2010                                  1    0.89573
S 10041.02     3010
S 10041.02     4010
S 10034.8      5010
!
*ELEMENTGROUP
! Group 1
! Element Group Definition
15       1    0     0.00042            Found Column
!
! Controle information
!
1    1    1    0    1    1    1    0    1
!
! Concrete Material Properties
! Controle Line
5    0    0.5       0.06
!
! Stress Strain Points for Compression
! Stress     Strain
7156       0.00036
9397       0.0005
13244      0.0008
17890      0.00171
15207      0.0035
!
! Stress Strain Points for Tension
! Stress     Strain
!
! Steel Material Properties
! Controle Line
2    1
!
! Stress Strain Points for Steel
! Stress     Strain
369506     0.0018
439712     0.24
!
! Fiber Cross Section Types
! Controle Line
8    1
!
! Fibers Data
!
0.077     0.077     0.0003      S1
0.077     -0.077    0.0003      S1
-0.077    0.077     0.0003      S1
```

```
-0.077   -0.077   0.0003     S1
0.111    0        0.0219     C1
0.037    0        0.0219     C1
-0.037   0        0.0219     C1
-0.111   0        0.0219     C1
! Pullout properties for connection Hinge Fibers
!  Basic Properties (1)
915743008 1       0.5      369506   439712   369506   439712   0.01    1
!  Degradation Parameters (1)
1        1        1        0.005    0.005    1        1        1
!
! Gap Properties for Connection Hinge Fibers
!
13244    17890    1.02E+15  1.01E+14  1.00E+13  0.5      1
!
! Connection Hinge Types
! Control Line
8
!
! Fibers Data for Connection Hinge types
!
0.077    0.077    0.0003     P1
0.077    -0.077   0.0003     P1
-0.077   0.077    0.0003     P1
-0.077   -0.077   0.0003     P1
0.111    0        0.0219     G1
0.037    0        0.0219     G1
-0.037   0        0.0219     G1
-0.111   0        0.0219     G1
!
!
! Element Geometry Types
! Controle Line
3        1
!
! Segment data, Eement Geometry Types
!
0.1        F01
0.8        F01
0.1        F01
!
! Element Generation Commands
!
1   1010     1910     900      1111     1
2   1020     1920     900      1111     1
3   1030     1930     900      1111     1
4   1040     1940     900      1111     1
5   1050     1950     900      1111     1
```

```
*ELEMENTGROUP
! Group 2
! Element Group Definition
15      1    0     0.00042            Floors Columns
!
! Controle information
!
1    1    1    0    1    1    1    0    1
!
! Concrete Material Properties
! Controle Line
5    0    0.5       0.06
!
! Stress Strain Points for Compression
! Stress     Strain
7156       0.00036
9397       0.0005
13244      0.0008
17890      0.00171
15207      0.0035
!
! Stress Strain Points for Tension
! Stress     Strain
!
! Steel Material Properties
! Controle Line
2    1
!
! Stress Strain Points for Steel
! Stress     Strain
369506     0.0018
439712     0.24
!
! Fiber Cross Section Types
! Controle Line
8    1
!
! Fibers Data
!
0.077      0.077      0.0003       S1
0.077      -0.077     0.0003       S1
-0.077     0.077      0.0003       S1
-0.077     -0.077     0.0003       S1
0.111      0          0.0219       C1
0.037      0          0.0219       C1
-0.037     0          0.0219       C1
-0.111     0          0.0219       C1
! Pullout properties for connection Hinge Fibers
```

```
!  Basic Properties (1)
915743008 1       0.5     369506   439712   369506   439712   0.01    1
!  Degradation Parameters (1)
1       1       1       0.005    0.005    1       1       1
!
! Gap Properties for Connection Hinge Fibers
!
13244    17890    1.02E+15  1.01E+14  1.00E+13  0.5     1
!
! Connection Hinge Types
! Control Line
8
!
! Fibers Data for Connection Hinge types
!
0.077    0.077    0.0003     P1
0.077    -0.077   0.0003     P1
-0.077   0.077    0.0003     P1
-0.077   -0.077   0.0003     P1
0.111    0        0.0219     G1
0.037    0        0.0219     G1
-0.037   0        0.0219     G1
-0.111   0        0.0219     G1
!
!
! Element Geometry Types
! Controle Line
3       1
!
! Segment data, Eement Geometry Types
!
0.1       F01
0.8       F01
0.1       F01
!
! Element Generation Commands
!
1   2110     2910     800      1111     1
2   2120     2920     800      1111     1
3   2130     2930     800      1111     1
4   2140     2940     800      1111     1
5   2150     2950     800      1111     1
6   3110     3910     800      1111     1
7   3120     3920     800      1111     1
8   3130     3930     800      1111     1
9   3140     3940     800      1111     1
10  3150     3950     800      1111     1
11  4110     4910     800      1111     1
```

```
12   4120     4920     800      1111     1
13   4130     4930     800      1111     1
14   4140     4940     800      1111     1
15   4150     4950     800      1111     1
*ELEMENTGROUP
! Group 3
! Element Group Definition
15       1    1     0.00042           Beam fibre
!
! Controle information
!
1    1    1    0    0    0    0    1    1
!
! Concrete Material Properties
! Controle Line
5    0    0.5       0.01
!
! Stress Strain Points for Compression
! Stress     Strain
7156      0.00036
9397      0.0005
13244     0.0008
17890     0.00171
15207     0.0035
!
! Stress Strain Points for Tension
! Stress     Strain
!
! Steel Material Properties
! Controle Line
2    1
!
! Stress Strain Points for Steel
! Stress     Strain
369506    0.0018
439712    0.24
!
! Fiber Cross Section Types
! Controle Line
10   1
!
! Fibers Data
!
0.119     0.043     0.0002      S1
0.119     -0.043    0.0002      S1
-0.119    0.043     0.0002      S1
-0.119    -0.043    0.0002      S1
-0.119    0         0.0002      S1
```

```
0.119    0       0.0002     S1
0.143    0       0.0218     C1
0.048    0       0.0218     C1
-0.048   0       0.0218     C1
-0.143   0       0.0218     C1
!
!
! Rigid End Zone Types
!
0.13
!
! Element Geometry Types
! Controle Line
3
!
! Segment data, Eement Geometry Types
!
0.1        F01
0.8        F01
0.1        F01
!
! Element Generation Commands
!
1   2010     2020     10       2222     1
2   2020     2030     10       2222     1
3   2030     2040     10       2222     1
4   2040     2050     10       2222     1
5   3010     3020     10       2222     1
6   3020     3030     10       2222     1
7   3030     3040     10       2222     1
8   3040     3050     10       2222     1
9   4010     4020     10       2222     1
10  4020     4030     10       2222     1
11  4030     4040     10       2222     1
12  4040     4050     10       2222     1
13  5010     5020     10       2222     1
14  5020     5030     10       2222     1
15  5030     5040     10       2222     1
16  5040     5050     10       2222     1
*ELEMENTGROUP
! Group 4
! Fiber Element
08   1   0     0.00000          JOINTS
! Input specific to element type 8
0   0   0   0   0   0   1   1   0   1
!shear
!234567890!234567890!234567890!234567890!234567890!234567890!234567890!
234567890
```

```
1E15    1E2     1E1     156     223     156     223     1       1
!DEGRADATION
!
1       1       1       0.3     0.3     1       1       1
!Material Properties
!234567890!234567890
29000000  1
!Cross section properties
1       0.00064  0.00064  0.0875  0       0
!Stiffness Factors
4       4       2
!Element geometry types
!234567890!234567890!234567890
1           1    1

! Element Generation Commands
!
!floors
1   1   1910    2010    100     3333
2   1   1920    2020    100     3333
3   1   1930    2030    100     3333
4   1   1940    2040    100     3333
5   1   1950    2050    100     3333
*ELEMENTGROUP
! Group 4
! Fiber Element
08   1   0    0.00000          JOINTS
! Input specific to element type 8
0   0   0   0   0   0   1   1   0   1
!shear
!234567890!234567890!234567890!234567890!234567890!234567890!234567890!
234567890
1E15    1E2     1E1     156     223     156     223     1       1
!DEGRADATION
!
1       1       1       0.3     0.3     1       1       1
!Material Properties
!234567890!234567890
29000000  1
!Cross section properties
1       0.00064  0.00064  0.0875  0       0
!Stiffness Factors
4       4       2
!Element geometry types
!234567890!234567890!234567890
1           1    1

! Element Generation Commands
```

```
!
!floors
1   1   2010    2110    100     3333
2   1   2020    2120    100     3333
3   1   2030    2130    100     3333
4   1   2040    2140    100     3333
5   1   2050    2150    100     3333
6   1   2910    3010    100     3333
7   1   2920    3020    100     3333
8   1   2930    3030    100     3333
9   1   2940    3040    100     3333
10  1   2950    3050    100     3333
11  1   3010    3110    100     3333
12  1   3020    3120    100     3333
13  1   3030    3130    100     3333
14  1   3040    3140    100     3333
15  1   3050    3150    100     3333
16  1   3910    4010    100     3333
17  1   3920    4020    100     3333
18  1   3930    4030    100     3333
19  1   3940    4040    100     3333
20  1   3950    4050    100     3333
21  1   4010    4110    100     3333
22  1   4020    4120    100     3333
23  1   4030    4130    100     3333
24  1   4040    4140    100     3333
25  1   4050    4150    100     3333
26  1   4910    5010    100     3333
27  1   4920    5020    100     3333
28  1   4930    5030    100     3333
29  1   4940    5040    100     3333
30  1   4950    5050    100     3333
!
*RESULTS
! Nodal Results: Sequential Generation
!
NSD   0015010    5010    1
!
!
!
*NODALOAD
! Pattern 1
! Pattern Name Line
 Vert                          Permanent Loads
!
! Nodal Loads: Sequential Generation
SF0     -52.9   0       2010    2010
SF0     -98.9   0       2020    2020
```

```
SF0     -98.9   0       2030    2030
SF0     -98.9   0       2040    2040
SF0     -52.9   0       2050    2050
SF0     -52.9   0       3010    3010
SF0     -98.9   0       3020    3020
SF0     -98.9   0       3030    3030
SF0     -98.9   0       3040    3040
SF0     -52.9   0       3050    3050
SF0     -52.9   0       4010    4010
SF0     -98.9   0       4020    4020
SF0     -98.9   0       4030    4030
SF0     -98.9   0       4040    4040
SF0     -52.9   0       4050    4050
SF0     -49.4   0       5010    5010
SF0     -80.8   0       5020    5020
SF0     -80.8   0       5030    5030
SF0     -80.8   0       5040    5040
SF0     -49.4   0       5050    5050
!
*NODALOAD
! Pattern 2
! Pattern Name Line
 horz                           Horizontal Load
!
! Nodal Loads: Sequential Generation
SF0.29  0       0       2010    2010
SF0.59  0       0       3010    3010
SF0.88  0       0       4010    4010
SF1     0       0       5010    5010
!
*NODALOAD
! Pattern 3
! Pattern Name Line
 nega                           Negative Loads
!
! Nodal Loads: Sequential Generation
SF-0.29 0       0       2010    2010
SF-0.59 0       0       3010    3010
SF-0.88 0       0       4010    4010
SF-1    0       0       5010    5010
!
*PARAMETERS
! Analysis Parameters
! Event Overshoot Scale Factors
!
F1  1
F2  1
F3  1
```

```
F4   1
F5   1
!
!
! Output Intervals for Static Analysis
!
OS   0    0    1    0    00
!
*MODE
!
! Controle Information
!
4              0    0    0
!
*STAT                        Static Gravity Analysis No. 1
!
! Static Analysis
!
! Nodal Loads
!
N     Vert 1
!
! Load Controle
!
L 1       1
*STAT                        Static Gravity Analysis No. 1
!
! Static Analysis
!
! Nodal Loads
!
N     horz 1
!
! Displacement Controle
!
D5010     1010         10.002     0.05      999  99   99999
!
*STAT                        Static Gravity Analysis No. 2
!
! Static Analysis
!
! Nodal Loads
!
N     nega 1
!
! Displacement Controle
!
D1010     5010         10.002     0.1       999  99   99999
```

```
!
*STAT                          Static Gravity Analysis No. 3
!
! Static Analysis
!
! Nodal Loads
!
N     horz 1
!
! Displacement Controle
!
D5010     1010         10.002     0.15      999  99   99999
!
*STAT                          Static Gravity Analysis No. 4
!
! Static Analysis
!
! Nodal Loads
!
N     nega 1
!
! Displacement Controle
!
D1010     5010         10.002     0.2       999  99   99999
!
*STAT                          Static Gravity Analysis No. 5
!
! Static Analysis
!
! Nodal Loads
!
N     horz 1
!
! Displacement Controle
!
D5010     1010         10.002     0.25      999  99   99999
!
*STAT                          Static Gravity Analysis No. 6
!
! Static Analysis
!
! Nodal Loads
!
N     nega 1
!
! Displacement Controle
!
D1010     5010         10.002     0.3       999  99   99999
```

```
!
*STAT                          Static Gravity Analysis No. 7
!
! Static Analysis
!
! Nodal Loads
!
N     horz 1
!
! Displacement Controle
!
D5010     1010         10.002     0.35      999  99   99999
!
*STAT                          Static Gravity Analysis No. 8
!
! Static Analysis
!
! Nodal Loads
!
N     nega 1
!
! Displacement Controle
!
D1010     5010         10.002     0.4       999  99   99999
!
*STAT                          Static Gravity Analysis No. 9
!
! Static Analysis
!
! Nodal Loads
!
N     horz 1
!
! Displacement Controle
!
D5010     1010         10.002     0.45      999  99   99999
!
*STAT                          Static Gravity Analysis No. 10
!
! Static Analysis
!
! Nodal Loads
!
N     nega 1
!
! Displacement Controle
!
D1010     5010         10.002     0.5       999  99   99999
```

```
!
*STAT                          Static Gravity Analysis No. 11
!
! Static Analysis
!
! Nodal Loads
!
N     horz 1
!
! Displacement Controle
!
D5010     1010         10.002     0.55      999  99   99999
!
*STAT                          Static Gravity Analysis No. 12
!
! Static Analysis
!
! Nodal Loads
!
N     nega 1
!
! Displacement Controle
!
D1010     5010         10.002     0.6       999  99   99999
!
*STAT                          Static Gravity Analysis No. 13
!
! Static Analysis
!
! Nodal Loads
!
N     nega 1
!
! Displacement Controle
!
D5010     1010         10.002     0.65      999  99   99999
!
*STAT                          Static Gravity Analysis No. 14
!
! Static Analysis
!
! Nodal Loads
!
N     horz 1
!
! Displacement Controle
!
D1010     5010         10.002     0.7       999  99   99999
```

```
!
*STAT                          Static Gravity Analysis No. 15
!
! Static Analysis
!
! Nodal Loads
!
N     nega 1
!
! Displacement Controle
!
D5010     1010         10.002     0.75      999  99   99999
!
*STAT                          Static Gravity Analysis No. 16
!
! Static Analysis
!
! Nodal Loads
!
N     horz 1
!
! Displacement Controle
!
D1010     5010         10.002     0.8       999  99   99999
!
*STAT                          Static Gravity Analysis No. 17
!
! Static Analysis
!
! Nodal Loads
!
N     nega 1
!
! Displacement Controle
!
D5010     1010         10.002     0.85      999  99   99999
!
*STAT                          Static Gravity Analysis No. 18
!
! Static Analysis
!
! Nodal Loads
!
N     horz 1
!
! Displacement Controle
!
D1010     5010         10.002     0.9       999  99   99999
```

```
!
*STAT                          Static Gravity Analysis No. 19
!
! Static Analysis
!
! Nodal Loads
!
N     nega 1
!
! Displacement Controle
!
D5010     1010         10.002     0.95      999  99   99999
!
*STAT                          Static Gravity Analysis No. 20
!
! Static Analysis
!
! Nodal Loads
!
N     horz 1
!
! Displacement Controle
!
D1010     5010         10.002     1         999  99   99999
!
*STAT                          Static Gravity Analysis No. 21
!
! Static Analysis
!
! Nodal Loads
!
N     nega 1
!
! Displacement Controle
!
D5010     1010         10.002     1.05      999  99   99999
!
*STAT                          Static Gravity Analysis No. 22
!
! Static Analysis
!
! Nodal Loads
!
N     horz 1
!
! Displacement Controle
!
D1010     5010         10.002     1.1       999  99   99999
```

```
!
*STAT                          Static Gravity Analysis No. 23
!
! Static Analysis
!
! Nodal Loads
!
N     nega 1
!
! Displacement Controle
!
D5010     1010         10.002     1.15      999  99   99999
!
*STAT                          Static Gravity Analysis No. 24
!
! Static Analysis
!
! Nodal Loads
!
N     horz 1
!
! Displacement Controle
!
D1010     5010         10.002     1.2       999  99   99999
!
*STAT                          Static Gravity Analysis No. 25
!
! Static Analysis
!
! Nodal Loads
!
N     nega 1
!
! Displacement Controle
!
D5010     1010         10.002     1.25      999  99   99999
!
*STAT                          Static Gravity Analysis No. 26
!
! Static Analysis
!
! Nodal Loads
!
N     horz 1
!
! Displacement Controle
!
D1010     5010         10.002     1.3       999  99   99999
```

```
!
! Nodal Loads
!
!
! Displacement Controle
*STOP
```

BIBLIOGRAPHY

BIBLIOGRAPHY

1. Barbat, A. Y. (1996). Damage Scenarios Simulation for Seismic Risk Assessment in Urban Zones. *Earthquake Spectra*, 371-394.
2. Calvi, G. (1999). A displacement-based approach for vulnerability evaluation of classes of buildings. *Journal of Earthquake Engineering*, 411-438.
3. Chopra, A. (1995). *Dynamics of Structures: Theory and Applications to Earthquake Engineering.* Prentice Hall.
4. Chopra, A., & Goel, R. (2000). Evaluation of NSP to estimate seismic deformation: SDF Systems. *Journal of Structural Engineering*, 482-490.
5. Deierlein, G., & Hsieh, S. (1990). Seismic response of steel frames with semi-rigid connections using the capacity spectrum method. *Proceedings 4th US National Conference on Earthquake Engineering*, (pp. 863-72).
6. Dumova-Jovanoska, E. (2004). Fragility Curves for RC Structures in Skopje Region. *Proceedings of the 13th World Conference on Earthquake Engineering*. Vancouver, Canada.
7. European Macroseismic Scale (EMS). (1998). Luxembourg: Centre Europeen de Geondynamique et de Seismologie.
8. Fajfar, P. (1996). Simple Push-Over Analysis of Buildings Structures. *11th World Conference on Earthquake Engineering*.
9. Goel, R., & Chopra, A. (2005). Response to B. Maison's Discussion of "Evaluation of Modal and FEMA Pushover Analyses: SAC Buildings. *Earthquake Spectra*, 277-279.
10. Gupta, B. (1998). Enhanced pushover procedure and inelastic demand estimation for performance-based seismic evaluation of buildings. *Ph.D. Dissertation*. Orlando, Florida: University of Central Florida.
11. Kappos, A. P. (1995). Cost-Benefit Analysis for the Seismic Rehabilitation of Buildings in Thessaloniki, Based on a Hybrid Method of Vulnerability Assessment. *Proceedings of the Fifth International Conference on Seismic Zonation*, (pp. 406-413). Nice, France.

12. Kilar, V. (1997). Simple Push-Over Analysis of Asymmetric Buildings. *Earthquake Engineering and Structural Dynamics*, 233-249.
13. Krawinkler, H., & Seneviratna, G. (1998). Pros and Cons of a Pushover Analysis for Seismic Performance Evaluation. *Engineering Structures*, 452-464.
14. Kyriakides, n. (2007). Vulnerability of rc buildings and risk assessment for cyprus. United Kingdom: University of Sheffield.
15. Lin, E., & Pankaj, P. (2004). Nonlinear static and dynamic analysis - the influence of material modelling in reinforced concrete frame structures. *13th World Conference on Earthquake Engineering.* Vancouver,Canada.
16. Paret, T., Sasaki, K., Eilbeck, D., & Freeman, S. (1996). Approximate Inelastic Procedures to Identify Failure Mechanisms from Higher Mode Effects. *Proceedings of the 11 th World Conference on Earthquake Engineering*. Acapulco, Mexico.
17. Park, Y. a. (1985). Mechanistic Seismic Damage Model for Reinforced Concrete. *Journal of Structural Engineering*, 722-739.
18. Pietra, D. (2008). Evaluation of Pushover Procedures for the Seismic Design of Buildings. Universita degli Studi di Pavia.
19. Priestley, M. (1993). Myths and Fallacies in Earthquake Engineering - Conflicts between Design and Reality. *Bulletin of New Zealand National Society for Earthquake Engineering*, 329-341.
20. Priestley, M. (1997). Displacement-based seismic assessment for reinforced concrete buildigns. *Journal of Earthquake Engineering*, 157-192.
21. Reinhorn , A. (1997). Inelastic analysis techniques in seismic evaluations. *Seismic design methodologies for the next generation of codes, Proc. of the International Workshop P. Fajfar and H. Krawinkler, eds., Bled, Slovenia.*
22. Rossetto, T., & Elnashai, A. (2003). Derivation of vulnerability functions for European-type RC structures based on observational data. *Engineering Structures*, 1241-1263.
23. Shahid, B., Anwar, G. A., Jilani, K., Islam, M., & Shakil, O. (2013). Seismic Analysis of Reinforced Concrete Structures in Pakistan. Pakistan: National University of Sciences and Technology.

24. Singhal, A. a. (1996). Method for Probabilistic Evaluation of Seismic Structural Damage. *Journal of Structural Engineering, ASCE*, 1459-1467.
25. Whitman, R. V., Reeds, J. W., & Hong, S.-T. (1974). Earthquake Damage Probability Matrices. *Proceedings of the fifth World Conference on Earthquake Engineering*, (pp. 2531-2540). Rome.
26. Bank, L. C. (2006). *Composites for construction: Structural design with FRP materials.* John Wiley & Sons.
27. Becque, J., Patnaik, A., & Rizkalla, S. (2003). Analytical Models for Concrete Confined with FRP Tubes. *Journal of Composites for Construction (7)1* , 31-38.
28. Benzaid, R., & Mesbah, H.-A. (2013). Circular and Square Concrete Columns Externally Confined by CFRP Composite: Experimental Investigation and Effective Strength Models. In *Fiber Reinforced Polymers - The Technology Applied for Concrete Repair.*
29. Berthet, J., Ferrier, E., & Hamelin., P. (2006). Compressive behavior of concrete externally confined by composite jackets. Part B: Modelling. *Construction and Building Materials* , 338-347.
30. Binici, B. (2005). An analytical model for stress–strain behavior of confined concrete. *Engineering Structures, (27)7* , 1040-1051.
31. Brighton, D., & Parvin, A. (2014). FRP Composites Strengthening of Concrete Columns under Various Loading Conditions. *Polymers Volume 6, Issue4* , 1040-1056.
32. Chun, S., & Park, H. (2002). Load carrying capacity and ductility of RC columns confined by carbon fiber reinforced polymer. *3rd international conference of composite materials in infrastructure.*
33. Fam, A. Z., & Rizkalla, S. H. (2001). Confinement Model for Axially Loaded Concrete Confined by Circular Fiber-Reinforced Polymer Tubes. *Structural Journal* , 451-461.
34. Fardis, M. N., & Khalili, H. H. (1982). FRP-encased concrete as a structural material. *Magazine of Concrete Research, Volume 34, Issue 121* , 191 –202.

35. Harajli, M., Hantouche, E., & Soudki, K. (2006). Stress-Strain Model for FRP Jacketed Concrete Columns. *ACI Structural Journal, Vol. 103, No. 5* , 672-682.
36. Lorenzis, L. D., & Tepfers, R. (2003). Comparative study of models on confinement of concrete cylinders with fiber reinforced polymer composites. *Journal of Composites for Construction, (7)3* , 219-237.
37. Marques, S., Marques, D., Lins da Silva, J., & Cavalcante, M. (2004). Model for Analysis of Short Columns of Concrete Confined by Fiber-Reinforced Polymer. *Journal of Composites for Construction* , 332-340.
38. Mirmiran, A., & Shahawy, M. (1997). Dilation characteristics of confined concrete. *Mechanics of Cohesive-frictional Materials* , 237-249.
39. MIYAUCHI, K., INOUE, S., KURODA, T., & KOBAYASHI, A. (1999). Strengthening effects of concrete columns with carbon fiber sheet. *Japan Concrete Institute 21 143 150* .
40. Rocca, S., Galati, N., & Nanni., A. (2006). LARGE-SIZE REINFORCED CONCRETE COLUMNS STRENGTHENED. *Third International Conference on FRP Composites in Civil Engineering (CICE 2006)* .
41. Saafi, M., Toutanji, H., & Li., Z. (1999). Behavior of Concrete Columns Confined with Fiber Reinforced Polymer Tubes. *Materials Journal, 96(4)* , 500-509.
42. Saenz, N., & Pantelides, C. (2007). Strain-Based Confinement Model for FRP-Confined Concrete. *Journal of Structural Engineering 133(6)* , 825-833.
43. Samaan, M., Mirmiran, A., & Shahawy, M. (1998). Model of Concrete Confined by Fiber Composites. *Journal of Structural Engineering (124)9* , 1025–1031.
44. Youssef, M. N., Feng, M. Q., & Mosallam, A. S. (2007). Stress-strain model for concrete confined by FRP composites. *Composites Part B: Engineering* , 614–628.
45. Shahida Manzoor, D. S. A., 2013. Characteristics of Grade 60 and Grade 72.5 Re-bars in P*akistan. International Journal of Modern Engineering Research (IJMER),* March-April, 3(2), pp. 667-673.

46. Shahzada, K., 2011. Vulnerability Assessment of Typical Buildings in Pakistan. *International Journal of Earth Sciences and Engineering,* Volume 4, pp. 208-211.
47. Usman, 2010. s.l.: NUST.
48. Uzair Maqbool Khan, M. W. U. A. U. S. M. U. M. W., 2010. *PROBABALISTIC SEISMIC VULNERABILTY ASSESEMENT OF RC FRAME STRUCTURES,* s.l.: NUST.